SAPIENZA
UNIVERSITÀ DI ROMA

Roma La Sapienza

Master in Chemical Engineering

Master thesis
21/01/2020

ANALYSIS OF TWO-PHASE FLOW MODELS THROUGH PRESSURE RELIEF VALVES.

Candidate:
Ana Rosa Vega Herrero
Matricola 1885761

Supervisor:
Roberto Bubbico

Acknowledgements

A mi familia por haberme estado apoyando desde España, siempre confiando en mí y dándome ánimos en todo momento.

A mis amigos por haberme soportado y ayudado en todo lo posible, y gracias a la gente que he conocido en Roma que han hecho de esta una experiencia única.

Gracias a todas.

“Analysis of two-phase flow models through pressure relief valve.”

ABSTRACT

Pressure relief valves are mechanical devices used in industry to protect systems against excessive pressure, thus preventing accidents from occurring. Nowadays, a multitude of flows can pass through these pressure relief valves, such as the biphasic ones, in which this master's thesis is going to be framed. These are used in industries such as the oil and chemical industries. The problem comes when trying to characterize them since there is not enough experimental data in the literature to be able to develop a good model, in addition to the fact that if the valves are over-sized or under-sized, it could lead to more economic costs and possible safety problems.

In this context, the present Master's thesis aims to find a calculation model that allows the adjustment of some experimental data to predict their behaviour. To achieve this goal, the different methods that can be used for pressure relief valves with two-phase flows will be studied and an analysis of the results will be carried out to find the model that best predicts the behaviour and adjusts to the experimental data provided.

In this thesis, we have taken as reference the experimental data provided by the University of La Sapienza, Rome, in which the mass flow rate of a steam/water mixture passing through a valve of 0.01 m diameter has been measured for different initial pressures and qualities of the inlet vapour of the mixture. Therefore, it was decided to try to fit some experimental data to some of the existing models (HEM, HNE-DS, API, ISO) to describe the behaviour of these fluids.

The results obtained have shown the differences that exist between the two homogeneous models (HEM, HNE-DS) as well as the similarity of each of them with the other two described (API, ISO). The conclusion has been reached that the model that best fits the behaviour of the data is the homogeneous non-equilibrium model, since it is in this model that a greater similarity is found between the experimental mass flow rate provided and the theoretical mass flow rate calculated. This hypothesis has been corroborated thanks to a comparison made to the HEM and HNE-DS models in which it has been concluded that at high pressures the homogeneous equilibrium model is the one that best fits the data but the model has wide spread results, but at the end, for all the experimental data the homogenous non-equilibrium model is the one that in the end best fits the them.

SUMMARY

MEMORY

FIGURE SUMMARY

TABLE SUMMARY

GRAPH SUMMARY

MEMORY

0.- Objectives and methodology

The pressure relief valves are mechanical devices that protect a system against excessive pressure, it has been used in industry for a long time, and together with two-phase fluids have been used and are still used for example in the petrochemical industry.

The sizing methods and equations for single-phase flow in safety relief valves have been well established and standardized for many years. However, in many practical applications, a two-phase flow can occur as previously mentioned in petrochemicals is the most common case, and despite the relatively high frequency of occurrence of this situation, at present, no method or equation It is considered reliable enough to be adopted as a standard. This is mainly due to two different reasons, the thermal and dynamic phenomena of fluids that occur between the two phases are very complex, it involves a large number of parameters.

However, in spite of these difficulties, a correct relief valve size is of the utmost importance to prevent the occurrence of dangerous accidents since an insufficient size of the valve will lead to a discharged mass flow rate lower than the required one, causing an overpressure in the process equipment and possibly its failure. On the contrary, due to oversizing, a discharged flow higher than expected could result in a smaller downstream pipe and effluent treatment systems. Therefore, a more thorough and thorough study of the process with more experimental data is needed. It must be taken into account that there are currently not enough experimental data on these flows through these valves, but there are different calculation methods in the literature, although most of them refer to some conditions of use and highly idealized cases.

This thesis considers the evaluation and analysis of the different resolution methods for a two-phase system to find the model that best predicts the behaviour and conforms to the experimental data provided.

For this work the following methodology will be followed:

- A bibliographic review of the two-phase flows with their characteristic parameters as well as a description of the pressure relief safety valves.
- A bibliographic review of the different models will be carried out for two-phase flows.
- A database provided by experiments carried out in La Sapienza will be used.
- A study and analysis of the data will be carried out to find several models that fit well and predict their behaviour. (homogeneous models (HEM, HNE) and API and ISO standards).
- As several models are expected to fit, a comparison will be made to find the most accurate models, as well as a review of future work that could be done to broaden the spectrum of study.

1.- Introduction to the flows

To begin, start by defining the single-phase and multi-phase flows and then give a more detailed explanation of the different two-phase flows that can be found as well as their main characteristic parameters. *[1]*

1.1.- Single-phase Flow:

A fluid can be in two different states, liquid phase (such as water) and is considered incompressible in most cases, waves and pressure shock mat occur and the flow is usually considered as laminar or turbulent. The other state is a gas phase (such as steam or air) and is considered compressible in many cases, density in the gas phase is very different from the liquid phase, gas phase properties vary considerably with temperature and can be considered laminar or turbulent flow equally.

An understanding of the physics of the single-phase flow and knowledge of the solution techniques for single-phase flow problems are important prerequisites for studying the two-phase or multiphase flow system. *[1]*

Normally, single-phase flows are well known and modelled for valves as if they were ideal, through modified adiabatic nozzles with a discharge coefficient Kd. This coefficient oscillates between 0.6-0.7 for liquids and almost the unit for gases. These discharge coefficients for single-phase fluids have been established for many years and are published by the manufacturers in their catalogues. *[2]*

To calculate the ideal G_{nozzle} mass flow, it is necessary to know the inlet and outlet pressure as well as the relationship between fluid density and pressure. So, the mass flow through the valve is obtained as

Eq 1.

$$G_{valve} = K_D G_{nozzle} = K_D \rho_n \sqrt{2 \int_{P_o}^{P_n} -\frac{dP}{\rho}} \qquad \textit{Eq 1}$$

G_{valve} : $mass\ flux\ through\ a\ valve\ (\frac{kg}{m^2 s})$

K_D: $dscharge\ coefficient$

G_{mozzle} : $mass\ flux\ through\ a\ nozzle\ (\frac{kg}{m^2 s})$

ρ: $density\ (\frac{kg}{m^3})$

ρ_n: $density\ in\ discharge\ satate\ (\frac{kg}{m^3})$

P_n: $Pressure\ in\ discharge\ state\ (Pa)$

P_o: $Pressure\ stagnation\ state, upstream\ (Pa)$

In gas-vapour flows, there is an important complication due to its compressibility, which causes the system to reach an acceleration point where it reaches sound velocity. At this speed, the so-called choke pressure is reached and, at this speed, the fluid reaches a maximum mass flow point that cannot be exceeded due to a narrowing of the useful section of the dynamic fluid passing through the gas. In most cases, there is a large pressure drop, so systems choke quickly.

1.2.- Multiphase flow:

Multiphase flow is defined as a flow in which more than one phase is produced, that is, a mixture of gas (g), liquid (l) or solid (s). These flows are commonly used in industry, such as, for example, gas-liquid flows in evaporators and condensers, gas-liquid-solid flows in chemical reactors, solid-gas flows in pneumatic transport.

Coming up next, the basic characteristics of these three types of phases of flow will be described. *[3]*

1.2.1.- Solids

The solid phase is usually found in the form of lumps or particles that are transported in the flow and their movements normally depend on the size of the individual elements and the movements of the associated fluids. It can be found that smaller particles accompany fluid movements, unlike larger particles that are less receptive to fluid movement. *[3]*

1.2.2.- Liquids

In multiphase flow, it can be found that it contains a liquid phase, this liquid can be in the continuous phase, that is, it contains dispersed elements of solids (particles), gases (bubbles) or other liquids (drops). Or it can also be in the discontinuous liquid phase, as in the form of droplets suspended in a gaseous phase or another different liquid phase.

Another important property of liquid phases is related to wettability. For example, when a liquid phase is in contact with a solid phase, a channel wall, and is adjacent to another phase that is also in contact with that wall, there is a triple interface on it, and the angle subtended on this interface by liquid-gas and liquid-solid is known as the contact angle. *[3]*

1.2.3.- Gas

Under some conditions, gas can be considered as a fluid with properties similar to liquids. Although it has an important difference concerning liquids and solids since gas has the additional property that it can be highly compressible, although, in practice, many multiphase flows containing gas phase can be treated as incompressible when the pressure is sufficiently high. *[3]*

1.3.- Two-phase flow

The most common class of multiphase flows are the two-phase flows, which the present work will focus on, and these include gas-liquid flow, gas-solid flow, liquid-liquid flow and liquid-solid flow, of which, the gas-liquid flow is the most characteristic for the study of them in pressure relief systems. There are different regimes for two-phase flows in the literature, but it may be difficult to specify specifically which regime the flow belongs to in a particular case.

Although there is no single set of regimes, the classification can be useful when interpreting how these affect the parameters (such as pressure, mass transfer coefficient or empty fraction) differently.

Detailed discussions of these patterns are given by Hewitt *[5]*, Whalley *[6]*, Dukler and Taitel *[7], [8]*. To begin with, the different flow regimes will be described, which can be divided mainly into types of interfacial distribution, called flow patterns or regimes. *[4].*

1.3.1.- Horizontal flow regimes in pipes

Where the heaviest phase (such as water) tends to be positioned near the bottom of the pipe due to the effect of gravity. Normally it is the gas phase that exerts a pressure job that pushes or guides the liquid phase in the direction of flow.

Horizontal flow (h) can be classified into six different regimes:

- Stratified flow (Figure 1) → it is the simplest flow regime in which the separation of the phases is completely gravitational, with the gas phase remaining in the upper part of the pipe and the liquid phase in the lower part. In this case, we can find that the contact surface between both parts is relatively smooth and not many variations are found. Keep in mind that these types of flows are not usually common in the industry since they only occur when the speed is sufficiently low.

Figure 1. Stratified flow h [4]

- Wavy flow (Figure 2) → It looks like a stratified flow only that it appears at higher flow rates. Waves form on the contact surface of the phases as a result of friction between the two. These waves move in the direction of flow.

Figure 2. Wavy flow h [4]

- Bubble flow (Figure 3) → Bubbles are present in the flow and are dispersed everywhere in the cross-section, with some separation due to the effect of gravity. What has been observed is that the bubbles accumulate at low speeds in the upper part of the pipe and that they behave like foam at high speeds.

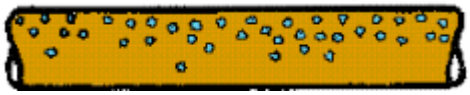

Figure 3. Bubble flow h [4]

- Plug Flow (Figure 4)→ In which there are large bubbles that flow near the top of the tube due to the effects of gravity and forming plugs; in this classification, you can also find the semi-slug flow, in which there are very large waves in the stratified layer and the bubbles when joined form larger gas plugs.

Figure 4. Plug flow h [4]

- Slug flow (Figure 5) → The waves in the flow reach the top of the pipe, closing the trajectory of the gas in that part, a different impulse of the two phases is produced due to the difference in speed of the same, the waves that touch the upper part of the tube forms a liquid slug that passes quickly along the canal, resulting in sudden and timely pressure changes causing the trajectory to close. These vibrations and pressure pulses should be avoided whenever possible.

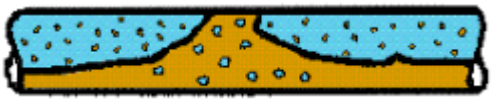

Figure 5. Slug flow h [4]

- Dispersed annular flow (Figure 6) → Is similar to the vertical flow, that we will see below, although there is an asymmetry in the thickness of the film due to the action of gravity, with thicker at the bottom, and a variety of intermittent currents since the liquid It forms a layer around the walls of the pipe with the gas flowing through, usually in the form of drops.

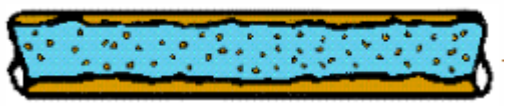

Figure 6. Dispersed annular flow h [4]

Despite the definitions discussed above, it is useful to provide some examples of flow regime diagrams along with the definitions that help distinguish the different regimes. The figure below (Figure 7) shows the map of gas/liquid flows in horizontal pipelines (based on studies by Weisman 1983). *[9] [10]*

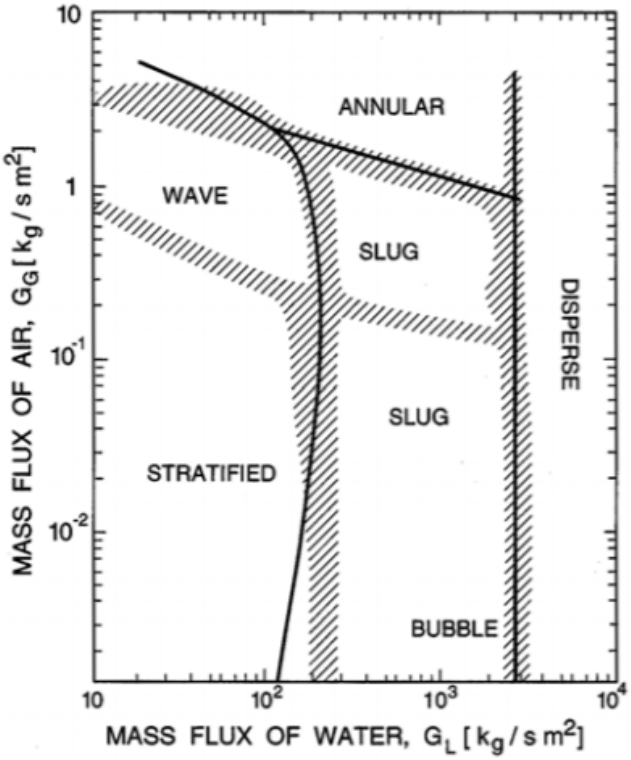

Figure 7. Flow regime map for the horizontal flow of an air/water mixture [10]

The different flow regimes for the flow of an air/water mixture in a horizontal pipe are shown, the transition observed experimentally the regions are shown by the shaded areas and the solid lines represent theoretical predictions.

Convective evaporation in a horizontal channel is similar to the evaporation in the vertical. But gravitational force tends to drain the liquid toward the bottom of the channel and the vapour phase concentrates at the top of the channel. At the inlet, the liquid enters subcooled, as the liquid heats up, the wall temperature correspondingly rises and subcooled boiling begins. The convective boiling process passes through bubbly, plug regimes and flow can be either stratified or unstratified. The channel dries out occurs at the top of the tube where the film thickness is thinner due to gravitational force. Dry out then progresses around the perimeter from top to bottom along the channel. Figure 8 shows the evolution

that could be expected in a horizontal boiler tube based on the flow regime maps given above.

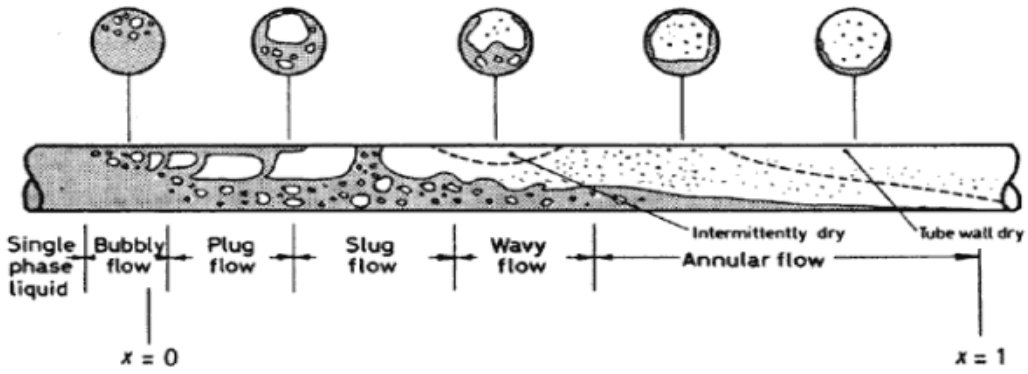

Figure 8. evolution of the steam/water flow in a horizontal boiler tube [11]

1.3.2.- Vertical flow regimes in pipes

In this case, it is the liquid phase that tends to be in the walls of the pipe, forming a stable or unstable film.

Vertical flow (v) can be classified into five different regimes:

- Bubble flow (Figure 9) → Liquid phase is continuous and there is a dispersion of bubbles within the liquid, these bubbles are distributed evenly although they tend to accumulate in the vicinity of the center of the pipe faster than near the walls. For these types of regimes, the speeds of both phases are considered very similar.

Figure 9. Bubble flow v [4]

- Slug flow (Figure 10) → The bubbles have coalesced to make larger bubbles which approach the diameter of the tube, in this regime, the bubble gas tends to get together and form bullet-shaped holes in the center of the pipe. The flow is usually considered unstable, which results in different pressure strokes and vibrations along the pipe as if it were a pulse flow

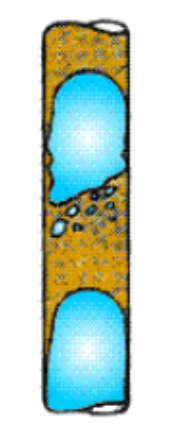

Figure 10. Slug flow v [4]

- Churn flow (Figure 11) → The bubbles have broken down to give oscillating churn regime, this means that the gas bubbles inside the pipe meet and form a gas path or path in the centre of the pipe. The flow is similar to that of the foam and quite unstable, which can usually lead to high-pressure variations within the pipe. The gas flow pushes the liquid up due to its high speed.

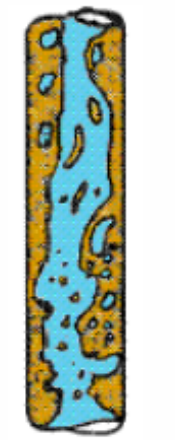

Figure 11. Churn flow v [4]

- Annular flow (Figure 12) → In this case, the liquid flows through the tube wall as if it were a film, with liquid trapped in the core, and the gas flows in the center of the pipe, another type of annular flow is the annular flow wispy, where, as the flow of liquid increases, the concentration of drops in the gas core also increases, which leads to the formation of large lumps of liquid.

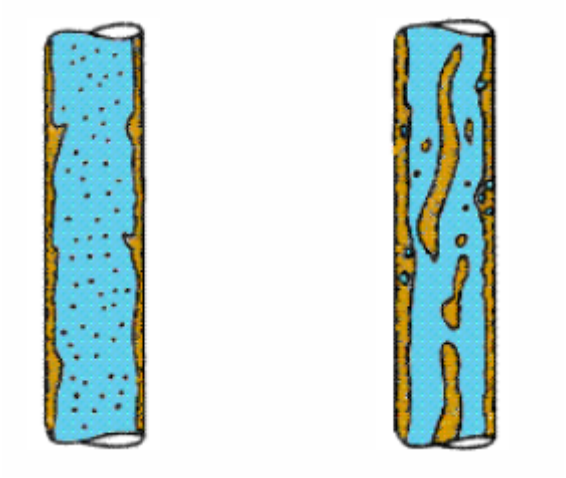

Figure 12. Annular flow v and annular flow wispy v [4]

Figure 13 shows a vertical flow regime map similar to the horizontal flow regime map, only that it is using moment flow axes rather than volumetric or mass flow axes. Based on Hewitt and Roberts flow regime map (1969) which correlates both air/water at atmospheric pressure and steam/water at high-pressure data.

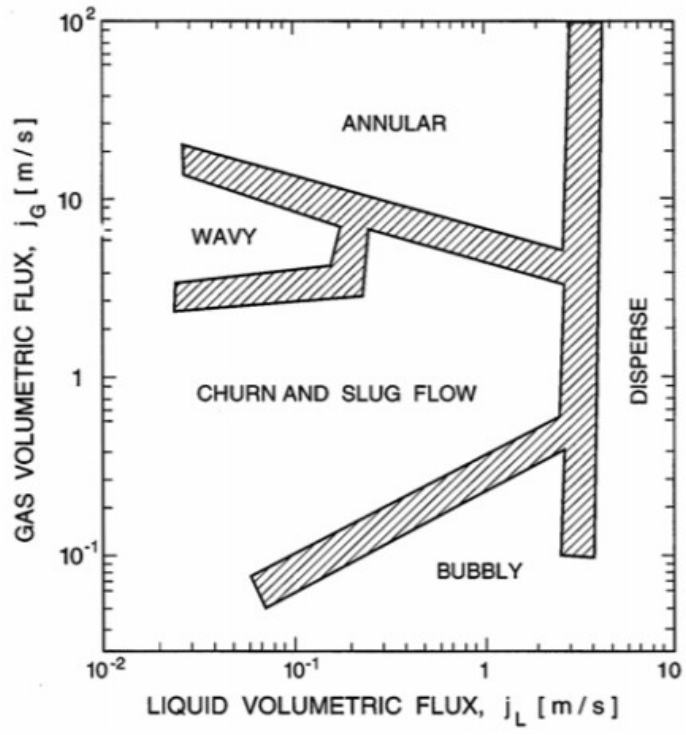

Figure 13. Flow regime map for the flow of an air/water mixture in a vertical pipe. [10]

As the volumetric fraction increases, the flow becomes unstable at some critical volumetric fraction. This instability produces large-scale mixing movements that dominate the flow. In even larger volume fractions, large volumes of unsteady gas accumulate within these mixing movements and produce the flow regime

known as turbulent rotational flow. Figure 14 shows the evolution that could be expected in a vertical boiler tube based on the flow regime maps given above.

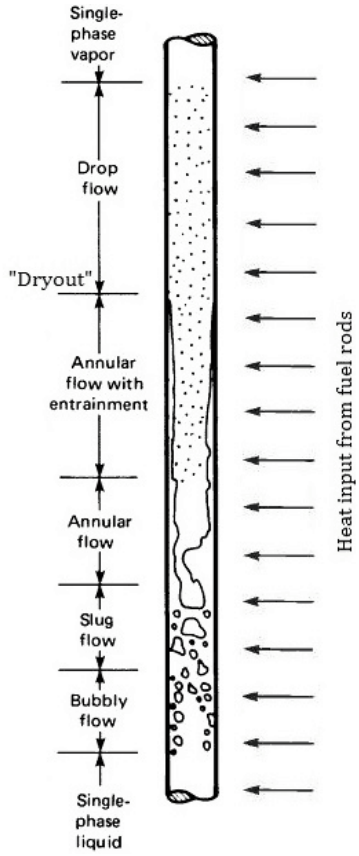

Figure 14. evolution of the steam/water flow in a vertical boiler tube [11]

1.3.3.- Schemes for inclined pipes

These regimes are the least known. The most important thing in these pipes is the angle of incidence of the flow, the slope, as well as its direction since the calculations can vary depending on whether it is upward or downward flow.

1.4.- Two-phase flow parameters

The most important design parameters for two-phase flow systems will be described below, these being the pressure drop, the heat, and mass transfer coefficient, the empty fraction, void fraction and slip ratio.

1.4.1.- Pressure drop:

In two-phase flow systems, the pressure drop occurs due to gravitational effects and friction between the phases. This pressure drop is what determines the power with which the fluid enters the pumping systems in the facilities, as in the

design of pumps. This parameter can be predicted using different models, homogeneous models, separate flow model or phenomenological models.

1.4.2.- Heat transfer coefficient

It is used to determine the size of heat exchangers in industrial facilities as in condensers in power plants.

1.4.3.- Mass transfer coefficient

This parameter is important in the design of separation equipment or in the prediction of heat and mass transfer, as in the condensation phenomena of steam mixtures.

1.4.4.- Average phase content

Represents the fraction in volume or area of the cross-section of a particular phase, that is, it denotes the fraction between the steam area and the total area of a cross-section of a pipe. In the case of gas-liquid flows, the gas phase is what is called the empty fraction and the liquid phase is called the liquid holdup (this parameter is considered important within the systems in which one of its phases can become toxic or valuable which is not the case in this thesis).

One of the problems presented by biphasic systems is the limitations in mass flows, produced by the critical flow when the speeds are very low, floods or minimum fluidization speeds; and in the heat fluxes in which the critical flux, in this case, can lead to poor system performance or unwanted temperature gradients in the channel wall.

This thesis will focus on the two-phase liquid-gas flow in safety systems, in this case, the pressure relief valves.

It has been explained in the previous point the liquid-gas flows with their characteristics, so it will proceed to oversee the safety systems, valves, as well as the different models that currently exist to interpret the operation of these. *[1] [12] [13] [14] [15] [16].*

The basic approach to sizing relief valves for two-phase flows, although is more complex, is similar as single-phase flows using the correct model choosing and determining the proper discharge coefficient. *[17]*

1.4.5.- Void fraction

This is one of the most important parameters used to characterize gas-liquid flows. It can be defined as the fraction of the channel volume that is occupied by the gas and it influences other parameters like viscosity, pressure drop or heat transfer. *[11]*

1.4.6.- Slip Ratio

The slip ratio or velocity ratio is defined as the ratio of the velocity of the vapour phase to the velocity of the liquid phase. In the homogeneous equilibrium model (HEM) of two-phase flow, that it's going to be explained later, the slip ratio is assumed to be unity, no slip. However, most industrial two-phase flows have different velocity of the gas and liquid phases. *[11]*

2.- Safety valves

In a system, a safety valve is a valve that acts as a fail-safe, which does not prevent the failure from ever occurring but that these systems prevent or stop the unsafe consequences of the failure.

The first record of the safety valves is from the Industrial Revolution, in which they were used for steam boilers since the first boilers that operated without them were more likely to explode.

2.1.- Pressure relief valve

Pressure relief valves may refer to a variety of terms, such as safety valves, pressure relief valves, and safety relief valves. These terms have been conventionally applied to valves for gas/steam service, liquid service or multi-service applications, respectively.

Within all the safety valves, the one of interest for the following thesis is the pressure relief valve, denoted as PRV, which releases a substance from a pressure vessel when temperatures or pressures are higher than those of the system limits. The valve normally opens in proportion to the increase in pressure over the opening pressure. These pressure relief valves are mainly used with incompressible fluids.

To better define it, a relief valve is a type of safety valve used to control or limit the pressure in a system as it can accumulate and cause system failure, including equipment and installation.

The operation of the valve is very simple since it is designed to open at a certain pressure and thus protect the equipment, when the pressure established by the limits is exceeded the valve opens to the force and a part of the fluid, could be liquid, gas or mixture, is diverted through the auxiliary route of pipes towards a high central gas flare where it is usually burned, sending to the atmosphere the combustion gases that have been generated.

So, when the inlet pressure is below the set pressure, the disc remains seated in the nozzle in the closed position and when the inlet pressure exceeds the set pressure, the pressure force on the disc exceeds the force of the spring and the

valve opens. When the inlet pressure drops below the set pressure, the valve closes again.

While this flow is diverted to the central flare, the pressure inside the system or vessel decreases causing the pressure to return to the established limits at a certain point and the pressure relief valve closes.

For the flow outlet, it can be outdoors as in high-pressure gas systems or connected to a pipeline as just explained.

These valves are commonly used in the petroleum refining, petrochemical, fine chemical manufacturing, natural gas processing, conventional or nuclear power generation *[18]*, food, cosmetics and pharmaceutical industries where it is necessary to control that operating pressure does not exceed unsafe limits.

Industries that have systems or pressure vessels have a legal obligation, in most countries, to use this type of pressure relief valves, which have certain codes with design standards provided by different institutions such as:

- The American Society of Mechanical Engineers, ASME. *[19]*
- The American Petroleum Institute, API 520 (2000). *[20]*
- The international standard, ISO 4126 (2004). *[21]*
- German Merkblatt A2 AD-2000 (2001).

There are different types of pressure relief valves. *[43] [44]*

- Mechanical: the relief system consists of a plug with a calibrated spring that allows its movement against changes in pressure.
- Electrical: these valves have a pressure switch that opens or closes a solenoid valve depending on the pressure reading.
- Electronics: where is a pressure transducer that sends a signal to a control room by having an operator manually or by programming decide at what pressure the solenoid valve is opened or closed.

The following figure (Figure 15) shows a pressure relief valve with its components.

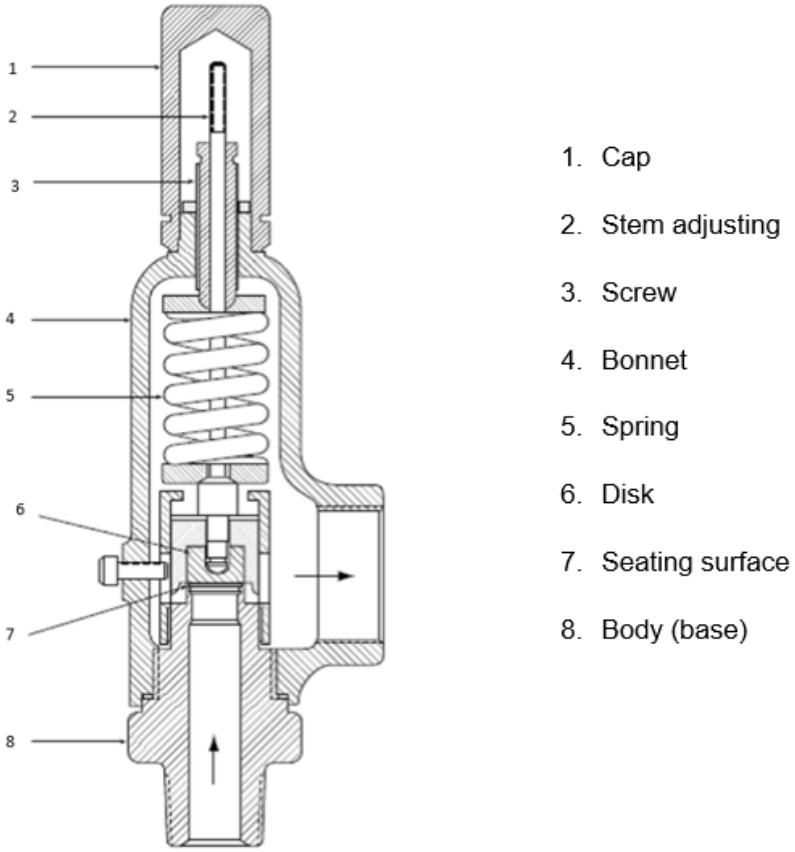

Figure 15. Components of a Pressure relief valve [22]

As mentioned previously, safety relief valves are one of the most important equipment in terms of the protection of any pressurized system. Their design and sizing are very important to ensure non-break conditions. *[23] [24] [25] [15]*

A good design prevents harmful pressures from occurring and ensures less loss of fluid products as well as minimizes the environmental impact they may have. *[26] [27] [23]*

The most characteristic factors when evaluating the stability and good performance of safety valves can be summarized in:

- Valve design
- Length of the inlet pipeline
- Regulator rings position
- Pressure vessel volume
- Valve opening length. *[28]*

The design is generally given by the operating conditions in which the valve acts, and the properties of the fluids that pass through it, although it must also be taken into account that its designs present complications due to the thermohydraulic phenomena that occur between the two phases of the fluid. some of the

dimensional characteristics of pressure relief devices may be the discharge area and effective discharge area or the inlet and outlet size. *[26]*

A difference has to be made between valves for steam or liquid applications because historically, many pressure relief valves used in liquid applications were safety relief valves or relief valves designed for compressible (steam) service. Most of these valves, when used in liquid service, require a high overpressure, 25%, to achieve a full spring lift since liquids, unlike vapours, do not provide sufficient expansive forces.

When required to operate within the 10% accumulation limit, a conservative factor of 0.6 was applied to the capacity of the valve in its sizing. Therefore, there are some industrial plants that are over-sized. (Liquid service valves have been developed that achieve full lift, stable operation and rated capacity at 10% overpressure following ASME requirements *[19]*.)

Some of these valves are designed to work with liquids and gases, however, they may have different operating characteristics, depending on whether the flow is liquid, gaseous or a combination of both. Capacity certification data for in-service sizing of liquids and gases must be obtained from the manufacturer for use in the final sizing and application of the valve.

For two-phase applications where the fluid being relieved may be liquid, gaseous, or a multiphase mixture, the use of spring-loaded valves designed for liquid and balanced applications is recommended to minimize the effects of backpressure when the percentage mass of the two-phase mixture at the valve inlet is 50% steam or less. Also, if the liquid-to-gas ratio in the flow stream is not safe, a valve designed specifically for liquid service or for liquid and gas service should be used. For example, if a liquid and gas service is located in the vapour region of a vessel containing a liquid level, the valve must be specified for gas service; or if there is a liquid and gas service valve in the water of a heat exchanger, then the valve must be specified for liquid service.

The operations conditions of these systems have been the subject of considerable discussion over the time since in most cases, the sizing of the valve is based on the flow-through an isentropic nozzle, the relationship between pressure and density of the fluid and the discharge coefficient (K_d). *[25]*

This presents a problem since for single-phase fluids the properties of the fluids are simple and the values of the discharge coefficient are available in the literature. Also, a general model is often used to calculate the specific mass flow at reference conditions, usually ideal or isentropic.

However, these methods are only different simplified hypotheses that attempt to predict the flow-rate through the valve knowing the inlet and outlet. Nevertheless, none of them is considered as a valid standard in two-phase flow design. *[26]*

For example, one of the problems can be observed in the size of the valves, since for monophasic it is usually smaller than two-phase due to the high velocity of the flows that can occur inside the valves. There is a clear need for further analysis concerning the availability of new experimental data for biphasic flows. *[26] [23]*

In order to choose an appropriate method different factors are considered, such as the assumption that the flow through the relief valves is homogeneous and the phases are mixed evenly. Different studies have led to the assumption that the two-phase mixture can be represented as a pseudo-homogeneous single-phase fluid. It is also important to know the thermodynamic state of the fluid since it changes as it crosses the valve and different states can occur, such as frozen where the quality of the fluid is not a function of pressure and then the quantities relative to gas and liquid are constant; or intermittent where the quality changes as the pressure drops in the valve and the liquid evaporates. Saturated and slightly cooled systems can also occur (the flow enters as a liquid and flashes when the saturation pressure is reached).

It is also important to know the choked conditions (they can drown at up to 90% of the inlet pressure), which are reached as mentioned above at sonic velocity, although this is less defined than for single-phase flows (they tend to drown at half the pressure than at the inlet), frozen flows can drown in a much wider rank of pressures, but lower than flashing flows. *[20] [17]*

3.- Discharge coefficient

The discharge coefficient, K_d, explains the difference between the mass flow in a real valve and that expected by the theoretical model being used. For example, it can be friction, since the theoretical model usually assumes an isentropic flow in an ideal nozzle, which is not normally found in reality.

Normally for single-phase air and water flows based on isentropic nozzle flow models for incompressible flow, water, and critical flow of an ideal gas, air, the valve manufacturers report the values of the discharge coefficients in the so-called Red Book (as introduced in the first chapter of the thesis). These coefficients have been determined by numerous experiments by different authors and are very standardized.

On the other hand, in the case of the two-phase flow, it is not so easy to find standardized data of the discharge coefficient although several different models can be found in the literature (if the theoretical model is accurate, the value of K_d would be 1).

This difficulty in tabulating different K_d values is due to the properties of complex fluids, an extremely wide rank of flow conditions, and the variety of theoretical models that can be found in practice. As mentioned above, a variety of suggestions have been made in the literature to estimate the appropriate value of K_d for use in two-phase flow in relief valves such as that performed by Darby

[25] in which experimental data collected for different valves under different operating conditions were compared with the predictions of the homogeneous equilibrium models, and average values of the discharge coefficient were obtained. Due to the various conditions under which the experimental data were generated, no general rule could be derived from the analysis.

Also, the correlation proposed by Lenzing *[29]* as a function of the discharge coefficients of liquid alone and vapour alone, weighted by the void fraction of the mixture is the most common suggestion (Eq 2).

$$Eq\ 2 \qquad K_d = \alpha K_{dv} + (1-\alpha) K_{dL}$$

K_{dv}: gas discharge coefficient,

K_{dL}: liquid discharge coefficient,

α: void fraction (gas volume fraction)

(1- α): liquid volume fraction

On the other hand, Darby *[25]* took another approach to the discharge coefficient in 2004, saying that it should depend solely on the type of flow, whether strangled or not, K_d being K_{dv} or K_{dL}, respectively, and Leung *[30]* proposes a discharge coefficient as a function of the ω-parameter.

The results of this theory have shown that:

- For nonflashing flow, such as air–water system, $K_{dL} < K_d < K_{dv}$.
- For flashing flow, such as steam–water system, $K_{dv} < K_d < 1$.

So, for the first time, the present theory demonstrates that for flashing flow discharge, the K_d is higher than K_{dv} and approaches unity for a wide range of omega values.

Although the calculations for the determination of the discharge coefficient of the valve are not going to be carried out in this work, it must be taken into account that this is much more a function of the flow conditions than of the specific properties of the fluid. The fact that K_{dv} is greater than K_{dL} is because K_{dv} is measured under conditions where the flow of gas is drowned, as opposed to liquids. Therefore, the appropriate value for K_d should depend on whether the flow is obstructed or not, so K_{dL} would be used if the flow is not drowned, and K_{dv} if the flow is drowned. *[31]*

4.- Models for two-phase flows

For single-phase flow models, the methods and equations have been well established for years, but it has to be understood that in many industrial applications a two-phase flow is observed and, although the frequency with which

it occurs is high, no method is considered reliable enough to be adopted with a good level of confidence. This is because the thermal and dynamic phenomena that occur between the two phases are complex, and a large number of parameters need to be controlled.

On the other hand, there are currently several different calculation methods available for two-phase flow sizing but their experimental database is very scarce and is often referred, as mentioned above, for ideal nozzles and pipes of different lengths, not so much on safety relief valves.

Also, the discharge coefficient adapted to each model has to be used and it represents an additional uncertainty due to the lack of data and those available in the literature refer to specific operating conditions so they cannot be used for any given condition. *[26]*

Unfortunately, relief valves not only present these problems, but they also impose limiting conditions. Critical flow occurs more easily by further limiting speed. Since the operation of these is based on the prediction of possible output flows, how a two-phase flow affects the performance of the valve is a matter of study. So, for the accurate prediction of the two-phase flow rate discharge through a pressure relief valve there are some issue that should be taken into account like the interaction between vapour quality and pressure drops, possible thermodynamic nonequilibrium or the sound velocity in two-phase flow.

Predictive models in the literature for two-phase discharge flows use mathematically simple semi-empirical algebraic approaches with uncertain precision and very general approaches to sizing and designing relief valves. *[23]*

4.1.- Background

Pressure relief valves in chemical, petrochemical, and power plants are sized for the discharge of gas-liquid mixtures in two phases and the flow is usually accompanied by a strong pressure drop between the inlet and the narrowest cross-section, which can lead to the vaporization of a subcooled or saturated liquid. In engineering sizing is usually based on the assumption of a homogeneous flow in the thermodynamic equilibrium, which corresponds to the Leung *[18]* homogeneous equilibrium model HEM (The American Petroleum Institute, API 520 published a report suggesting a method for dimensioning two-phase flow PSV, based on the HEM). *[20] [32] [33]*

This model is known to be conservative, leading to oversizing of safety valves and in applications with high levels of vessel filling, oversizing is not acceptable.

Therefore, Diener and Schmidt *[34]* developed a model, incorporating the thermodynamic (boiling delay) and mechanical (slip) non-equilibrium of the flow that is called the HNE homogeneous non-equilibrium model. The size of the Pressure Relief valves is one of the most important parameters used to choose

between these two main prediction models, HEM and HNE. Homogeneous models calculate the mass flow assuming that the mixture of two phases is homogeneous and liquid and vapour phases have the same speed, as a result of this estimate, all physical parameters are determined by weighted averages in steam quality Eq 3. *[26] [22]*

$$W_r = k_d G_t A \qquad \text{Eq 3}$$

W_r: dischargeable mass flow rate.

A: geometric valve seat area.

G_t: theoretical max flux through an ideal nozzle.

k_d: discharge coefficient for two-phase flow.

For four main models, HEM, HNE-DS, ISO, and API, the homogenous can be based on the so-called omega methods, where omega, ω, is the compressibility factor that defines an equation of state for two-phase flow. Numerous papers have discussed the differences between these four models through a comparison based on experimental data and with different types of safety valves. For example, comparisons have been made where flow rates are measured for various types of two-phase flow such as saturated liquid plus flashing vapour, initially subcooled liquid with flashes and non-flashing gas/liquid mixtures, to validate the accuracy of the different models. *[22]*

To sum up, the homogeneous equilibrium model, HEM, was chosen by DIERS (Design Institute for Emergency Relief Systems) *[35]* for the design and sizing of emergency systems. Although one of the problems that this model presents when the omega parameter is not used is that it is considered very conservative when performing the required calculations, since it involves a very long iterative procedure with a very detailed tabulation of the thermodynamic properties of the flow.

Therefore, in 1986, J. C. Leung *[36]* published a generalized correlation for the homogeneous equilibrium choked flow of a single component to simplify this procedure, explained later in this document. This simplification is known as the omega method in which the ω-parameter, first proposed by Epstein in 1983 *[38]*, is introduced. In this parameter, groups of dimensionless physical properties are included, which allowed characterizing a wide range of fluid conditions. J. C. Leung himself, in 1994 *[37]*, proposed a small modification of parameter ω, by means of which key parameters could be brought to light in relation to the compressible nature of a two-phase flow system.

In relation to the ω-parameter, this is based on the assumption of a change in the isothermal state of the two-phase mixture. After this assumption, the deviations from the critical mass flow rate versus the change of state of gas or normally isentropic steam appeared. It was therefore questioned to what extent these correlations affect the predictions of critical mass flow in the two-phase flow.

One of the advantages of the ω-method is, in addition to the possibility of explicit calculation of the critical mass flow, the low number of properties of the fluid needed for its resolution, although depending on the fluid being worked with, these simplifications can lead to considerable deviations in the calculated values of the mass flow rate compared to the values calculated by the iterative method of the HEM.

In general, theoretical models adapted to each case tend to overestimate the actual flow through a device. These methods present different ways of sizing the valves by calculating the mass flow rate, the discharge coefficient or the required minimum adjustment area of the valves, but it must be taken into account that they are not suitable for determining the pressure Loss when the mixture flows through the system. *[18]*

4.2.- HEM

The assumption of a homogeneous flow in thermodynamic equilibrium results in a compressibility coefficient that depends solely on the properties of the inlet fluid. The HEM is a computer model described by CCPS (Center for Chemical Process Safety). *[31]*

One of the most recently developed forms of HEM is the so-called ω-method, mainly based on Leung's work whose characteristic parameter ω is defined in the model. The flow is considered as a quasi-single-phase compressible fluid that undergoes an isentropic expansion that crosses the valve and, besides, is in conditions of thermodynamic equilibrium at the outlet. Two-phase density is represented as a linear function of pressing the thermal/physical properties of the fluid in the stagnant state.

The ω-methods present a series of advantages since they can be applied in different conditions such as in systems, both intermittent and not, in strangled and not strangled flows as well as in conditions of saturation or subcooling of the flow at its inlet (API is almost entirely based on this model). *[18] [33]*

Based on HEM alone, there are two main methods of calculation, based on a pipe or a nozzle. For the nozzle the following integral equation Eq 4 is used in which the density is calculated according to the pseudo-homogenous-single-phase-flow assumption Eq 5.

$$G_{nozzle} = \rho_n \sqrt{2 \int_{P_o}^{P_n} -\frac{dP}{\rho}} \qquad \textit{Eq 4}$$

Terms of Eq 4 defined in

Eq 1.

$$\rho = \alpha\, \rho_G + (1-\alpha)\rho_L \qquad \textit{Eq 5}$$

α: volume fraction of gas phase

ρ_G: gas density $(\frac{kg}{m^3})$

ρ_L: liquid density $(\frac{kg}{m^3})$

The HEM model incorporates a series of possible models for the pressure-density relationship and depending on the model pressure, mass fraction, and density data are entered for one or several points of the system (the way to calculate the density-pressure relationship varies depending on the points that are taken into account in the system) (Table 1 shows the different equations that can be used to calculate the flow depending on the system with which you are working, in our case to make the analysis of data has been used the equation of state for the calculation of gas densities).

*Table 1. HEM density models**

MODEL	POINTS	EQUATIONS
A	1	$(\rho_o/\rho - 1) = a\left(P_o/P - 1\right)$
B	3	$(\rho_o/\rho - 1) = a\left(P_o/P - 1\right)^b$
C	3	$(\rho_o/\rho - 1) = a\left[\left(P_o/P - 1\right)^b - 1\right]$
D	2	$(\rho_o/\rho - 1) = a\left(P_o/P - 1\right) + b\left[\left(P_o/P - 1\right)^2\right]$
E	2	$x = a_o + a_1 P$ $\rho_G = b_o P^{b_1}$ $\rho_L = c_o + c_1 P$
F	3	$x = a_o + a_1 P + a_2 P^2$ $\frac{\rho_G}{\rho_L} - 1 = b_o\left[\left(\frac{P_o}{P}\right)^{b_1} - 1\right]$ $\rho_L = c_o + P + c_2 P^2$

*a,b,c: empirical parameters of the model in [17]

The model parameters are evaluated with the entered data and the mass flow from stagnation to discharge pressure is numerically integrated. If the flow is drowned, the most common situation, a maximum flow will be found before the discharge pressure is reached at the critical choke pressure. The quality or mass fraction can be calculated by assuming the flow through the nozzle is isenthalpic like the next Eq 6.

Eq 6 $$x = \frac{H_o - H_L}{H_G - H_L}$$

H_o: Initial enthalpy $(\frac{J}{mol})$

H_G: $Gas\ enthalpy\ (\frac{J}{mol})$

H_L: $Liquid\ enthalpy\ (\frac{J}{mol})$

Nozzle case also can take into account both the thermal and mechanical nonequilibrium called "slip", as the pressure drops through the valve body, the gas phase expands, i.e. the density decreases, the specific volume increases, while the density of the liquid phase remains constant. Thus, the gas phase will accelerate concerning the liquid phase, and the condition of "slip".

There are many slip models and little or no experimental confirmation of which is the most suitable and what is necessary is the slip ratio, S, which is calculated as (parameter introduced by Diener and Schmidt):

$$Eq\ 7 \qquad S = (1 - x + x\frac{\rho_L}{\rho_G})^{k_S}$$

k_s: $empirical\ parameter\ for\ slip$

S: $slip\ ratio, ration\ of\ gas\ phase\ velocity\ to\ liquid\ phase\ velocity$

For nonequilibrium the quality x has to be changed by a nonequilibrium quality x_{NE} where $x_{NE}<x$.

$$Eq\ 8 \qquad x_{NE} = x_o + k_{NE}(x^2 - x_o^2)$$

k_{NE}: $empirical\ parameter\ for\ nonequilibrium$

x_o: $quality\ at\ the\ stagnation\ condition$

As explained above, one of the most developed forms of HEM currently; they are called ω-methods based on Leung's Work from 1990 to 1995 *[30] [36] [37]*, which are recognized as one of the best methodologies to analyse the two-phase flow and Relief systems, although more experimental data is needed to fully prove the validity of the model and it is rigorous for pure fluids and only in limited cases it can be extended to multi-component systems and is accurate only below the critical point $T_r \leq 0.9$ or $P_r \leq 0.5$.

The following are the most important parameters and equations when applying the method.

1. Two-phase equation state and ω-parameter.

The two-phase equation of state is calculated using Eq 9, this is an approximation of the two-phase system behaviour and for some fluids/conditions it may give incorrect values

$$Eq\ 9 \qquad \frac{\rho_o}{\rho} = \omega\left(\frac{P_o}{P} - 1\right) + 1$$

ω: compressible flow parameter as a function of the fluid properties at the inlet conditions only and, for saturated or two-phase inlet conditions calculated by Eq 10.

$$Eq\ 10 \qquad \omega = \frac{x_o v_{LGo}}{v_o k} + \frac{C_{Lo} T_o P_o}{v_o}\left(\frac{v_{LGo}}{h_{LGo}}\right)^2$$

The first term of the equation represents the compressibility of the two-phase mixture due to the existing vapour. The second term of the equation takes into account the compressibility due to phase change caused by depressurisation.

It must be taken into account that this method is based on the homogeneous equilibrium of the phases, so the density value can be calculated as indicated by Eq 5 or with its equivalent presented in Eq 11.

$$Eq\ 11 \qquad \frac{1}{\rho} = x\left(\frac{1}{\rho_G}\right) + (1 - x)\left(\frac{1}{\rho_L}\right)$$

With the homogenous void fraction calculated as:

$$Eq\ 12 \qquad \alpha = \frac{x}{x + (1-x)\rho_G/\rho_L}$$

2. Dimensionless mass flow

Combining Eq 4 and Eq 9 mass flow can be obtained dimensionless by the next equation (like mass flow in the first scenario of the API models), and it must be taken into account if the system has in critical conditions, in this case, pressure value, P, should be considered as critical pressure P_c.

$$Eq\ 13 \qquad Gs = \frac{\left\{-2\left[\omega Ln\left(\frac{P}{P_o}\right) + (\omega - 1)\left(1 - \left(\frac{P}{P_o}\right)\right)\right]\right\}^{1/2}}{\omega\left(\frac{P_o}{P} - 1\right) + 1}\sqrt{\frac{P_o}{v_o}}$$

In this method is important to know the inlet conditions of the stagnation (subscript "o" at the equations) as well as the calculation of the physical parameters, like quality or void fraction, calculation of the ω-parameter and the critical pressure (Eq 26). And it is important to know to the initial liquid conditions, saturated or subcooled, because the calculation of the parameters is different (see in the API chapter).

4.3.- ISO

The ISO model *[21]* is based on the work of Diener and Schmidt *[34]* considering the boiling delay of the liquid. They proposed a boiling delay coefficient, N, based on the quality of the mass flow in the narrowest flow cross-section of the valve.

This is included to take into account the phenomenon of partial thermal equilibrium, which means that when the pressure in the safety valve is reduced a flicker occurs, such as an intermittence of the liquid that does not reach the thermodynamic equilibrium due to the short travel length.

- N=1 implies a complete equilibrium.
- N=0 implies that there is neither boiling nor frozen flow (the so-called "frozen flow" is obtained when the thermal insulation hypothesis is added, i.e. when there is no heat transfer between the phases).

The N factor depends on the pressure in the narrowest cross-section of the fluid which is easy to calculate since a first flow hypothesis is used. *[32]*

The ISO model and the HNE-DS model differ only by a factor to account for mechanical nonequilibrium (internal friction). Diener and Schmidt introduced the widely validated slip factor for non-flashing two-phase flows in the HNE-DS model (see below).

4.4.- HNE

Diener and Schmidt *[34]* introduced the slip factor for non-intermittent biphasic flows (HNE-DS model) and is only an extended omega method. This method was extended by one term to account for a boiling delay, not thermodynamic equilibrium and requires physical properties only in the stagnant condition. *[18]*

Non-homogeneous equilibrium models are mainly used in the case of small nozzles where the fluid residence time is too short for significant vaporization, for this model the flow equations are integrated with constant steam quality.

It can also be studied according to the HNE model developed by Henry and Fauske *[39]*, for which simplifications such as incompressible liquid phase supposition, constant liquid temperature or isotropic vaporization are used (Fauske´s model doesn´t include the effect of slip).

The Fauske model uses both the liquid flow from stagnation to saturation for subcooled inputs and the throttled or critical mass flow resulting from the phase change that occurs, as well as the liquid flow from saturation to discharge pressure. For throttled flows, the model discharge pressure is replaced by the throttle pressure. Also, the parameter is introduced for the non-equilibrium that represents the delayed flashing for lengths less than 10 cm, according to the studies of Fauske the flash is completed before the 10cm of the entry. *[34] [40] [41] [42].*

This model could be simplified in the next six equations:

$$Eq\ 14 \qquad \frac{G_C}{G_I} = \left[\frac{\frac{1}{N_{NE}} + \left(\frac{G_O}{G_I}\right)^2}{1+K_f}\right]^{\frac{1}{2}}$$

$$Eq\ 15 \quad N_{NE} = \left(\frac{G_I}{G_3}\right)^2 + \frac{L}{L_e}\ for\ L \leq L_e$$

$$Eq\ 16 \quad N_{NE} = 1\ for\ L > L_e$$

$$Eq\ 17 \quad G_O = \sqrt{2\rho_o(P_o - P_s)}$$

$$Eq\ 18 \quad G_I = \frac{h_{GLo}}{v_{GLo}\sqrt{T_o C_{p,Lo}}}$$

$$Eq\ 19 \quad G_3 = \sqrt{2\rho_o(P_s - P_2)}$$

G_C: two-phase mass flux

G_I: equilibrium rate

N_{NE}: nonequilibrium parameter

K_f: loss coefficient

L_e: equilibrium length = 10 cm

P_c: liquid density at stagnation condition

P_o: stagnation pressure

P_s: saturation pressure

h_{GLo}: heat of vaporization at stagnation conditions

v_{GLo}: specific volume of gas minus specific volume of liquid at stagnation conditions

T_o: stagnation temperature

$C_{p,Lo}$: specific heat of liquid at stagnation conditions

P_2: discharge pressure (choke pressure if flow is choked)

Numerous studies have been carried out to validate the HNE-DS model applied to initially subcooled liquids, which show that there is no unequivocal tendency in nozzle diameter and length and that very small deviations in mass flow quality result in large mass flow deviations with low subcooling so that experimental data often have a high degree of uncertainty.

The HNE-DS model studies were extended to the initially subcooled liquids by the non-equilibrium N coefficient which led to quite good results compared to the experimental data treated in the studies. in terms of subcooling under the HNE-DS model it is much better than the HEM-model, but it also can be applied for saturated inlet conditions

The model has two most important equations, similar to the HEM-model but with and extra parameter. The first is that of the omega parameter, ω, which is the same as the equation that describes the omega parameter in the homogeneous

model, only in this case it is multiplied by a N-parameter in the second term of the equation (see Eq 20 and Eq 21).

$$\omega = \frac{x_o v_{LGo}}{v_o k} + \frac{C_{Lo} T_o P_o}{v_o} \left(\frac{v_{LGo}}{h_{LGo}}\right)^2 * N \quad \text{Eq 20}$$

$$N = \left(x_o + C_{Lo} T_o P_o * \left(\frac{v_{LGo}}{h_{LGo}^2}\right) * Ln\left(\frac{1}{\eta_{cr}}\right)\right)^{0.4} \quad \text{Eq 21}$$

4.5.- API

API Standard 520 defines a pressure relief device as one that handles a liquid in vapour-liquid equilibrium or a mixed-phase fluid that will flash with steam generation as the fluid moves through it, in which steam generation must be considered as it can reduce effective mass flow capacity.

It should be aware that there are currently no pressure relief devices with certified capacities for biphasic flow as there are no test methods for certification. The effect of any self-cooling that may arise from the liquid flash should also be investigated to avoid flow blockage.

The document also shows that a pilot-operated or balanced pressure relief valve may be necessary when increased backpressure due to intermittent or two-phase flow conditions is excessive or cannot be adequately predicted. The actual flow through a device can be many times greater if nozzle equilibrium is not achieved.

It should be noted that the methods presented in the API document have not been validated by testing, nor is there any recognized procedure to certify the capability of pressure relief valves in a two-stage flow service.

Many different scenarios are possible in the general category of two-phase liquid/vapour relief. In all of these scenarios, a two-phase mixture is produced that enters the pressure relief valve or a two-phase mixture as the fluid moves through the valve. Steam generation as a result of flashing must be taken into account, as it can reduce, as mentioned above, the effective mass flow capacity of the valve. *[20]*

The methods presented in the document can be used to dimension pressure relief valves in two-phase liquid/vapour scenarios. Some of them can be used in the case of encountering a supercritical fluid in two-phase flow condensation.

Most are based on the Leung *[37]* omega method, but for high moment discharges from two-phase systems, thermal and mechanical equilibrium can be assumed. These assumptions correspond to the homogeneous equilibrium model (HEM).

The revised version of API 520 (2000) recommends a two-point ω-method; it considers all the different fluid inlet conditions (subcooled, saturated and biphasic), as well as evaluate the occurrence of critical conditions.

Due to the assumed hypotheses, the parameter ω is a function of the input conditions and thus the specific volume of the biphasic mixture is calculated at the input conditions and a pressure of 90% of the input pressure. (The API method consists of a HEM model based on a more rigorous treatment of the property data). *[20]*

Within the scenarios that the API collects can be found:

- Liquid and saturated steam enters the valve and flashes. No non-condensable gas is present and includes fluids above and below the thermodynamic equilibrium point in the two-phase condensation flow (scenario 1).

- Highly subcooled liquid and non-condensable gas, condensable vapour or both enter the valve and does not flash (scenario 1).

- Subcooled or saturated liquid enters the valve and flashes. No condensable vapour or non-condensable gas present (scenario 2).
- Non-condensable gas or condensable vapour and non-condensable gas and subcooled or saturated liquid, which enters the valve and flashes. Presence of non-condensable gas (scenario 3).

Depending on the scenario in which the system is found, different resolution methods will be used as shown below. *[22]*

4.5.1.- Scenario 1: Two-phase flashing or non-flashing flow

If the two-phase system has a saturated liquid and vapour and contain a noncondensable gas, it is a flashing flow; if the two-phase system has a highly subcooled liquid and either a noncondensable gas, condensable vapour or both, it is a non-flashing flow (fluids above and below the thermodynamic critical point can also be handled in the condensation of the two-phase flow). The main parameters for this method are:

1. Omega parameter ω.

For flashing multi-component systems with nominal boiling range less than 150°F or flashing single-component systems (must be far from its thermodynamic critical point $T_r \leq 0.9$ or $P_r \leq 0.5$, use either Eq 22 and Eq 23.

$$\text{Eq 22} \qquad \omega = \frac{x_o v_{vo}}{v_o}\left(1 - \frac{0.37 P_o v_{vlo}}{h_{vlo}}\right) + \frac{0.185 C_p T_o P_o}{v_o}\left(\frac{v_{vlo}}{h_{vlo}}\right)^2$$

$$\text{Eq 23} \qquad \omega = \frac{x_o v_{vo}}{v_o k} + \frac{0.185 C_p T_o P_o}{v_o}\left(\frac{v_{vlo}}{h_{vlo}}\right)^2$$

x_o: vapour mass fraction at the valve inlet.

v_{vo}: specific volume of the vapour at the valve inlet (ft^3/lb).

v_o: specific volume of the two-phase system at the valve inlet (ft^3/lb).

P_o: pressure at the valve inlet (psia) (valve set pressure (psig) plus the allowable overpressure (psi) plus atmospheric pressure).

v_{vlo}: difference between the vapour and liquid specific volumes at the valve inlet (ft^3/lb).

h_{vlo}: latent heat of vaporization at the valve inlet (Btu/lb) (for multi-component systems, h_{vlo} is the difference between the vapour and liquid specific enthalpies).

C_p: liquid specific heat at constant pressure at the PRV inlet (Btu/lb • R).

T_o: temperature at the valve inlet (R).

k: ratio of specific heats of the vapour (If the specific heat ratio is unknown, a value of 1.0 can be used).

Use Eq 24 for flashing multi-component systems with nominal boiling range greater than 150°F (single-component systems near the thermodynamic critical point, or supercritical fluids in condensing two-phase flow), and for nonflashing flow use Eq 25.

$$\text{Eq 24} \qquad \omega = 9\left(\frac{v_9}{v_o} - 1\right)$$

$$\text{Eq 25} \qquad \omega = \frac{x_o v_{vgo}}{v_o k}$$

v_9: specific volume evaluated at 90% of the valve inlet pressure P_o (ft^3/lb). When determining v_9, the flash calculation should be carried out isentropically, but an isenthalpic (adiabatic) flash is sufficient.

v_o: specific volume of the two-phase system at the valve inlet (ft^3/lb).

x_o: vapour, gas, or combined vapour and gas mass fraction at the valve iinlet.

v_{vgo}: specific volume of the vapour, gas or combined vapour and gas at the valve inlet (ft^3/lb).

v_o: specific volume of the two-phase system at the valve inlet (ft^3/lb).

k: ratio of specific heats of the vapour, gas or combined vapour and gas. If the specific heat ratio is unknown, a value of 1.0 can be used.

2. Critical or subcritical flow.

Pc as critical pressure (psia), calculated by $P_c = \eta_c P_o$ with η_c as critical pressure obtained from the following expression:

$$Eq\ 26 \qquad \eta_c^2 + (\omega^2 - 2\omega)(1-\eta_c)^2 + 2\omega^2 Ln\eta_c + 2\omega^2(1-\eta_c) = 0$$

and P_a as the downstream back pressure (psia).

So, if $P_c < P_a$ → critical flow; if $P_c < P_a$ → subcritical flow.

3. Mass flux.

In this parameter two distinctions are made, for critical flow Eq 27 and for subcritical flow Eq 28

$$Eq\ 27 \qquad G = 68.09\eta_c\sqrt{\frac{P_o}{v_o\omega}}$$

$$Eq\ 28 \qquad G = \frac{68.09\{-2[\omega Ln\eta_a + (\omega-1)(1-\eta_a)]\}^{1/2}}{\omega\left(\frac{1}{\eta_a}-1\right)+1}\sqrt{\frac{P_o}{v_o}}$$

G = mass flux ($lb/s \bullet ft^2$).

ηa = back pressure ratio (Pa/Po)

4. Area of the pressure relief valve.

To calculate the required effective discharge area (in^2) it is used the next equation:

$$Eq\ 29 \qquad A = \frac{0.04W}{K_d K_b K_c G}$$

W: mass flow rate (lb/hr)

Kd: discharge coefficient obtained from the valve manufacturer, usually the first estimation of Kd is 0.85.

Kb: back pressure correction factor for vapour obtained from the valve manufacturer, oly applies to balanced-bellow valves.

Kc: combination correction factor for installations with a rupture disk upsteam. Kc=1 without disk and Kc=0.9 with disk installed and does not exist a published value.

4.5.2.- Scenario 2: Subcooled liquid

This is used for subcooled or saturated liquid with no condensable vapour or gas at the inlet of the valve. Depending on the subcooling region in which the flow is located, the subcooled liquid flashes before or after the valve throat pressure. The main parameters are quite similar to those described in scenario 1.

1. Saturated Omega Parameter ω_s

With the same conditions as the below scenario, for multi-component systems with nominal boiling range less than 150°F or flashing single-component systems (must be far from its thermodynamic critical point $T_r \leq 0.9$ or $P_r \leq 0.5$, use Eq 30 and for multi-component systems with nominal boiling range greater than 150°F use the Eq 31.

$$\omega_s = 0.185\rho_{lo}C_pT_oP_s\left(\frac{v_{vls}}{h_{vls}}\right)^2 \quad \text{Eq 30}$$

ρ_{lo}: liquid density at the valve inlet (lb/ft^3).

Cp: liquid specific heat at constant pressure at the valve inlet (Btu/lb • R).

Ps: saturation vapour pressure corresponding to To (psia). For a multi-component system, use the bubble point pressure corresponding to To.

v_{vls}: difference between the vapour and liquid specific volumes at Ps (ft^3/lb).

h_{vls}: latent heat of vaporization at Ps (Btu/lb). For multi-component systems, h_{vls} is the difference between the vapour and liquid specific enthalpies at Ps.

$$\omega_s = 9\left(\frac{\rho_{lo}}{\rho_9} - 1\right) \quad \text{Eq 31}$$

ρ_9: density evaluated at 90% of the Ps corresponding to the valve inlet temperature To (lb/ft^3). For a multi-component system, use the bubble point pressure corresponding to To for Ps. When determining ρ_9, the flash calculation should be carried out isentropically, but an isenthalpic (adiabatic) flash is sufficient.

2. Subcooling region.

P_o as the pressure (psia) at the inlet of the valve and η_{st} as the transition saturation pressure ratio calculated by:

$$\eta_{st} = \frac{2\omega_s}{1+2\omega_s} \quad \text{Eq 32}$$

So if $P_s < P_o \cdot \eta_{st}$ → high subcooling region, flashing occurs at the throat, and if $P_s < P_o \cdot \eta_{st}$ → low subcooling region, flashing occurs upstream of throat.

3. Critical or subcritical flow.

Pc as critical pressure (psia), calculated by $P_c = \eta_c \cdot P_o$ with η_c as critical pressure obtained using η_s as P_s/P_o, and P_a as the downstream back pressure (psia).

So, for the low subcooling region, if $P_c > P_a$ → critical flow; if $P_c < P_a$ → subcritical flow; and for the high subcooling region if $P_s > P_a$ → critical flow; if $P_s < P_a$ → subcritical flow.

4. Max flux.

It is use Eq 33 for the low subcooling region, and if the flow is critical use η_c and for subcritical use η_a. Eq 34 is use in the high subcooling region, and if the flow is critical use P_s, and if the flow is subcritical use P_a (all terms have been described in the previous point).

$$Eq\ 33 \qquad G = \frac{68.09\{2(1-\eta_s)+2\left[\omega_s\eta_s Ln\left(\frac{\eta_s}{\eta}\right)-(\omega_s-1)(\eta_s-\eta)\right]\}^{1/2}}{\omega_s\left(\frac{\eta_s}{\eta}-1\right)+1}\sqrt{P_o\rho_{lo}}$$

$$Eq\ 34 \qquad G = 96.3[\rho_{lo}(P_o - P)]^{\frac{1}{2}}$$

5. Area of the pressure relief valve.

To calculate the required effective discharge area (in^2) it is used the next equation, only applicable to turbulent flow systems, the most two-phase scenarios will be within the turbulent flow regime (all terms have been described in the previous point).

$$Eq\ 35 \qquad A = 0.3208\frac{Q\rho_{lo}}{K_d K_b K_c G}$$

Q: volumetric flow rate (gal/min).

4.5.3.- Scenario 3: Flashing flow with noncondensable gas.

The method can be used for two-phase flashing flow with a noncondensable gas or both a condensable vapour and noncondensable gas. It is not valid when the solubility of the noncondensable gas in the liquid is appreciable (for these situations, the method presented in scenario 1 should be used). The term vapour will be used to refer to the condensable vapour and the term gas will be used to refer to the noncondensable gas.

1. Inlet void fraction α_o.

The void fraction can be calculated using the next equation:

$$Eq\ 36 \qquad \alpha_o = \frac{x_o v_{vgo}}{v_o}$$

x_o: gas or combined vapour and gas mass fraction at the valve inlet.

v_{vgo}: specific volume of the gas or combined vapour and gas at the valve inlet (ft^3/lb).

v_o: specific volume of the two-phase system at the valve inlet (ft^3/lb).

2. Omega parameter ω.

To calculate this parameter, Eq 37 will be used if the system contains less than 0.1% weight hydrogen, nominal boiling range less than 150ºF, P_{vo}/P_o less than 0.9 or P_{go}/P_o greater than 0.1 and $T_r \leq 0.9$ or $P_r \leq 0.5$ (**CASE 1**). And Eq 38 will be used if the system contains more than 0.1% weight hydrogen, nominal boiling range greater than 150ºF, P_{vo}/P_o greater than 0.9 or P_{go}/P_o less than 0.1 and $T_r \geq 0.9$ or $P_r \geq 0.5$ (**CASE 2**).

$$Eq\ 37 \qquad \omega = \frac{\alpha_o}{k} + 0.185(1-\alpha_o)\rho_{lo}C_pT_oP_s\left(\frac{v_{vlo}}{h_{vlo}}\right)^2$$

$$Eq\ 38 \qquad \omega = 9\left(\frac{v_9}{v_o} - 1\right)$$

P_{vo}: saturation pressure corresponding to the inlet temperature T_o (psia).

P_{go}: noncondensable gas partial pressure at the valve inlet (psia).

3. Critical or subcritical flow

For CASE 1:

Pc is critical pressure (psia) calculated like $[y_{gc}\cdot\eta_{gc}+(1-y_{go})\cdot\eta_{vc}]P_o$, and y_{go} is the inlet gas mole fraction in the vapour phase, determined using $y_{go}=P_{go}/P_o$. The term η_{gc} is nonflashing critical pressure ratio and η_{vc} is flashing critical pressure

So, if $P_c > P_a \Rightarrow$ critical flow and if $P_c < P_a \Rightarrow$ subcritical flow.

For CASE 2:

Pc as critical pressure (psia), calculated by $P_c = \eta_c P_o$ with η_c as critical pressure obtained from Eq 26.

and P_a as the downstream back pressure (psia).

So, if $P_c < P_a \rightarrow$ critical flow; if $P_c < P_a \rightarrow$ subcritical flow.

4. Mass flux.

For CASE 1:

Equation V will be used if the system has critical flow, and equations Eq 39, Eq 40 and Eq 41 will be used if the system has subcritical flow and G is calculated by equations Eq 42, Eq 43 and Eq 44.

$$Eq\ 39 \qquad G = 68.09\left[\frac{P_o}{v_o}\left(\frac{y_{go}\eta_{gc}^2 k}{\alpha_o} + \frac{(1-y_{go})\eta_{vc}^2}{\omega}\right)\right]^{\frac{1}{2}}$$

$$Eq\ 40 \qquad \eta_a = y_{go}\eta_g + (1-y_{go})\eta_v$$

$$Eq\ 41 \qquad \frac{\alpha_0}{k}\left(\frac{1}{\eta_g}-1\right) = \omega\left(\frac{1}{\eta_v}-1\right)$$

$$Eq\ 42 \qquad G = \left[y_{go}G_g^2 + (1-y_{go})G_v^2\right]^{\frac{1}{2}}$$

$$Eq\ 43 \qquad G_g = \frac{68.09\left\{-2\left[\frac{\alpha_o}{k}Ln\eta_g + \left(\frac{\alpha_o}{k}-1\right)(1-\eta_g)\right]\right\}^{\frac{1}{2}}}{\frac{\alpha_0}{k}\left(\frac{1}{\eta_g}-1\right)+1}\sqrt{\frac{P_o}{v_o}}$$

$$Eq\ 44 \qquad G_v = \frac{68.09\{-2[\omega Ln\eta_v + (\omega-1)(1-\eta_v)]\}^{\frac{1}{2}}}{\omega\left(\frac{1}{\eta_v}-1\right)+1}\sqrt{\frac{P_o}{v_o}}$$

η_g: nonflashing partial pressure ratio.

η_v: flashing partial pressure ratio.

G_g = nonflashing mass flux (lb/s ft^2).

G_v = flashing mass flux (lb/s ft^2).

For CASE 2:

Eq 45 will be used if the system has critical flow, and Eq 46 will be used if the system has subcritical flow.

$$Eq\ 45 \qquad G = 68.09\eta_c\sqrt{\frac{P_o}{\omega v_o}}$$

$$Eq\ 46 \qquad G = \frac{68.09\{-2[\omega Ln\eta_a + (\omega-1)(1-\eta_a)]\}^{\frac{1}{2}}}{\omega\left(\frac{1}{\eta_a}-1\right)+1}\sqrt{\frac{P_o}{v_o}}$$

5. Area of the pressure relief valve.

To calculate the required effective discharge area (in^2) it is used the next equation (all terms have been described in the previous point).

$$Eq\ 47 \qquad A = \frac{0.04W}{K_d K_b K_c G}$$

5. Experimental data

In order to carry out the analysis of the models, a series of experimental data have been used with which to work corresponding to a two-phase system consisting of liquid water and water steam through a commercial relief valve.

These data have been provided by the University of La Sapienza, Rome. The experiments carried out were aimed at measuring, not calculating, the different pressure parameters, both inlet, and outlet, as well as the mass flow through the valve during runs. Data have also been provided on the quality of the vapour in the mixture at the entrance of the system. The discharge coefficients given for the single liquid and vapour flow were K_v=0.85 and K_l=0.68 and the diameter of the reference area of the system is 10 mm.

The parameters provided next to their units are shown in the following table.

Table 2. Experimental data

PARAMETERS	UNITS	PAAMTERS	UNITS
P_{in}	bar	x_{in}	%
P_{out}	bar	φ	mm
Dp (P_{in}-P_{out})	bar	G_{exp}	Kg/s
η (P_{out}/P_{in})	Non-dimensional		

At the time of making all the calculations, the relevant unit changes have been made to work in the international system (see Table 3).

Table 3. S.I. Units

Cp_{lo}	J/kg K	x_{in}	%
ρ_l	kg/m^3	G_{exp}	kg/s
P_{in}	Pa	G_{steo}	kg/m^{2}s
φ	m	G_{theo}	kg/s
T@	K	R (G_{theo}/G_{exp})	Non-dimensional
ρ_v	kg/m^3		
v_g	m^3/kg	K_d (C_{exp}/G_{theo})	Non-dimensional
v_{lg}	m^3/kg		
v_o	m^3/kg	α	Non-dimensional
h_{fg}	J/kg	R_{gas}	kPaL/molK
ω	Non-dimensional	Area	m^2
P_{out}	Pa	MW	g/mol
η (P_{out}/P_{in})	Non-dimensional	Dp (P_{in}-P_{out})	Pa

Thanks to these data, the pertinent analyses will be able to be carried out to evaluate if any of the models proposed in the previous chapters can predict with greater certainty the behaviour of the system giving rise to a method to which the data can be adjusted to thus being able to predict future work with the liquid-water vapour mixture.

5.1.- Methods

In order to evaluate the data, only the homogenous models, HEM and HNE-DS that are two of the most common method to use, are going to be completely analysed. The other methods that have been briefly described in the report of this thesis have been ISO and API standards.

- ISO Standard and HNE-DS model are similar, differs only by one factor that takes into account mechanical non-equilibrium or internal friction, although both models have been validated by comparison with experimental data from literature from more than 2000 measurements made with safety valves of various sizes, in this case the flow is flashing (steam/water flow) so, the HNE-DS has been decided to be the representative to analyse and compare the data and no to use the ISO standard.

- At the API standard, the HEM model is proposed to be followed to analyse the data but based on a more rigorous treatment of the property data, and like HEM, does not take into account the thermodynamic and mechanical non-equilibriums. Due to HEM model is generally recognized as one of the best methodologies to use with two phase flow in relief devices, it was decided to carry out the analysis with it and not with API standard.

6. HEM model with experimental data

As explained above, this method can be applied to both flashing and non-flashing systems, to choked or non-choked flows and to two-phase input conditions, saturated or even subcooled; in this case the omega parameter, ω, only depends on the inlet flow conditions, which are obtained thanks to the experimental data provided.

It is one of the most widely used methodologies to analyse the two-phase flows in relief devices and for this reason, will begin analysing this model. According to the data provided at the inlet conditions, what is going to be assumed is that the two-phase flow system is flowing as a saturated mixture (Figure 16) since nothing suggests otherwise and the inlet vapour quality data is so close to the unit, so it will be assumed that the mixture is always saturated and not subcooled in these

first cases, so the parameters corresponding to temperature, densities, specific volumes, and enthalpies are going to be calculated from data tables, in this case, the tables corresponding to saturated liquid from the Cengel manual have been used. *[9]*

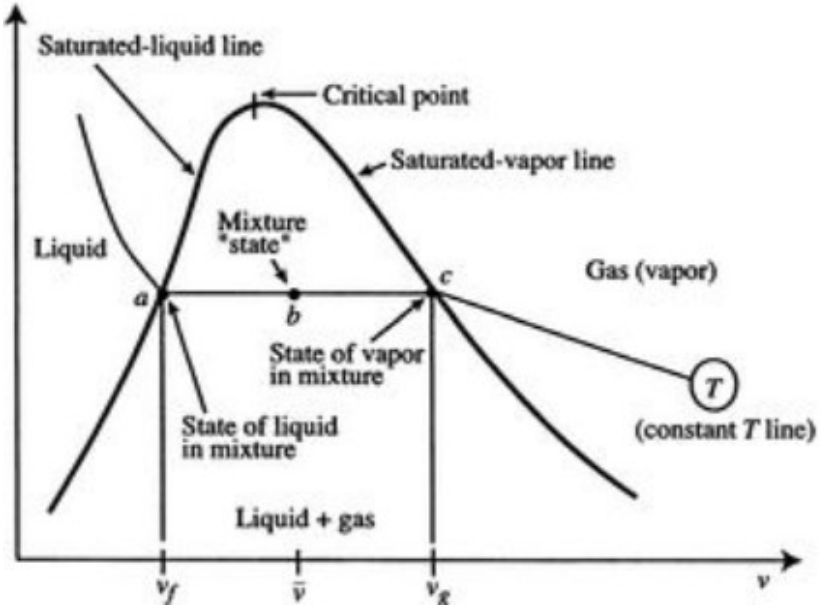

Figure 16. Behaviour of Two-Phase Systems [9].

As can be seen in Figure 16, the system can be found under different inlet conditions or states, like saturated mixture corresponding to the central zone of the diagram, subcooled liquid, corresponding to the left part of the diagram or also under critical conditions, the higher point of the saturated line at the diagram. In our case, the system is in the saturated region corresponding to the state of the mixture according to the assumptions assumed and the calculations carried out below (to identify if the system is under critical or subcooled inlet conditions). Due to this, some of the parameters to be used will be able to assume constants throughout the system such as liquid water density, because it changes quite short with the pressure, as well as liquid specific volume as it corresponds to the inverse of this density.

The specific heat capacity of the liquid, Cp, is also going to be assumed constant. The quantity of heat required to raise the temperature of 1 kg of water by 1 K is approximately 4,184 KJ. Therefore, the specific heat capacity of water is 4184 J/kgK.

Thanks to these assumptions the data corresponding to the temperature, specific volumes of the mixture and enthalpies will be able to be calculated directly by interpolation of the tables of the Cengel manual corresponding to the saturated liquid for each inlet pressure given in the experimental data. *[9]*

What will be compared in this analysis is the experimental mass flux rate provided with the theoretical mass flux rate calculated according to the homogeneous model. It is known from the literature that the most common is to find that the experimental one is usually smaller than the calculated one because when it is calculated theoretically, small errors in the installation or system are not consider; furthermore, this usually leads overdesigning of the pressure relief valves.

If the model did not predict fluid composition well, the calculation of the discharge coefficient will be necessary to correct any errors being made; this will be done in two situations:

- The most common $G_{theo} > G_{exp} \rightarrow K_d < 1$
- The least common but also possible $G_{theo} < G_{exp} \rightarrow K_d > 1$ if it is this case that will be found does not mean that the system is more but sometimes the fluids behave in different ways than expected, in both cases should analyse another method that is more appropriate for the data provided.

In general, for the calculation of the theoretical two-phase mass flow (steam/water in this case), the following steps are required:

1. Evaluation of stagnation input conditions, in this case, the data has already been calculated by previous experiments.
2. Calculation of the physical parameters (specific volumes, enthalpies, etc.) and the empty fraction, calculated from the tables in the Cengel manual and the equation next at this document. [9]
3. Calculation of the mass flux calculation according to Eq 13
4. It must be taken in account that the method is accurate only far from the critical point ($T_r \leq 0.9$ or $P_r \leq 0.5$).

6.1.- Theorical calculations of the HEM model

Following the steps mentioned above, the system inlet parameters will be searched and calculated according to the following equations. Table 4 shows the parameters that have been considered constant due to the assumptions assumed.

Table 4. Constant parameters

CONSTANT PARAMETERS		
ρ_l	998	kg/m^3
v_l	0.001	m^3/kg
R_{gas}	8.314	kPaL/molK
MW H_2O	18	g/mol
Cp_{lo}	4184	J/kg K
Area	7.854E-05	m^2
ϕ	0.01	m
r	0.005	m
K_l	0.68	-
K_v	0.85	-

Eq 48 $$v_o = v_g x_{in} + (1 - x_{in}) v_l$$

Eq 49 $$v_{lg} = v_g - v_l$$

Eq 50 $$\alpha = \frac{x_{in}}{x_{in} + \frac{(1-x_{in})\rho_G}{\rho_L}}$$

Eq 51 $$\rho_g = \frac{MWP_{in}}{R_{gas} T_o}$$

Eq 52 $$T_o = Tsat = T@$$

Eq 53 $$A = \pi * r^2$$

$$Eq\ 54 \quad G_{teo} = G_{steo} * A$$

$$Eq\ 55 \quad \omega = \frac{x_o v_{LGo}}{v_o k} + \frac{C_{Lo} T_o P_o}{v_o} \left(\frac{v_{LGo}}{h_{LGo}}\right)^2$$

The other parameters have been calculated by interpolating the data with the tables of saturated liquid with Eq 56 and the ω-parameters, void fraction, specific mass flux (G_{stheo}), equations Eq 10, Eq 12 and Eq 13 have been followed.

$$Eq\ 56 \quad y = \frac{(x - x_1)}{(x_2 - x_1)} (y_2 - y_1) + y_1$$

y: value to calculate

x1, x2, y1, y2: data of the table

x: given value

Figure 17 shows a graphic linear interpolation of known data points, given the two red points, the line is the linear interpolating between the points, and “y” is the value at “x” that must be found.

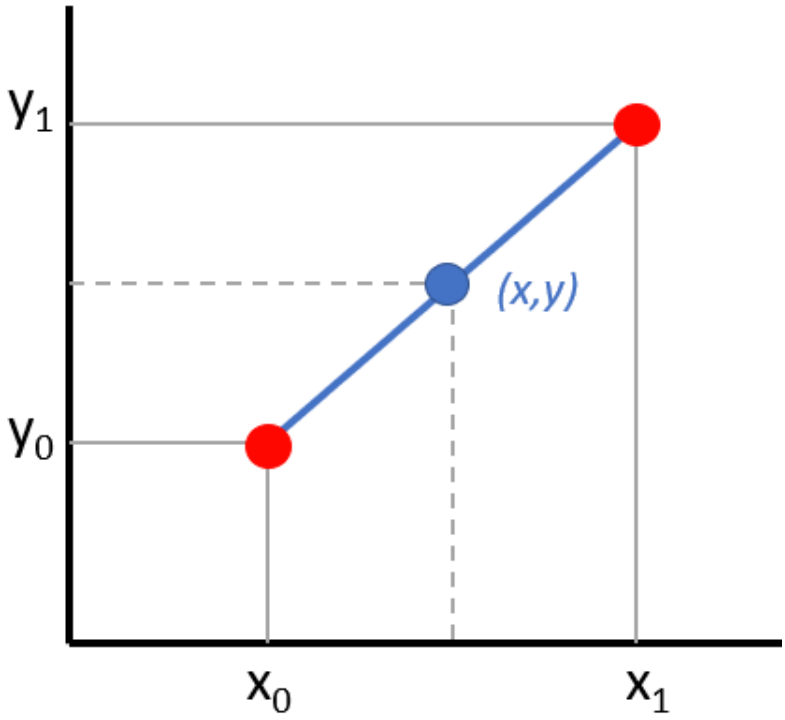

Figure 17. Linear interpolation

Once the parameters and the inlet conditions have been calculated, the analysis will be proceeded in which state the system with which we are dealing is, the hypothesis of saturated mixture has been assumed, but to verify it has been decided to calculate the critical pressure ratio. This relationship is calculated using the following implicit equation:

$$\text{Eq 57} \quad \eta_c^2 + (\omega^2 - 2\omega)(1-\eta_c)^2 + 2\omega^2 Ln\,\eta_c + 2\omega^2(1-\eta_c) = 0$$

To solve it, the SOLVER tool belonging to the excel program, with which the relevant calculations are being made, has been used. In all cases it is obtained that the initial inlet pressure is greater than the critical pressure obtained, according to the Eq 58, which leads us to think that the system is not in conditions of critical flow, so no modification is necessary to the raised model.

(See Table 5)

$$\text{Eq 58} \quad \eta_c = \frac{P_c}{P_o}$$

Table 5. Critical ratio for the experimental data

Pin	Pout	η	Dp	xin	Gexp	**η crit**	Pin	Pout	η	Dp	xin	Gexp	**η crit**
bar	bar	-	bar	%	kg/s		bar	bar	-	bar	%	kg/s	
4.93	4.71	0.96	0.21	0.93	0.21	0.87	4.93	4.60	0.93	0.33	4.90	0.14	0.71
7.56	6.61	0.87	0.95	0.97	0.42	0.82	7.49	7.25	0.97	0.25	4.94	0.14	0.72
9.98	9.46	0.95	0.52	0.99	0.35	0.82	7.47	6.83	0.92	0.63	4.95	0.21	0.72
4.94	4.48	0.91	0.46	1.01	0.28	0.82	5.07	4.05	0.80	1.02	4.97	0.21	0.71
17.53	17.26	0.98	0.27	1.01	0.28	0.81	10.03	9.82	0.98	0.22	5.00	0.14	0.72
10.00	9.67	0.97	0.33	0.98	0.28	0.82	12.48	11.61	0.93	0.88	4.98	0.28	0.72
7.51	7.16	0.95	0.35	0.99	0.28	0.82	7.56	6.17	0.82	1.38	4.99	0.28	0.72
4.91	4.01	0.82	0.90	0.99	0.35	0.82	15.06	13.76	0.91	1.30	5.02	0.35	0.72
17.55	16.91	0.96	0.64	1.01	0.42	0.81	9.97	9.44	0.95	0.53	5.02	0.21	0.72
14.92	14.63	0.98	0.30	1.00	0.28	0.81	17.50	17.14	0.98	0.37	5.00	0.21	0.73
7.51	6.91	0.92	0.61	1.01	0.35	0.82	12.56	10.12	0.81	2.44	5.02	0.41	0.72
14.93	14.44	0.97	0.49	1.02	0.35	0.81	14.93	14.20	0.95	0.73	5.02	0.27	0.72
12.48	11.72	0.94	0.76	1.04	0.42	0.81	9.99	8.95	0.90	1.04	5.00	0.28	0.72
12.53	12.04	0.96	0.50	1.04	0.35	0.81	10.06	8.17	0.81	1.90	5.04	0.35	0.72
12.44	12.11	0.97	0.32	1.04	0.28	0.81	12.53	11.05	0.88	1.49	5.05	0.35	0.72
9.89	9.03	0.91	0.85	1.04	0.42	0.81	12.51	12.05	0.96	0.45	5.05	0.21	0.72
17.54	17.08	0.97	0.46	1.10	0.35	0.81	14.99	14.58	0.97	0.41	5.11	0.21	0.72
4.99	3.77	0.76	1.21	1.32	0.35	0.80	17.60	16.47	0.94	1.12	5.14	0.35	0.72
5.04	3.55	0.70	1.49	1.54	0.35	0.79	17.41	16.71	0.96	0.70	5.12	0.28	0.72
12.43	12.00	0.97	0.43	1.94	0.28	0.78	17.54	15.77	0.90	1.77	5.21	0.42	0.72
7.46	7.18	0.96	0.28	1.97	0.21	0.78	7.50	5.32	0.71	2.17	6.67	0.28	0.70
14.99	14.59	0.97	0.39	1.96	0.28	0.78	4.99	3.21	0.64	1.79	6.85	0.21	0.69
4.99	4.16	0.83	0.83	1.95	0.28	0.77	15.06	13.94	0.93	1.12	8.04	0.27	0.70
9.97	9.71	0.97	0.26	1.98	0.21	0.78	17.45	14.47	0.83	2.98	8.54	0.41	0.70
7.47	6.92	0.93	0.56	2.00	0.28	0.78	7.38	5.94	0.81	1.43	9.46	0.21	0.68
4.87	4.53	0.93	0.34	1.82	0.21	0.78	12.51	10.83	0.87	1.68	9.30	0.28	0.69
7.54	5.63	0.75	1.90	2.00	0.42	0.78	4.97	4.18	0.84	0.80	9.74	0.14	0.67
14.94	14.72	0.99	0.22	2.00	0.21	0.78	5.04	4.82	0.96	0.22	9.88	0.08	0.67
14.98	14.32	0.96	0.66	2.00	0.35	0.78	7.58	7.05	0.93	0.52	9.88	0.14	0.68
17.46	16.87	0.97	0.59	1.99	0.35	0.78	7.42	6.89	0.93	0.53	9.88	0.14	0.68
12.48	11.43	0.92	1.06	2.02	0.42	0.78	17.58	16.92	0.96	0.66	9.89	0.21	0.69
17.47	17.27	0.99	0.21	2.03	0.21	0.78	17.53	16.87	0.96	0.66	9.95	0.21	0.69
17.46	17.09	0.98	0.38	2.04	0.28	0.78	12.65	10.95	0.87	1.70	9.60	0.28	0.69
12.48	12.24	0.98	0.24	2.03	0.21	0.78	17.48	16.21	0.93	1.28	9.93	0.28	0.69
9.94	8.59	0.86	1.35	2.05	0.42	0.78	10.00	8.91	0.89	1.09	9.94	0.21	0.68
7.51	6.49	0.86	1.02	2.04	0.35	0.77	17.53	17.25	0.98	0.28	9.97	0.14	0.69
10.03	9.24	0.92	0.79	1.98	0.35	0.78	10.00	9.57	0.96	0.43	9.96	0.14	0.68
12.42	11.71	0.94	0.71	2.06	0.35	0.78	12.55	12.20	0.97	0.35	9.98	0.14	0.68
17.46	16.57	0.95	0.89	2.07	0.42	0.78	15.03	14.72	0.98	0.31	10.00	0.14	0.69
9.96	9.47	0.95	0.49	2.07	0.28	0.78	12.60	11.73	0.93	0.87	9.99	0.21	0.68
7.62	5.07	0.66	2.56	2.49	0.42	0.76	15.07	14.32	0.95	0.75	10.02	0.21	0.68
5.07	3.65	0.72	1.42	2.93	0.28	0.75	10.01	7.57	0.76	2.44	10.04	0.28	0.68
7.46	5.35	0.72	2.10	3.73	0.35	0.74	17.53	15.33	0.87	2.19	10.08	0.35	0.69

Once it is known that the system is not under a critical flow, it must be verified that it is not under a choked flow regime, which is checked with the backpressure (P_b) measured downstream (experimental data). In this case $P_b > P_c$ so the flux is not strangled and the specific mass flux rate can be calculated from Eq 13.

In addition, the calculations are being performed according to the omega model, which can only be used below the critical point, which is fulfilled since it is obtained for all experiments given that $T_o / T_c < 0.9$ and $P_o / P_c < 0.5$ being $T_c = 647.3$ K and $P_c = 220.5$ bars.

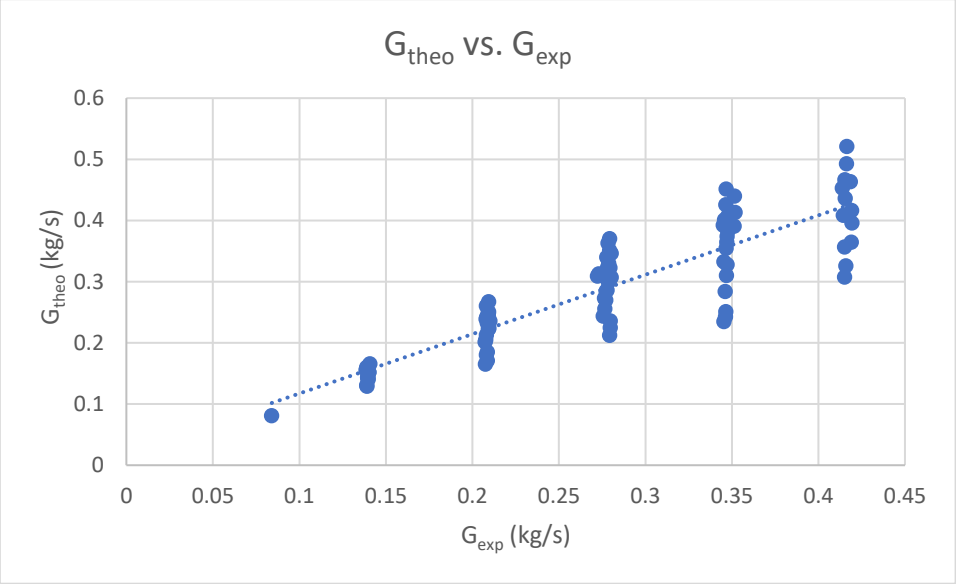

Graph 1. G_{theo} versus G_{exp}

When analysing the data, it has begun by comparing the experimental mass flux provided and the theoretical mass flux calculated by the model. As can be seen in Graph 1, the data follow a linear tendency although the calculated data does not have exactly the same values as the experimental ones. The following graphs show the experimental versus theoretical mass flux for different ranks of initial pressures given, corresponding to the following intervals:

- ➔ 4-6 bar: Rank 1
- ➔ 7-9-11 bar: Rank 2
- ➔ 12-15 bar: Rank 3
- ➔ 15-18 bar: Rank 4

In these graphs the linear tendency of the data can be seen more clearly, the fact that the data does not exactly coincide suggests that the model needs a K_d, discharge coefficient, to make the model a better prediction and thus be able to take into account the differences between the ideal flow through an ideal nozzle and the actual flow through a real valve, the calculation process of this parameter will be further advanced. To complement the graphs, the following tables show the results of the calculations made with excel to analyse the system.

Table 6. Data for Rank 1

P_{in}	T@	ρ_{gas}	v_g	v_{lg}	v_o	h_{fg}	ω	P_{out}	η	Dp	x_{in}	G_{exp}	G_{theo}	R
Pa	K	kg/m³	m³/kg	m³/kg	m³/kg	J/kg	-	Pa	-	Pa	-	kg/s	kg/s	-
4.93E+05	424.41	2.51	0.38	0.38	0.005	1.47E+06	13.64	4.71E+05	0.96	0.21	0.009	0.21	0.17	0.82
4.94E+05	424.52	2.52	0.38	0.38	0.005	2.11E+06	6.64	4.48E+05	0.91	0.46	0.010	0.28	0.24	0.84
4.91E+05	424.27	2.51	0.38	0.38	0.005	2.11E+06	6.73	4.01E+05	0.82	0.90	0.010	0.35	0.25	0.72
4.99E+05	424.87	2.54	0.38	0.37	0.006	2.11E+06	5.54	3.77E+05	0.76	1.21	0.013	0.35	0.24	0.70
5.04E+05	425.29	2.57	0.37	0.37	0.007	2.11E+06	5.00	3.55E+05	0.70	1.49	0.015	0.35	0.23	0.68
4.99E+05	424.89	2.54	0.38	0.37	0.008	2.11E+06	4.25	4.16E+05	0.83	0.83	0.019	0.28	0.22	0.80
4.87E+05	423.98	2.49	0.38	0.38	0.008	2.11E+06	4.45	4.53E+05	0.93	0.34	0.018	0.21	0.18	0.89
4.93E+05	424.43	2.51	0.38	0.38	0.020	2.11E+06	2.39	4.60E+05	0.93	0.33	0.049	0.14	0.13	0.93
5.07E+05	425.49	2.58	0.37	0.37	0.019	2.11E+06	2.38	4.05E+05	0.80	1.02	0.050	0.21	0.18	0.87
4.99E+05	424.94	2.54	0.38	0.37	0.027	2.11E+06	2.01	3.21E+05	0.64	1.79	0.068	0.21	0.16	0.79
4.97E+05	424.76	2.53	0.38	0.38	0.038	2.11E+06	1.72	4.18E+05	0.84	0.80	0.097	0.14	0.13	0.94
5.04E+05	425.27	2.57	0.37	0.37	0.038	2.11E+06	1.71	4.82E+05	0.96	0.22	0.099	0.08	0.08	0.96

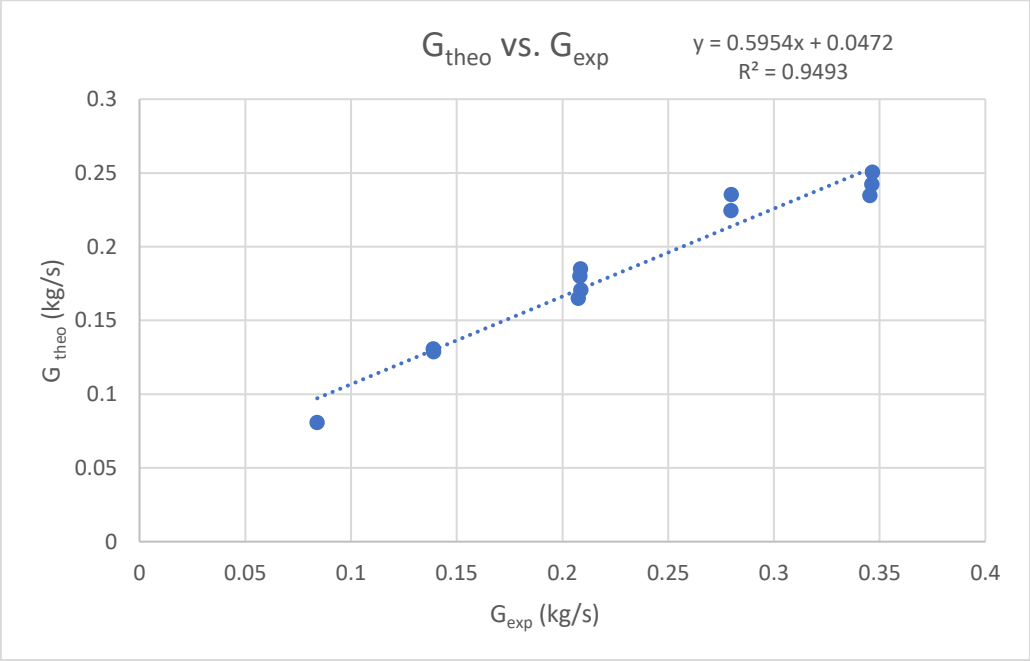

Graph 2. G_{theo} versus G_{exp} in Rank 1

Table 7. Data for Rank 2

P_{in}	T@	ρ_{gas}	v_g	v_{lg}	v_o	h_{fg}	ω	P_{out}	η	Dp	x_{in}	G_{exp}	G_{theo}	R
Pa	K	kg/m^3	m^3/kg	m^3/kg	m^3/kg	J/kg	-	Pa	-	Pa	-	kg/s	kg/s	-
7.56E+05	441.22	3.71	0.25	0.25	0.003	2.06E+06	6.84	661024.00	0.87	0.95	0.010	0.42	0.36	0.86
9.98E+05	452.94	4.77	0.19	0.19	0.003	2.01E+06	6.65	945561.00	0.95	0.52	0.010	0.35	0.37	1.08
1.00E+06	453.01	4.78	0.19	0.19	0.003	2.01E+06	6.70	966750.00	0.97	0.33	0.010	0.28	0.32	1.16
7.51E+05	440.94	3.69	0.26	0.25	0.004	2.06E+06	6.75	715629.00	0.95	0.35	0.010	0.28	0.28	1.03
7.51E+05	440.97	3.69	0.26	0.25	0.004	2.06E+06	6.66	690704.00	0.92	0.61	0.010	0.35	0.33	0.94
9.89E+05	452.53	4.73	0.20	0.20	0.003	2.02E+06	6.45	903321.00	0.91	0.85	0.010	0.42	0.42	0.99
7.46E+05	440.67	3.66	0.26	0.26	0.006	2.06E+06	4.36	717963.00	0.96	0.28	0.020	0.21	0.21	1.02
9.97E+05	452.89	4.76	0.19	0.19	0.005	2.02E+06	4.40	971103.00	0.97	0.26	0.020	0.21	0.24	1.12
7.47E+05	440.76	3.67	0.26	0.26	0.006	2.06E+06	4.32	691638.00	0.93	0.56	0.020	0.28	0.27	0.97
7.54E+05	441.09	3.70	0.25	0.25	0.006	2.06E+06	4.32	563354.00	0.75	1.90	0.020	0.42	0.33	0.78
9.94E+05	452.76	4.75	0.20	0.19	0.005	2.02E+06	4.32	859143.00	0.86	1.35	0.020	0.42	0.40	0.94
7.51E+05	440.97	3.69	0.26	0.25	0.006	2.06E+06	4.26	649186.00	0.86	1.02	0.020	0.35	0.31	0.89
9.96E+05	452.84	4.76	0.20	0.19	0.005	2.02E+06	4.29	946723.00	0.95	0.49	0.021	0.28	0.30	1.07
7.62E+05	441.56	3.74	0.25	0.25	0.007	2.05E+06	3.76	506801.00	0.66	2.56	0.025	0.42	0.31	0.74
1.01E+06	453.27	4.80	0.19	0.19	0.009	2.01E+06	2.88	725592.00	0.72	2.80	0.040	0.42	0.36	0.87
7.49E+05	440.87	3.68	0.26	0.25	0.014	2.06E+06	2.49	724841.00	0.97	0.25	0.049	0.14	0.14	1.00
7.47E+05	440.71	3.67	0.26	0.26	0.014	2.06E+06	2.48	683170.00	0.92	0.63	0.050	0.21	0.21	0.99
1.00E+06	453.17	4.79	0.19	0.19	0.011	2.01E+06	2.54	981889.00	0.98	0.22	0.050	0.14	0.15	1.08
7.56E+05	441.21	3.71	0.25	0.25	0.014	2.06E+06	2.48	617408.00	0.82	1.38	0.050	0.28	0.26	0.92
9.97E+05	452.91	4.77	0.19	0.19	0.011	2.02E+06	2.54	944194.00	0.95	0.53	0.050	0.21	0.22	1.07
9.99E+05	452.97	4.77	0.19	0.19	0.011	2.01E+06	2.54	894757.00	0.90	1.04	0.050	0.28	0.29	1.03
1.01E+06	453.29	4.81	0.19	0.19	0.011	2.01E+06	2.53	816557.00	0.81	1.90	0.050	0.35	0.33	0.96
7.50E+05	440.89	3.68	0.26	0.25	0.018	2.06E+06	2.12	532432.00	0.71	2.17	0.067	0.28	0.24	0.88
7.38E+05	440.21	3.63	0.26	0.26	0.025	2.06E+06	1.80	594409.00	0.81	1.43	0.095	0.21	0.20	0.97
7.58E+05	441.31	3.72	0.25	0.25	0.026	2.06E+06	1.77	705474.00	0.93	0.52	0.099	0.14	0.14	1.03
7.42E+05	440.46	3.65	0.26	0.26	0.026	2.06E+06	1.77	688911.00	0.93	0.53	0.099	0.14	0.14	1.03
1.00E+06	453.04	4.78	0.19	0.19	0.020	2.01E+06	1.81	891490.00	0.89	1.09	0.099	0.21	0.22	1.06
1.00E+06	453.01	4.78	0.19	0.19	0.020	2.01E+06	1.81	956956.00	0.96	0.43	0.100	0.14	0.15	1.08
1.00E+06	453.07	4.78	0.19	0.19	0.020	2.01E+06	1.81	757090.00	0.76	2.44	0.100	0.28	0.27	0.99

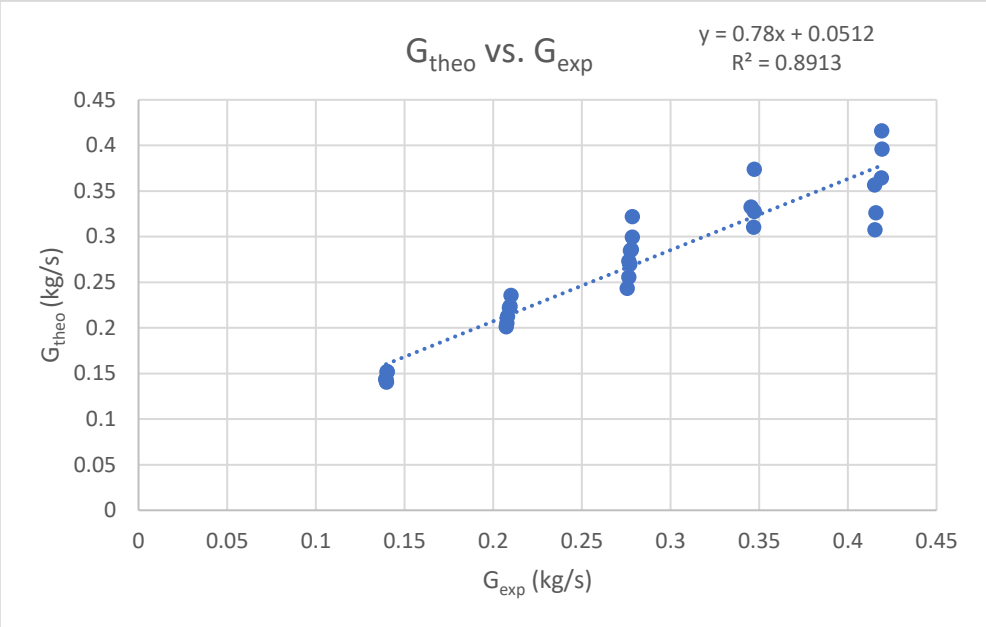

Graph 3. G_{theo} versus G_{exp} in Rank 2

Table 8. data for Rank 3

P_{in}	T@	ρ_{gas}	v_g	v_{lg}	v_o	h_{fg}	ω	P_{out}	η	Dp	x_{in}	G_{exp}	G_{theo}	R
Pa	K	kg/m³	m³/kg	m³/kg	m³/kg	J/kg	-	Pa	-	Pa	-	kg/s	kg/s	-
1.49E+06	471.19	6.86	0.13	0.13	0.002	1.95E+06	6.36	1.46E+06	0.98	0.30	0.010	0.28	0.36	1.30
1.49E+06	471.20	6.86	0.13	0.13	0.002	1.95E+06	6.30	1.44E+06	0.97	0.49	0.010	0.35	0.44	1.25
1.25E+06	462.84	5.84	0.16	0.16	0.003	1.98E+06	6.37	1.17E+06	0.94	0.76	0.010	0.42	0.46	1.11
1.25E+06	463.05	5.86	0.16	0.16	0.003	1.98E+06	6.37	1.20E+06	0.96	0.50	0.010	0.35	0.41	1.17
1.24E+06	462.70	5.82	0.16	0.16	0.003	1.98E+06	6.36	1.21E+06	0.97	0.32	0.010	0.28	0.35	1.24
1.24E+06	462.66	5.81	0.16	0.16	0.004	1.98E+06	4.49	1.20E+06	0.97	0.43	0.019	0.28	0.32	1.15
1.50E+06	471.40	6.88	0.13	0.13	0.004	1.95E+06	4.47	1.46E+06	0.97	0.39	0.020	0.28	0.34	1.22
1.49E+06	471.24	6.86	0.13	0.13	0.004	1.95E+06	4.41	1.47E+06	0.99	0.22	0.020	0.21	0.26	1.25
1.50E+06	471.36	6.88	0.13	0.13	0.004	1.95E+06	4.41	1.43E+06	0.96	0.66	0.020	0.35	0.41	1.17
1.25E+06	462.87	5.84	0.16	0.16	0.004	1.98E+06	4.39	1.14E+06	0.92	1.06	0.020	0.42	0.44	1.05
1.25E+06	462.85	5.84	0.16	0.16	0.004	1.98E+06	4.37	1.22E+06	0.98	0.24	0.020	0.21	0.25	1.19
1.24E+06	462.64	5.81	0.16	0.16	0.004	1.98E+06	4.33	1.17E+06	0.94	0.71	0.021	0.35	0.38	1.10
1.25E+06	462.87	5.84	0.16	0.16	0.009	1.98E+06	2.60	1.16E+06	0.93	0.88	0.050	0.28	0.31	1.09
1.26E+06	463.14	5.87	0.16	0.16	0.009	1.98E+06	2.60	1.01E+06	0.81	2.44	0.050	0.41	0.41	0.99
1.49E+06	471.21	6.86	0.13	0.13	0.008	1.95E+06	2.63	1.42E+06	0.95	0.73	0.050	0.27	0.31	1.15
1.25E+06	463.06	5.86	0.16	0.16	0.009	1.98E+06	2.59	1.10E+06	0.88	1.49	0.050	0.35	0.36	1.05
1.25E+06	462.95	5.85	0.16	0.16	0.009	1.98E+06	2.58	1.21E+06	0.96	0.45	0.050	0.21	0.23	1.12
1.50E+06	471.40	6.88	0.13	0.13	0.008	1.95E+06	2.61	1.46E+06	0.97	0.41	0.051	0.21	0.24	1.16
1.25E+06	462.97	5.85	0.16	0.16	0.016	1.98E+06	1.91	1.08E+06	0.87	1.68	0.093	0.28	0.30	1.08
1.27E+06	463.48	5.91	0.16	0.15	0.016	1.98E+06	1.88	1.09E+06	0.87	1.70	0.096	0.28	0.30	1.08
1.25E+06	463.10	5.86	0.16	0.16	0.017	1.98E+06	1.85	1.22E+06	0.97	0.35	0.100	0.14	0.16	1.12
1.26E+06	463.29	5.89	0.16	0.16	0.016	1.98E+06	1.85	1.17E+06	0.93	0.87	0.100	0.21	0.23	1.11

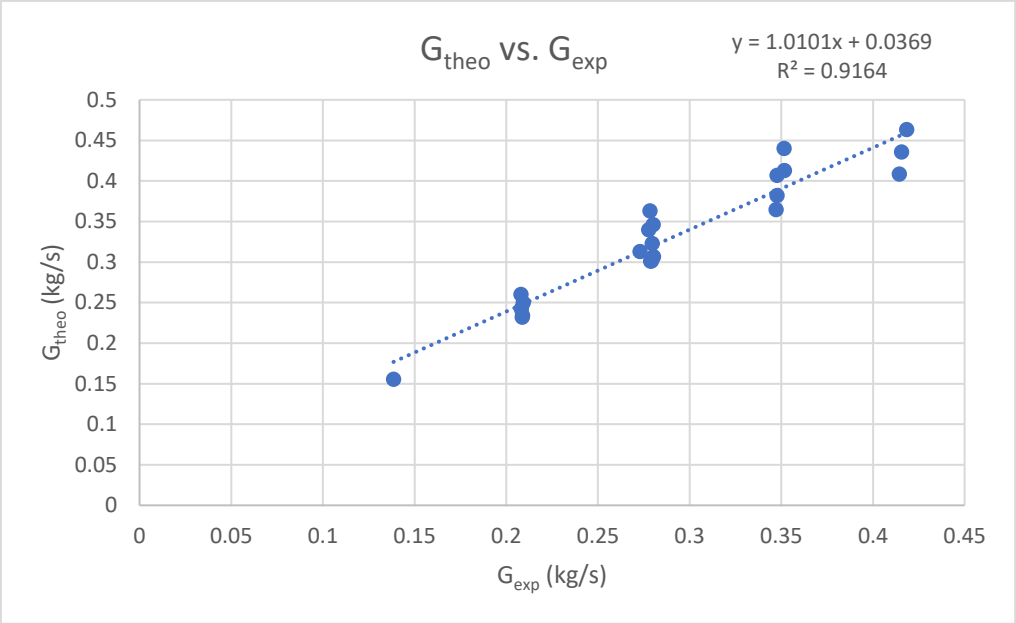

Graph 4. G_{theo} versus G_{exp} in Rank 3

Table 9. Data for Rank 4

P_{in}	T@	ρ_{gas}	v_g	v_{lg}	v_o	h_{fg}	ω	P_{out}	η	Dp	x_{in}	G_{exp}	G_{theo}	R
Pa	K	kg/m³	m³/kg	m³/kg	m³/kg	J/kg	-	Pa	-	Pa	-	kg/s	kg/s	-
1.75E+06	478.96	7.92	0.11	0.11	0.002	1.92E+06	6.18	1.73E+06	0.98	0.27	0.010	0.28	0.37	1.33
1.75E+06	479.00	7.93	0.11	0.11	0.002	1.92E+06	6.18	1.69E+06	0.96	0.64	0.010	0.42	0.52	1.25
1.75E+06	478.98	7.93	0.11	0.11	0.002	1.92E+06	5.93	1.71E+06	0.97	0.46	0.011	0.35	0.45	1.30
1.75E+06	478.75	7.89	0.11	0.11	0.003	1.92E+06	4.41	1.69E+06	0.97	0.59	0.020	0.35	0.43	1.23
1.75E+06	478.80	7.90	0.11	0.11	0.003	1.92E+06	4.36	1.73E+06	0.99	0.21	0.020	0.21	0.27	1.27
1.75E+06	478.76	7.90	0.11	0.11	0.003	1.92E+06	4.36	1.71E+06	0.98	0.38	0.020	0.28	0.35	1.26
1.75E+06	478.75	7.90	0.11	0.11	0.003	1.92E+06	4.32	1.66E+06	0.95	0.89	0.021	0.42	0.49	1.18
1.51E+06	471.62	6.91	0.13	0.13	0.008	1.95E+06	2.63	1.38E+06	0.91	1.30	0.050	0.35	0.39	1.11
1.75E+06	478.88	7.91	0.11	0.11	0.007	1.92E+06	2.67	1.71E+06	0.98	0.37	0.050	0.21	0.25	1.20
1.76E+06	479.12	7.95	0.11	0.11	0.007	1.92E+06	2.63	1.65E+06	0.94	1.12	0.051	0.35	0.40	1.16
1.74E+06	478.59	7.87	0.11	0.11	0.007	1.92E+06	2.64	1.67E+06	0.96	0.70	0.051	0.28	0.33	1.18
1.75E+06	478.98	7.93	0.11	0.11	0.007	1.92E+06	2.61	1.58E+06	0.90	1.77	0.052	0.42	0.47	1.12
1.51E+06	471.62	6.91	0.13	0.13	0.011	1.95E+06	2.07	1.39E+06	0.93	1.12	0.080	0.27	0.31	1.13
1.74E+06	478.72	7.89	0.11	0.11	0.011	1.92E+06	2.04	1.45E+06	0.83	2.98	0.085	0.41	0.45	1.09
1.76E+06	479.07	7.94	0.11	0.11	0.012	1.92E+06	1.91	1.69E+06	0.96	0.66	0.099	0.21	0.25	1.17
1.75E+06	478.96	7.93	0.11	0.11	0.012	1.92E+06	1.91	1.69E+06	0.96	0.66	0.099	0.21	0.25	1.17
1.75E+06	478.82	7.90	0.11	0.11	0.012	1.92E+06	1.91	1.62E+06	0.93	1.28	0.099	0.28	0.32	1.16
1.75E+06	478.95	7.92	0.11	0.11	0.012	1.92E+06	1.91	1.72E+06	0.98	0.28	0.100	0.14	0.17	1.18
1.50E+06	471.52	6.90	0.13	0.13	0.014	1.95E+06	1.88	1.47E+06	0.98	0.31	0.100	0.14	0.16	1.15
1.51E+06	471.64	6.92	0.13	0.13	0.014	1.95E+06	1.88	1.43E+06	0.95	0.75	0.100	0.21	0.24	1.15
1.75E+06	478.94	7.92	0.11	0.11	0.012	1.92E+06	1.90	1.53E+06	0.87	2.19	0.101	0.35	0.39	1.14

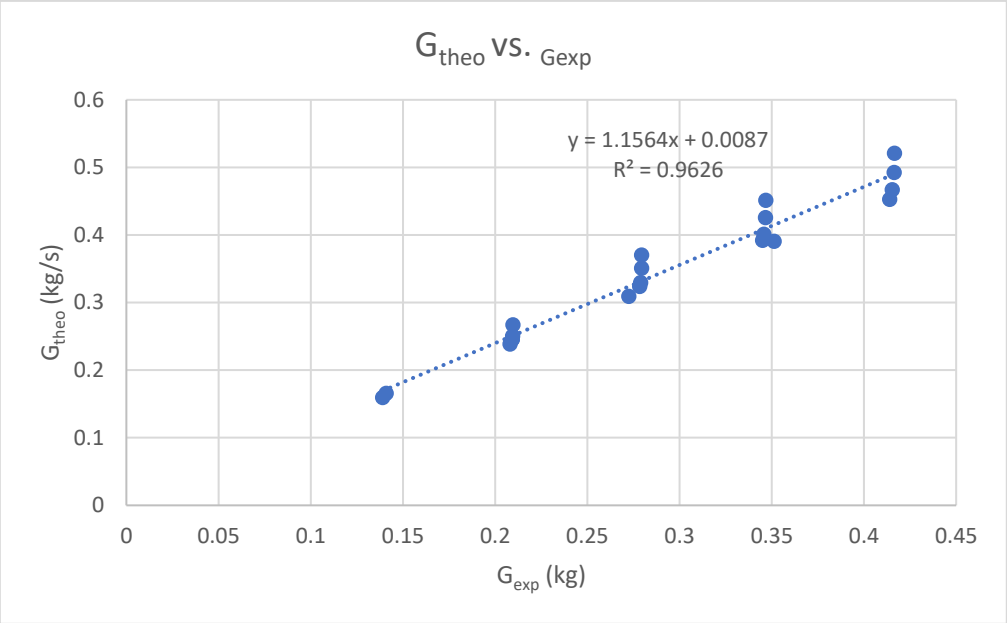

Graph 5. G_{theo} versus G_{exp} in Rank 4

As has been done previously in the literature, it has been decided to adopt the mass flux ratio, R (G_{theo}/G_{exp}), in order to analyse the results. In this case, different representations of this value have been made based on various parameters such as the inlet vapour quality, the inlet pressure or the pressure ratio, using the initial pressure Pin in the ranks described above as the input parameter.

The following graphs show the relationship between R and inlet vapour quality for all pressures and for the different ranks.

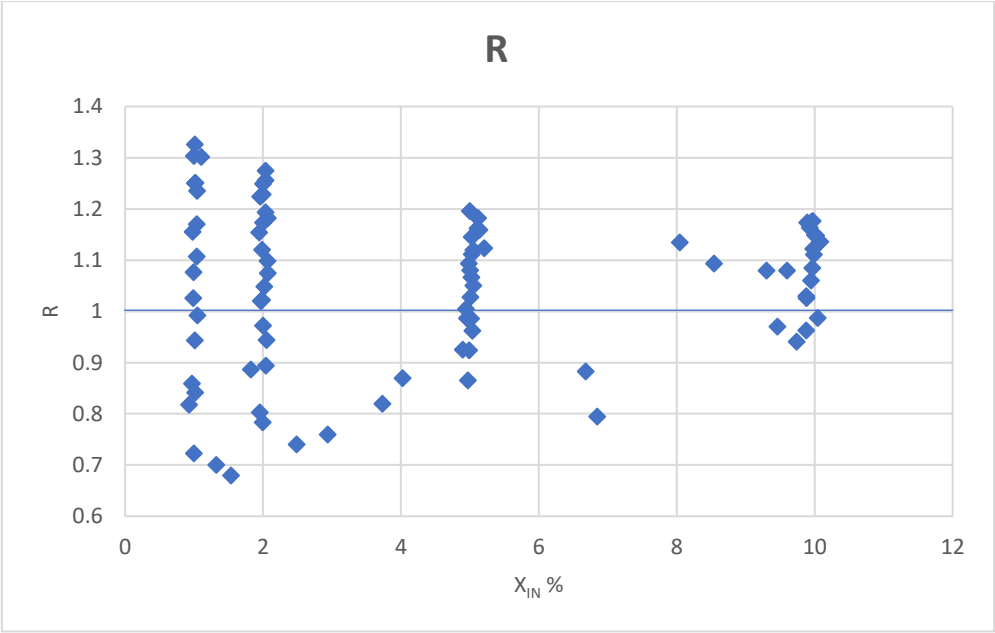

Graph 6. R versus x_{in} for all the experimental data

In the graphs Graph 7, Graph 8, Graph 9 and Graph 10 can be observed at different pressure ranks.

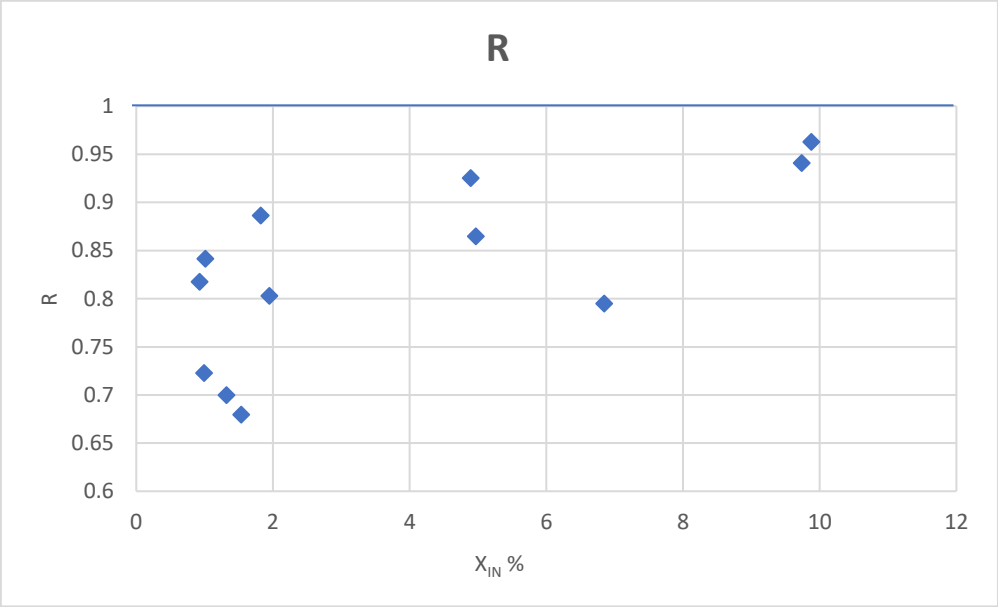

Graph 7. R versus x_{in} (Rank 1)

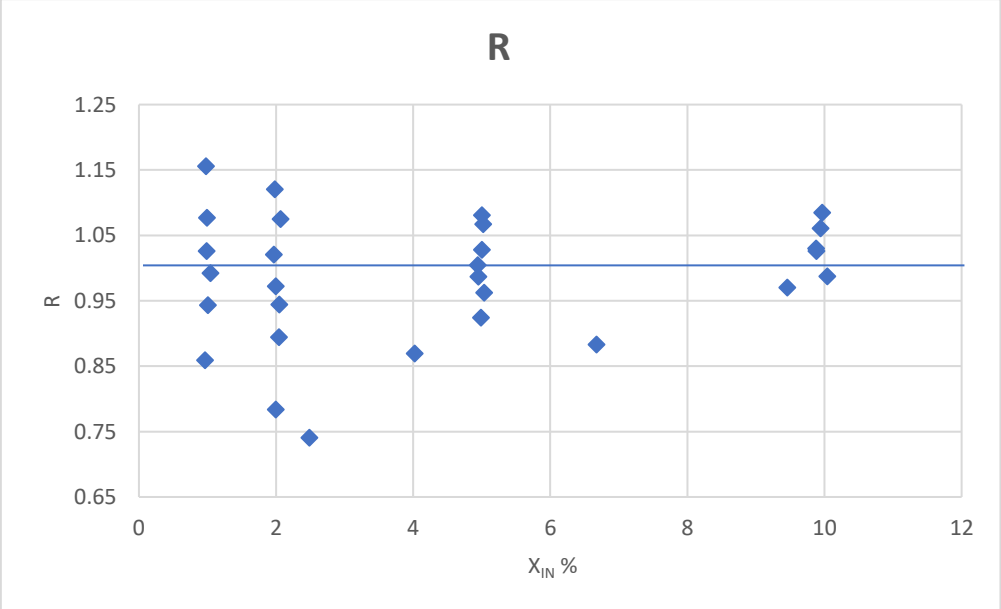

Graph 8. R versus x_{in} (Rank 2)

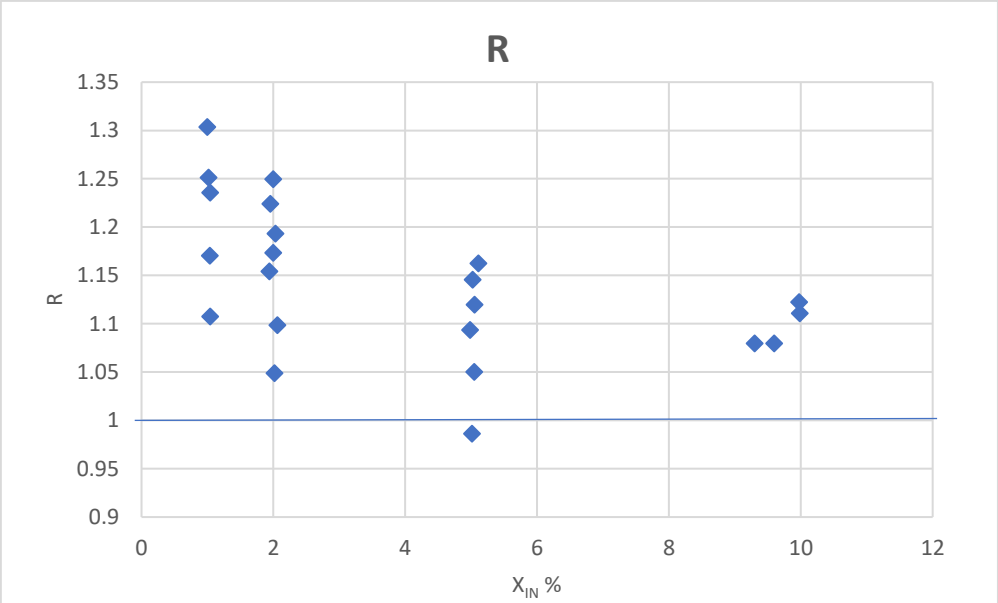

Graph 9. R versus x_{in} (Rank 3)

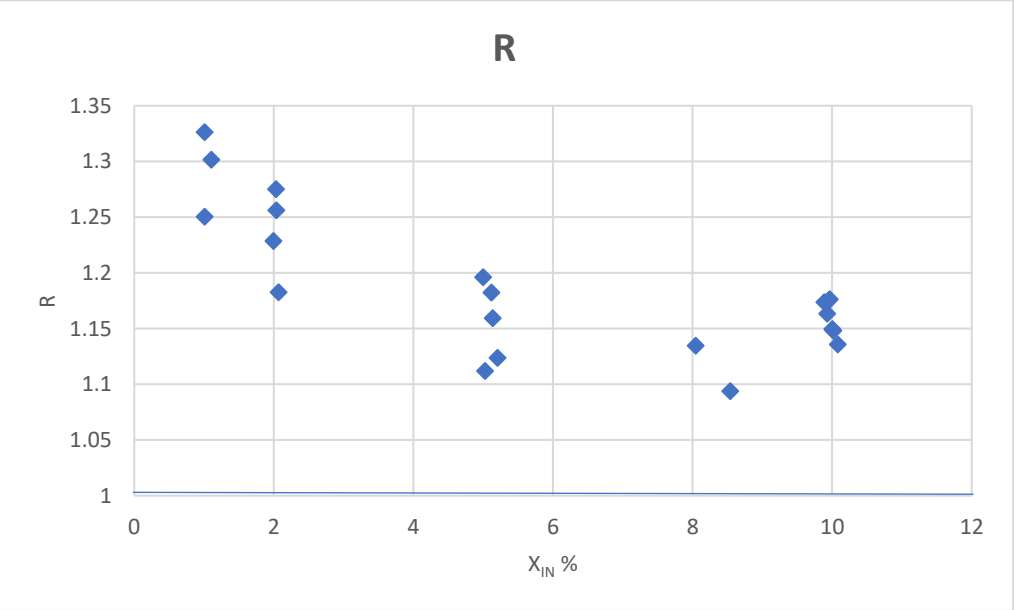

Graph 10. R versus x_{in} (Rank 4)

It can be seen that there are areas where the models are over-predicting the value of the mass flux and in other areas underestimating this value. The most common case recorded in literature is that in which the R-values are above the unit as this means that the real flux rate is lower than the theoretical one, which is what usually happens in reality as in the theoretical circle neither instrumental nor human errors that can occur in the system are being taken into account. Although, as can be seen, there are also areas where the model is predicting a lower flux rate than what is actually being measured in the system, which suggests that it may be working with a model that does not predict the behaviour of this data.

Likewise, a greater dispersion of the data is observed in the smaller values of the vapour quality, which tends to reduce as this parameter increases. It must be taken into account that the calculation methods of the HEM model have been used according to the ω-parameter which is sensitive to vapour quality, so any error in the measurement of this can result in incorrect values of the calculated flux. For this reason, this diffusion of the data may exist at lower quality as it has been possible to measure incorrectly in previous experiments.

When analysing the R-values, when closer to the unit, it means a greater prediction of the model, in this case, it can be observed that the R-values are between 0.68 and 1.32, being this difference higher with lower qualities which is where these higher and lower R-values are found.

Table 10. R- Values in different ranks of inlet pressure

[P]	R_{max}	R_{min}
Rank 1	0.96	0.68
Rank 2	1.15	0.74
Rank 3	1.3	0.98
Rank 4	1.32	1.09

Table 10 shows the maximum and minimum values for each given pressure rank. These data give an idea that the values of the calculated theoretical mass flux depend not only on the inlet vapour quality but also on the pressures measured. Graph 11 shows a comparison for the two ranks of pressures of the extremes, it is observed that to smaller inlet qualities the difference between the mass fluxes is greater and decreases as the quality increases. There is also a major difference with the pressures so we will also analyse their effect on the system.

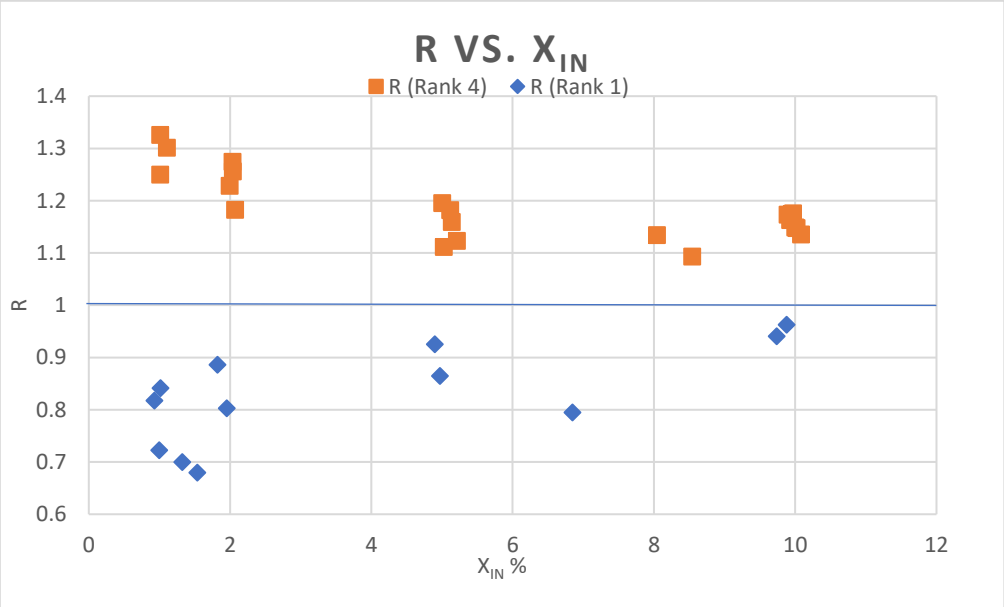

Graph 11. R versus x_{in} at two different ranks of inlet pressure

To analyse the effect of pressure, it has been decided to use R-parameter and the pressure ranks mentioned above. The pressure is an additional variable that is involved in the process, being important at the inlet as well as outlet or backpressure.

Taking as a reference one of the pressure ranks, for example, rank 3, the graph of the mass flux ratio, R, as function of pressure drop, Dp (P_{in}-P_{out}), has been made, which refers to the pressure drop as the difference between the pressures measured at the inlet and the outlet.

When comparing the two graphics (Graph 12), it can be seen that depending on the inlet vapour quality, the R-values approximate to each other as the vapour quality increases, but at lower qualities, this difference does not become very significant, so it is found that some R-values could be considered relatively constant, but when evaluating these values according to the pressure drop, the graph shows something different about the R-values.

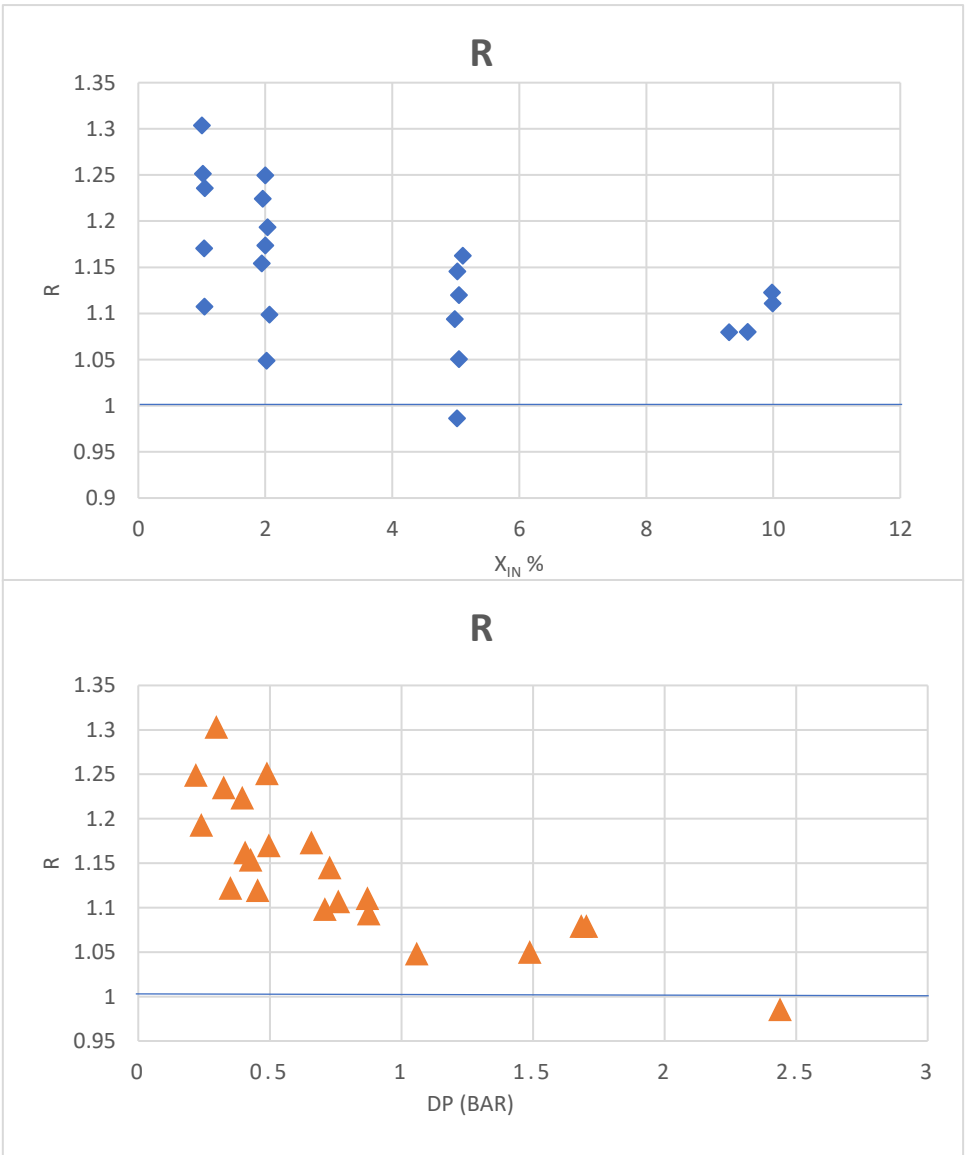

Graph 12. Comparison of the influence of the pressure difference and the vapour quality for Rank 3

The graph shows how there is a tendency to decrease the R-value as the Dp increases seeing that a slight change in pressures causes greater changes in the theoretical mass flux than the changes that may occur due to the different qualities of vapour at the inlet. This more marked influence of Dp that we find, can be one of the causes of the dispersion of data that have been seen in the previous graphs and gives an idea that the model depends more on the operating conditions than on the quality of the vapour of the mixture that flows. The comparison has also been made for the other pressure ranks, see the next graphs.

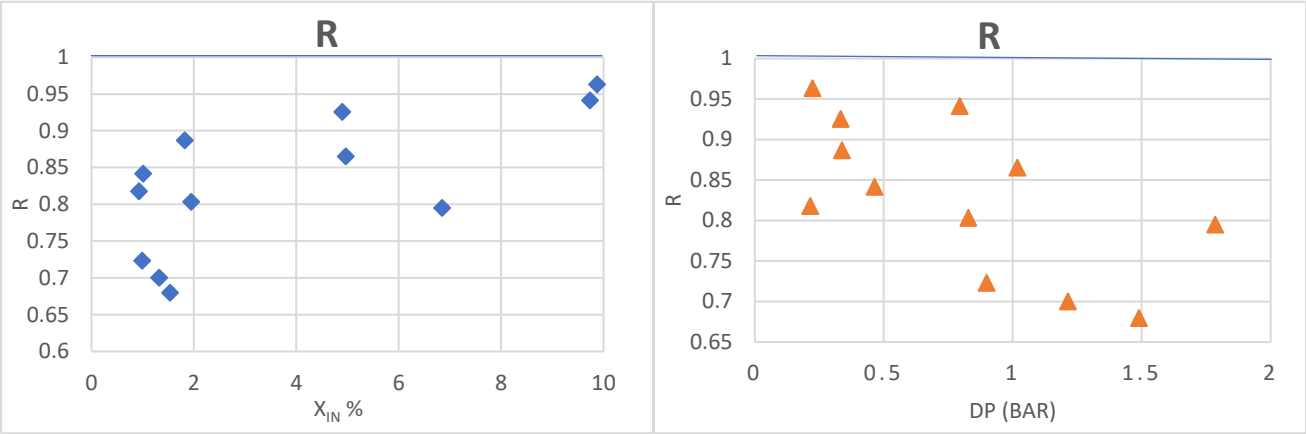

Graph 13. Comparison of the influence of the pressure difference and the vapour quality for Rank 1

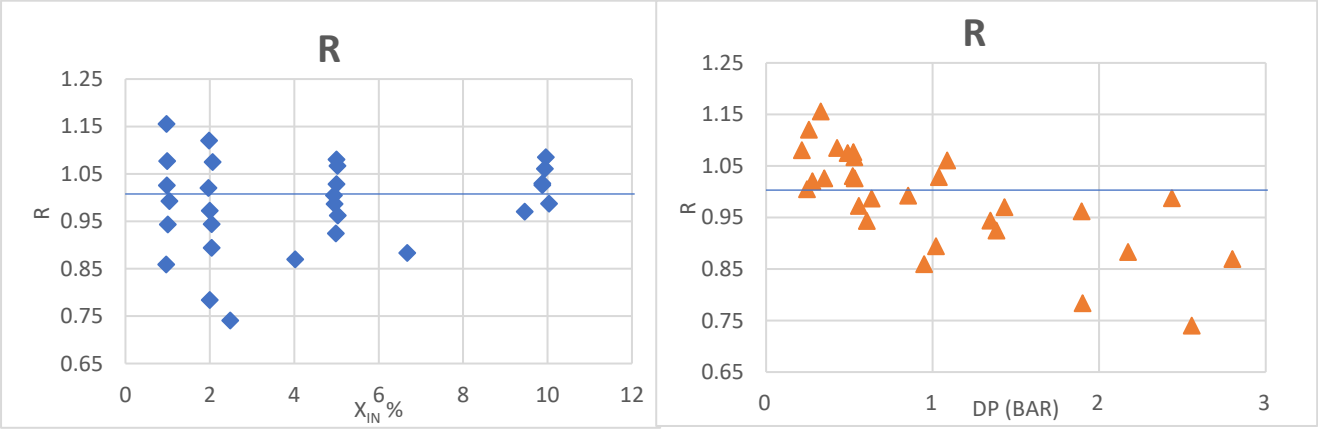

Graph 14. Comparison of the influence of the pressure difference and the vapour quality for Rank 2

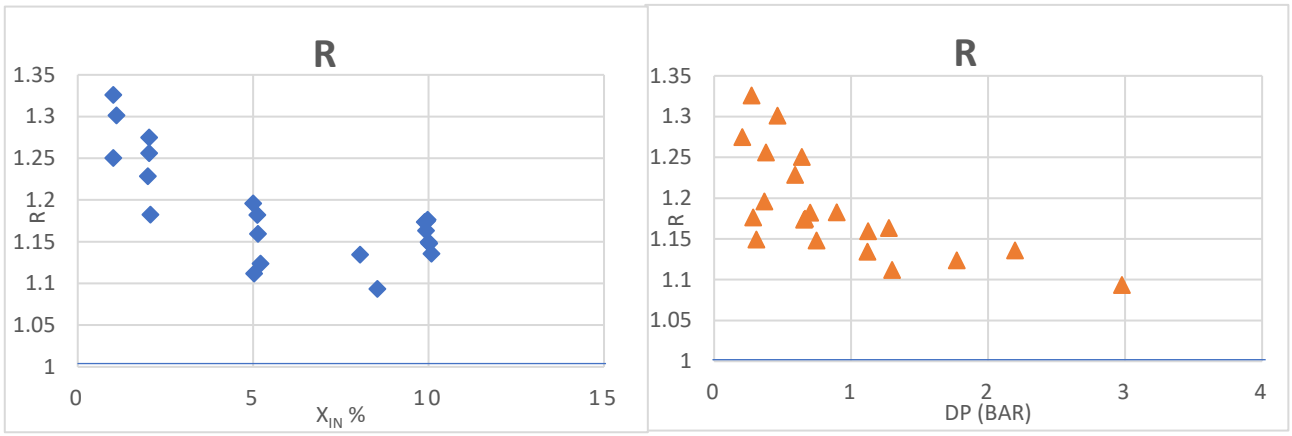

Graph 15. Comparison of the influence of the pressure difference and the vapour quality for Rank 4

As can be seen, the comparison shows that for all the pressure ranks, in which work is being done, the value of the ratio R decreases more markedly with the increase in the pressure drop, Dp. Seeing as described above, the greater influence of the upstream and downstream pressures of the system than the quality of the inlet vapour.

Once we see that the influence of the pressures is important, the graphs that report the R-parameter in function of the ratio of pressures, η, will be made. What can be observed in the graphs is that the R-value decreases considerably as the ratio of pressures η also does.

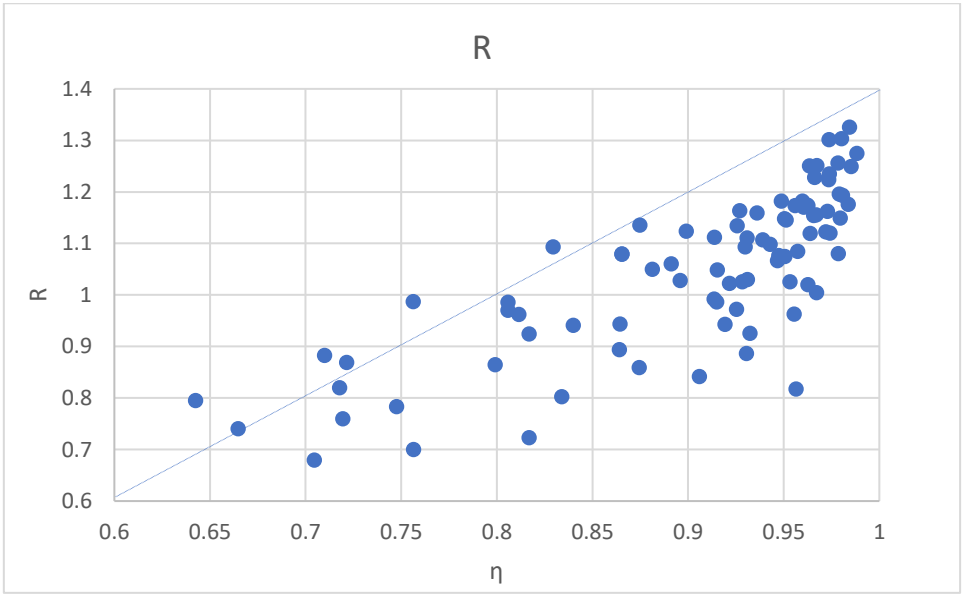

Graph 16. Mass flux ratio versus pressure ratio for all the experimental data

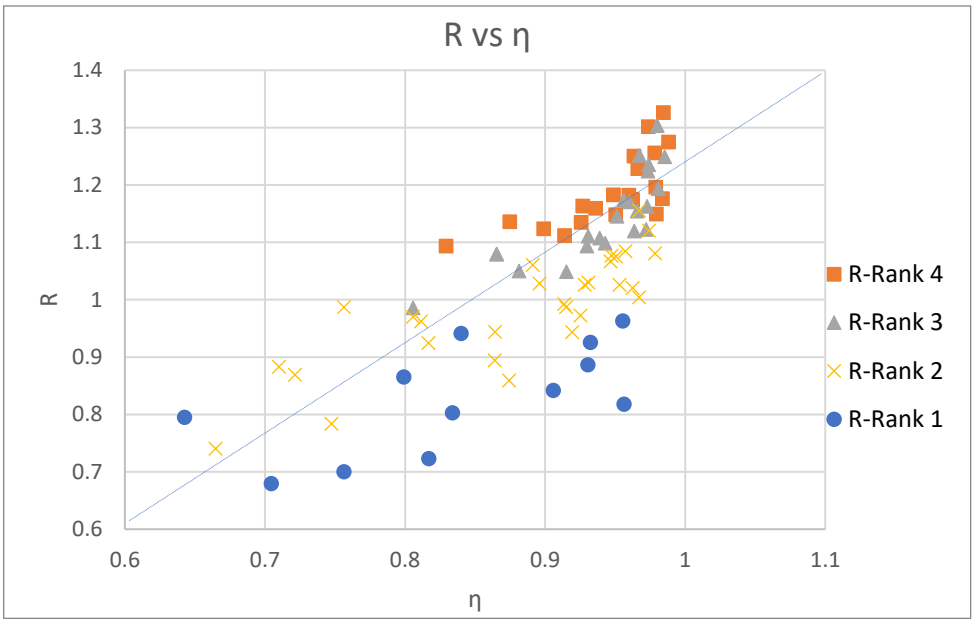

Graph 17. Mass flux ratio versus pressure ratio for the different ranks of pressure

Comparing the data for the different ranks of pressure, it is observed that they follow a increasing exponential tendency rather than a linear one with the values of η, and although this is not very marked, gives an idea of the growth of the value of R as the η increases, it is also observed that for the pressure ranks given the tendency is to go towards R-values around 1.2 and 1.4 since they are in these points in which it is observed that the data set close more their limits and more approach each other for values of the ratio of pressures, η, near to the unit (which would correspond to an ideal system in which the experimental mass flux would be equal to the measured one and the HEM model would predict perfectly the system, in this case, the analysis does not show these results).

To be able to see more clearly these results, it has been decided to use one of the pressure ranks, in this case rank 3, to analyse his behaviour further. Within these experiments, the data has been divided again into other different rank, but in this case in function of the inlet quality of the vapour, being these:

- Rank x1 → between 0.9-1.1 %
- Rank x2 → between 1.9-2.1 %
- Rank x3 → between 4.9-5.2%
- Rank x4 → between 9-10%

The next table shows the results for these ranks of inlet quality that has been used for the analysis.

Table 11. Data for the ranks of inlet quality

	x_{in}	η	R
	%	–	-
RANK X1	1.00	0.98	1.30
	1.02	0.97	1.25
	1.04	0.94	1.11
	1.04	0.96	1.17
	1.04	0.97	1.24
RANK X2	1.94	0.97	1.15
	1.96	0.97	1.22
	2.00	0.99	1.25
	2.00	0.96	1.17
	2.02	0.92	1.05
	2.03	0.98	1.19
	2.06	0.94	1.10
RANK X3	4.98	0.93	1.09
	5.02	0.81	0.99
	5.02	0.95	1.15
	5.05	0.88	1.05
	5.05	0.96	1.12
	5.11	0.97	1.16
RANK X4	9.30	0.87	1.08
	9.60	0.87	1.08
	9.98	0.97	1.12
	9.99	0.93	1.11

The following graph shows the evolution of R as function of the pressure ratio, η, for the quality ranks explained. It is observed, as it has been deduced previously, that all the data follow the same exponential tendency as the pressure ratio increases, thus corroborating what has been explained in the previous paragraphs. What can also be deduced from this graph is that for all quality ranks the evolution is the same, which gives an idea that the data do not depend on the input quality since all these converge towards the same R-values (1.2-1.4) regardless of the inlet quality that has been measured in the experiments.

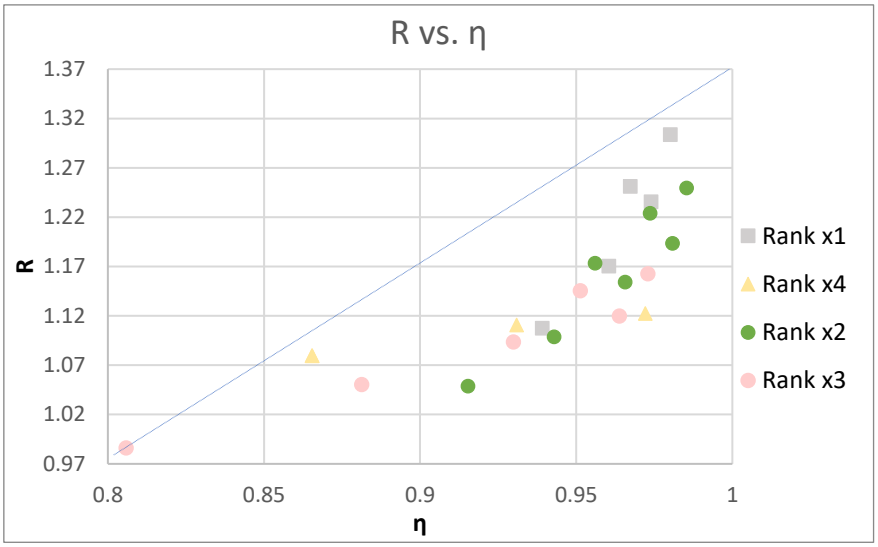

Graph 18. R versus η for the different ranks of inlet quality for Rank 3 of pressures

As a conclusion of this analysis, it can be said that:

- The mass flux ratio, R, decreases as the pressure ratio, also decreases.
- Higher R-values are obtained when there is a higher value of the inlet pressures at the system.
- The values of R follow an exponential tendency with η in addition that for η values close to the unit the R values converge around 1.2-1.4.

7.- HNE-DS model with experimental data

As it has been seen in the previous point, the model of homogeneous equilibrium is not the one that better adapts the behaviour of the experimental data, that as it has been possible to see the experimental mass fluxes do not coincide with the calculated or theoretical mass fluxes, being this superior in most of the cases although always depending on the inlet pressure.

Therefore, it has been decided to carry out the same analysis with the following model, which in this case is the homogeneous non-equilibrium model, HNE-DS.

To summarize and clarify the method explained in a previous point of this thesis, it can be said that the idea of the method is to consider that the valve has no friction, being the liquid a practically monophasic mixture with a balance between the gas and the liquid.

The flow model takes into account the non-equilibrium effects and the properties of the fluids, at the end of the analysis it must be taken into account the potential need for a discharge coefficient like in the HEM model.

In this model, the equations described in the section of the thesis in which the model is described will be used, but in order to facilitate the reading of that, the two most important equations on which the model is based will be written below.

The first is the one for the omega parameter, ω, which is the same as the equation that describes the ω-parameter in the homogeneous model (HEM), only that in this case it is multiplied by a parameter N in the second term of the equation.

$$\omega = \frac{x_o v_{LGo}}{v_o k} + \frac{C_{Lo} T_o P_o}{v_o} \left(\frac{v_{LGo}}{h_{LGo}}\right)^2 * N \qquad \text{Eq 59}$$

$$N = \left(x_o + C_{Lo} T_o P_o * \left(\frac{v_{LGo}}{h_{LGo}^2}\right) * Ln\left(\frac{1}{\eta_{cr}}\right)\right)^{0.4} \qquad \text{Eq 60}$$

The other equations and steps to be followed will be the same as in the previous model, the corresponding densities, pressures and temperatures will be calculated as in the previous section and then both, the N and ω-parameters, will be calculated to finally obtain the theoretical mass flux rate of the model, to make a comparison with the experimental mass flux rate that has been provided as data for this work.

The range of variability for N is $0<N\leq 1$; for high values of N, the method tends to the HEM model, when N=1 the equations of the HEM model are used while for low values the non-equilibrium hypothesis is fulfilled. This parameter is used to take into account the possibility of an intermediate situation between equilibrium and non-equilibrium.

As it will be observed later in the resolution tables, in which the parameters are defined for all the experimental data, it can be observed that the value of the N-parameter is always between 0 and 1, which corroborates that we are facing a situation between equilibrium and non-equilibrium, so this method can be used.

7.1.- Theorical calculations of the HNE-DS model

In analysing the data, we have started, as in the previous model, by comparing the experimental mass flux provided and the theoretical mass flux calculated by the model. As can be seen from the graph, the data follow a somewhat more linear tendency than in the previous model, although the calculated data do not have exactly the same values as the experimental data (See Graph 19).

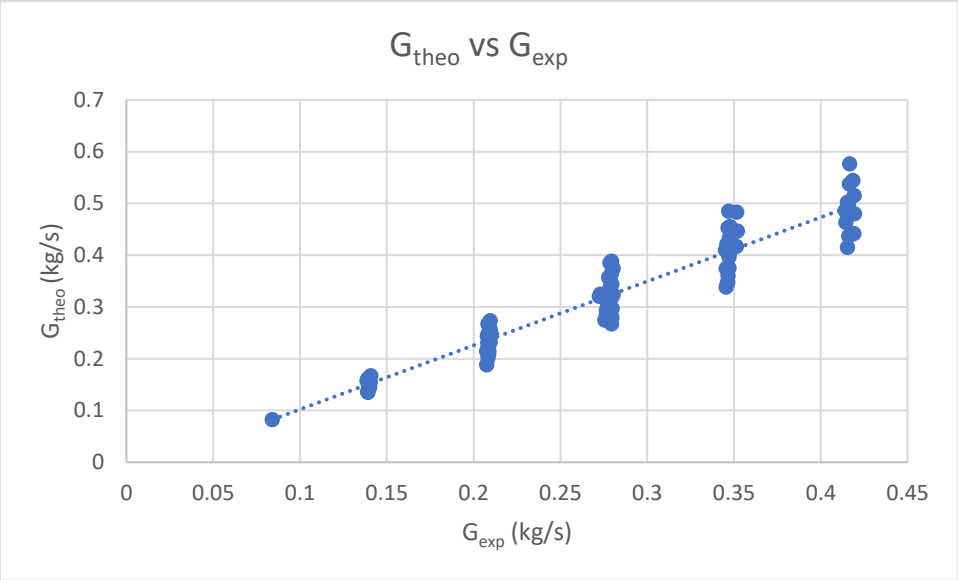

Graph 19. G_{theo} versus G_{exp} HNE-DS model

The following graphs (Graph 20, Graph 21, Graph 22, Graph 23) show the experimental versus theoretical mass flux for different given initial pressure ranks, corresponding to the following intervals, the same as in the previous model.

- ➔ 4-6 bar: Rank 1
- ➔ 7-9-11 bar: Rank 2
- ➔ 12-15 bar: Rank 3
- ➔ 15-18 bar: Rank 4

In these graphs it can be seen more clearly the linear tendency of the data, being more pronounced for the lower pressure ranks than for the higher-pressure ranks. Although the data fits much better with this model than with the homogeneous one. The fact that the data do not match exactly suggests that the model needs a Kd, discharge coefficient, to make a better prediction and thus be able to take into account the differences between the ideal flux through an ideal nozzle and the real flux through a real valve, the process of calculating this parameter will be explained in next chapters.

As a complement to the graphs, the following tables (Table 12, Table 13, Table 14, Table 15) show the results of the calculations made with Excel to analyse the system. At the end of the description of this model, a comparison will be made between the two models studied to see which one best predicts the behaviour of the system.

Table 12. Data for Rank 1

P_{in}	T@	ρ_{gas}	v_g	v_{lg}	v_o	h_{fg}	ω	P_{out}	η	Dp	x_{in}	N	G_{exp}	G_{theo}	R
Pa	K	kg/m^3	m^3/kg	m^3/kg	m^3/kg	J/kg	-	Pa	-	Pa	-	-	kg/s	kg/s	-
4.93E+05	424.41	2.51	0.38	0.38	0.005	1.47E+06	3.96	4.71E+05	0.96	0.21	0.009	0.25	0.21	0.21	1.03
4.94E+05	424.52	2.52	0.38	0.38	0.005	2.11E+06	2.14	4.48E+05	0.91	0.46	0.010	0.23	0.28	0.30	1.06
4.91E+05	424.27	2.51	0.38	0.38	0.005	2.11E+06	2.15	4.01E+05	0.82	0.90	0.010	0.23	0.35	0.36	1.04
4.99E+05	424.87	2.54	0.38	0.37	0.006	2.11E+06	1.99	3.77E+05	0.76	1.21	0.013	0.25	0.35	0.35	1.00
5.04E+05	425.29	2.57	0.37	0.37	0.007	2.11E+06	1.91	3.55E+05	0.70	1.49	0.015	0.26	0.35	0.34	0.98
4.99E+05	424.89	2.54	0.38	0.37	0.008	2.11E+06	1.80	4.16E+05	0.83	0.83	0.019	0.27	0.28	0.28	1.00
4.87E+05	423.98	2.49	0.38	0.38	0.008	2.11E+06	1.83	4.53E+05	0.93	0.34	0.018	0.27	0.21	0.21	1.00
5.07E+05	425.51	2.58	0.37	0.37	0.012	2.11E+06	1.63	3.65E+05	0.72	1.42	0.029	0.30	0.28	0.27	0.95
4.93E+05	424.43	2.51	0.38	0.38	0.020	2.11E+06	1.46	4.60E+05	0.93	0.33	0.049	0.35	0.14	0.13	0.97
5.07E+05	425.49	2.58	0.37	0.37	0.019	2.11E+06	1.46	4.05E+05	0.80	1.02	0.050	0.36	0.21	0.20	0.97
4.99E+05	424.94	2.54	0.38	0.37	0.027	2.11E+06	1.37	3.21E+05	0.64	1.79	0.068	0.39	0.21	0.19	0.90
4.97E+05	424.76	2.53	0.38	0.38	0.038	2.11E+06	1.30	4.18E+05	0.84	0.80	0.097	0.44	0.14	0.14	0.98
5.04E+05	425.27	2.57	0.37	0.37	0.038	2.11E+06	1.30	4.82E+05	0.96	0.22	0.099	0.44	0.08	0.08	0.98

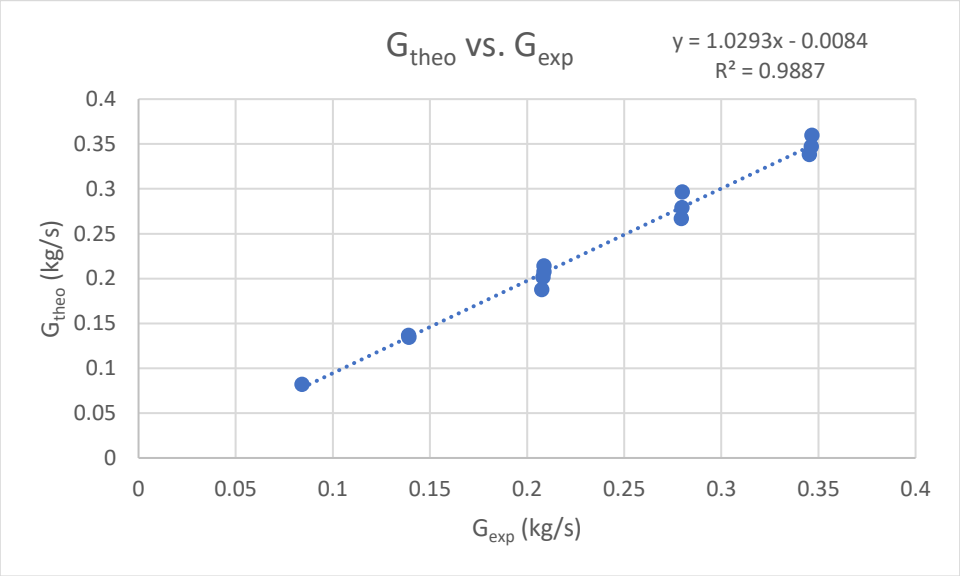

Graph 20. G_{theo} versus G_{exp} for Rank 1

Table 13. Data for Rank 2

P_{in}	T@	ρ_{gas}	v_g	v_{lg}	v_o	h_{fg}	ω	P_{out}	η	Dp	x_{in}	N	G_{exp}	G_{theo}	R
Pa	K	kg/m^3	m^3/kg	m^3/kg	m^3/kg	J/kg	-	Pa	-	Pa	-	-	kg/s	kg/s	-
7.56E+05	441.22	3.71	0.25	0.25	0.003	2.06E+06	2.14	6.61E+05	0.87	0.95	0.010	0.23	0.42	0.48	1.15
9.98E+05	452.94	4.77	0.19	0.19	0.003	2.01E+06	2.10	9.46E+05	0.95	0.52	0.010	0.24	0.35	0.43	1.25
1.00E+06	453.01	4.78	0.19	0.19	0.003	2.01E+06	2.10	9.67E+05	0.97	0.33	0.010	0.24	0.28	0.36	1.28
7.51E+05	440.94	3.69	0.26	0.25	0.004	2.06E+06	2.13	7.16E+05	0.95	0.35	0.010	0.23	0.28	0.33	1.18
7.51E+05	440.97	3.69	0.26	0.25	0.004	2.06E+06	2.12	6.91E+05	0.92	0.61	0.010	0.24	0.35	0.40	1.16
9.89E+05	452.53	4.73	0.20	0.20	0.003	2.02E+06	2.08	9.03E+05	0.91	0.85	0.010	0.24	0.42	0.51	1.23
7.46E+05	440.67	3.66	0.26	0.26	0.006	2.06E+06	1.81	7.18E+05	0.96	0.28	0.020	0.28	0.21	0.23	1.09
9.97E+05	452.89	4.76	0.19	0.19	0.005	2.02E+06	1.81	9.71E+05	0.97	0.26	0.020	0.28	0.21	0.25	1.17
7.47E+05	440.76	3.67	0.26	0.26	0.006	2.06E+06	1.81	6.92E+05	0.93	0.56	0.020	0.28	0.28	0.30	1.09
7.54E+05	441.09	3.70	0.25	0.25	0.006	2.06E+06	1.81	5.63E+05	0.75	1.90	0.020	0.28	0.42	0.44	1.05
9.94E+05	452.76	4.75	0.20	0.19	0.005	2.02E+06	1.80	8.59E+05	0.86	1.35	0.020	0.28	0.42	0.48	1.14
7.51E+05	440.97	3.69	0.26	0.25	0.006	2.06E+06	1.80	6.49E+05	0.86	1.02	0.020	0.28	0.35	0.37	1.08
1.00E+06	453.15	4.79	0.19	0.19	0.005	2.01E+06	1.81	9.24E+05	0.92	0.79	0.020	0.28	0.35	0.40	1.16
9.96E+05	452.84	4.76	0.20	0.19	0.005	2.02E+06	1.80	9.47E+05	0.95	0.49	0.021	0.29	0.28	0.33	1.17
7.62E+05	441.56	3.74	0.25	0.25	0.007	2.05E+06	1.72	5.07E+05	0.66	2.56	0.025	0.30	0.42	0.41	1.00
7.46E+05	440.67	3.66	0.26	0.26	0.011	2.06E+06	1.57	5.35E+05	0.72	2.10	0.037	0.33	0.35	0.35	1.00
1.01E+06	453.27	4.80	0.19	0.19	0.009	2.01E+06	1.57	7.26E+05	0.72	2.80	0.040	0.34	0.42	0.44	1.05
7.49E+05	440.87	3.68	0.26	0.25	0.014	2.06E+06	1.49	7.25E+05	0.97	0.25	0.049	0.36	0.14	0.14	1.03
7.47E+05	440.71	3.67	0.26	0.26	0.014	2.06E+06	1.49	6.83E+05	0.92	0.63	0.050	0.36	0.21	0.22	1.05
1.00E+06	453.17	4.79	0.19	0.19	0.011	2.01E+06	1.50	9.82E+05	0.98	0.22	0.050	0.36	0.14	0.15	1.10
7.56E+05	441.21	3.71	0.25	0.25	0.014	2.06E+06	1.48	6.17E+05	0.82	1.38	0.050	0.36	0.28	0.29	1.03
9.97E+05	452.91	4.77	0.19	0.19	0.011	2.02E+06	1.50	9.44E+05	0.95	0.53	0.050	0.36	0.21	0.23	1.11
9.99E+05	452.97	4.77	0.19	0.19	0.011	2.01E+06	1.50	8.95E+05	0.90	1.04	0.050	0.36	0.28	0.31	1.10
1.01E+06	453.29	4.81	0.19	0.19	0.011	2.01E+06	1.50	8.17E+05	0.81	1.90	0.050	0.36	0.35	0.37	1.08
7.50E+05	440.89	3.68	0.26	0.25	0.018	2.06E+06	1.41	5.32E+05	0.71	2.17	0.067	0.39	0.28	0.27	1.00
7.38E+05	440.21	3.63	0.26	0.26	0.025	2.06E+06	1.33	5.94E+05	0.81	1.43	0.095	0.44	0.21	0.21	1.03
7.58E+05	441.31	3.72	0.25	0.25	0.026	2.06E+06	1.32	7.05E+05	0.93	0.52	0.099	0.44	0.14	0.15	1.05
7.42E+05	440.46	3.65	0.26	0.26	0.026	2.06E+06	1.32	6.89E+05	0.93	0.53	0.099	0.44	0.14	0.15	1.05
1.00E+06	453.04	4.78	0.19	0.19	0.020	2.01E+06	1.34	8.91E+05	0.89	1.09	0.099	0.45	0.21	0.23	1.10
1.00E+06	453.01	4.78	0.19	0.19	0.020	2.01E+06	1.34	9.57E+05	0.96	0.43	0.100	0.45	0.14	0.15	1.10
1.00E+06	453.07	4.78	0.19	0.19	0.020	2.01E+06	1.34	7.57E+05	0.76	2.44	0.100	0.45	0.28	0.29	1.06

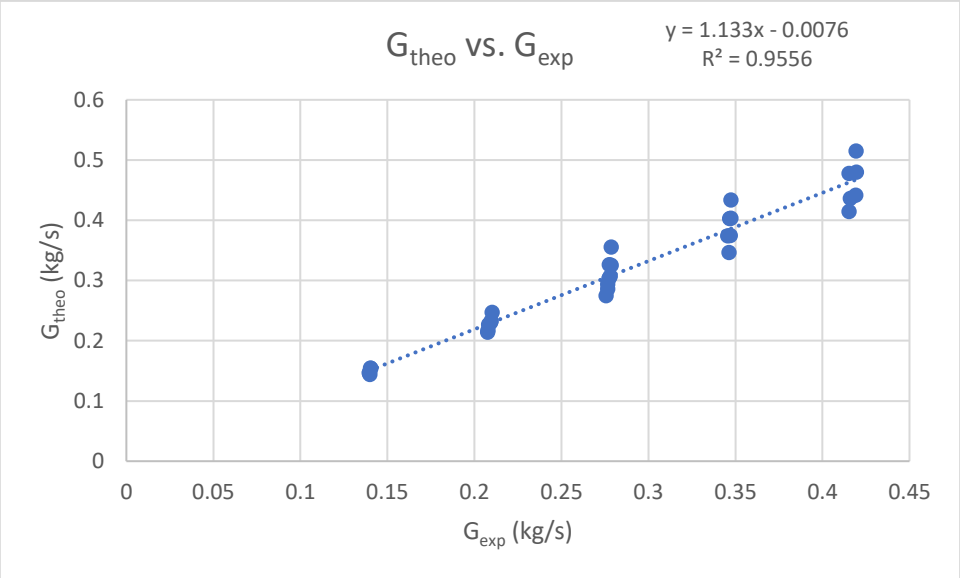

Graph 21. G_{theo} versus G_{exp} for Rank 2

Table 14. Data for Rank 3

P_{in}	T@	ρ_{gas}	v_g	v_{lg}	v_o	h_{fg}	ω	P_{out}	η	Dp	x_{in}	N	G_{exp}	G_{theo}	R
Pa	K	kg/m³	m³/kg	m³/kg	m³/kg	J/kg	-	Pa	-	Pa	-	-	kg/s	kg/s	-
1.49E+06	471.19	6.86	0.13	0.13	0.002	1.95E+06	2.01	1.46E+06	0.98	0.30	0.010	0.25	0.28	0.39	1.38
1.49E+06	471.20	6.86	0.13	0.13	0.002	1.95E+06	2.01	1.44E+06	0.97	0.49	0.010	0.25	0.35	0.48	1.37
1.25E+06	462.84	5.84	0.16	0.16	0.003	1.98E+06	2.04	1.17E+06	0.94	0.76	0.010	0.25	0.42	0.54	1.30
1.25E+06	463.05	5.86	0.16	0.16	0.003	1.98E+06	2.04	1.20E+06	0.96	0.50	0.010	0.25	0.35	0.45	1.31
1.24E+06	462.70	5.82	0.16	0.16	0.003	1.98E+06	2.04	1.21E+06	0.97	0.32	0.010	0.25	0.28	0.37	1.33
1.24E+06	462.66	5.81	0.16	0.16	0.004	1.98E+06	1.82	1.20E+06	0.97	0.43	0.019	0.29	0.28	0.34	1.23
1.50E+06	471.40	6.88	0.13	0.13	0.004	1.95E+06	1.80	1.46E+06	0.97	0.39	0.020	0.29	0.28	0.36	1.29
1.49E+06	471.24	6.86	0.13	0.13	0.004	1.95E+06	1.80	1.47E+06	0.99	0.22	0.020	0.29	0.21	0.27	1.28
1.50E+06	471.36	6.88	0.13	0.13	0.004	1.95E+06	1.80	1.43E+06	0.96	0.66	0.020	0.29	0.35	0.45	1.27
1.25E+06	462.87	5.84	0.16	0.16	0.004	1.98E+06	1.80	1.14E+06	0.92	1.06	0.020	0.29	0.42	0.50	1.20
1.25E+06	462.85	5.84	0.16	0.16	0.004	1.98E+06	1.80	1.22E+06	0.98	0.24	0.020	0.29	0.21	0.26	1.24
1.24E+06	462.64	5.81	0.16	0.16	0.004	1.98E+06	1.80	1.17E+06	0.94	0.71	0.021	0.29	0.35	0.42	1.21
1.25E+06	462.87	5.84	0.16	0.16	0.009	1.98E+06	1.52	1.16E+06	0.93	0.88	0.050	0.37	0.28	0.32	1.15
1.51E+06	471.62	6.91	0.13	0.13	0.008	1.95E+06	1.52	1.38E+06	0.91	1.30	0.050	0.37	0.35	0.42	1.19
1.26E+06	463.14	5.87	0.16	0.16	0.009	1.98E+06	1.51	1.01E+06	0.81	2.44	0.050	0.37	0.41	0.46	1.12
1.49E+06	471.21	6.86	0.13	0.13	0.008	1.95E+06	1.52	1.42E+06	0.95	0.73	0.050	0.37	0.27	0.32	1.19
1.25E+06	463.06	5.86	0.16	0.16	0.009	1.98E+06	1.51	1.10E+06	0.88	1.49	0.050	0.37	0.35	0.40	1.14
1.25E+06	462.95	5.85	0.16	0.16	0.009	1.98E+06	1.51	1.21E+06	0.96	0.45	0.050	0.37	0.21	0.24	1.15
1.50E+06	471.40	6.88	0.13	0.13	0.008	1.95E+06	1.52	1.46E+06	0.97	0.41	0.051	0.37	0.21	0.25	1.19
1.51E+06	471.62	6.91	0.13	0.13	0.011	1.95E+06	1.41	1.39E+06	0.93	1.12	0.080	0.42	0.27	0.32	1.17
1.25E+06	462.97	5.85	0.16	0.16	0.016	1.98E+06	1.36	1.08E+06	0.87	1.68	0.093	0.44	0.28	0.32	1.13
1.27E+06	463.48	5.91	0.16	0.15	0.016	1.98E+06	1.36	1.09E+06	0.87	1.70	0.096	0.45	0.28	0.32	1.13
1.25E+06	463.10	5.86	0.16	0.16	0.017	1.98E+06	1.35	1.22E+06	0.97	0.35	0.100	0.45	0.14	0.16	1.13
1.50E+06	471.52	6.90	0.13	0.13	0.014	1.95E+06	1.36	1.47E+06	0.98	0.31	0.100	0.45	0.14	0.16	1.16
1.26E+06	463.29	5.89	0.16	0.16	0.016	1.98E+06	1.35	1.17E+06	0.93	0.87	0.100	0.45	0.21	0.24	1.14
1.51E+06	471.64	6.92	0.13	0.13	0.014	1.95E+06	1.36	1.43E+06	0.95	0.75	0.100	0.45	0.21	0.24	1.17

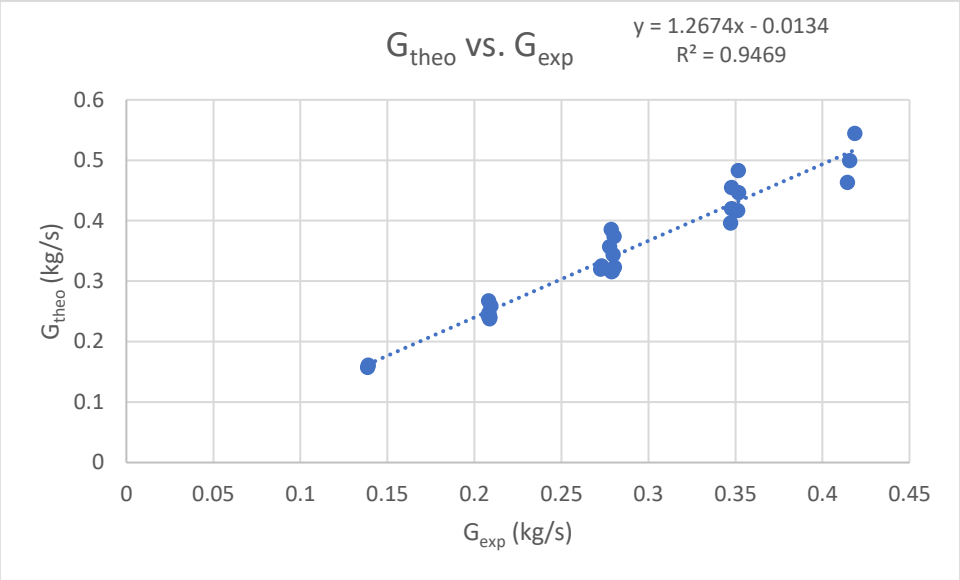

Graph 22. G_{theo} versus G_{exp} for Rank 3

Table 15. Datta for Rank 4

P_{in}	T@	ρ_{gas}	v_g	v_{lg}	v_o	h_{fg}	ω	P_{out}	η	Dp	x_{in}	N	G_{exp}	G_{theo}	R
Pa	K	kg/m^3	m^3/kg	m^3/kg	m^3/kg	J/kg	-	Pa	-	Pa	-	-	kg/s	kg/s	-
1.75E+06	478.96	7.92	0.11	0.11	0.002	1.92E+06	1.97	1.73E+06	0.98	0.27	0.010	0.25	0.28	0.39	1.39
1.75E+06	479.00	7.93	0.11	0.11	0.002	1.92E+06	1.97	1.69E+06	0.96	0.64	0.010	0.25	0.42	0.58	1.38
1.75E+06	478.98	7.93	0.11	0.11	0.002	1.92E+06	1.95	1.71E+06	0.97	0.46	0.011	0.26	0.35	0.48	1.40
1.75E+06	478.75	7.89	0.11	0.11	0.003	1.92E+06	1.79	1.69E+06	0.97	0.59	0.020	0.29	0.35	0.45	1.31
1.75E+06	478.80	7.90	0.11	0.11	0.003	1.92E+06	1.78	1.73E+06	0.99	0.21	0.020	0.30	0.21	0.27	1.30
1.75E+06	478.76	7.90	0.11	0.11	0.003	1.92E+06	1.78	1.71E+06	0.98	0.38	0.020	0.30	0.28	0.36	1.31
1.75E+06	478.75	7.90	0.11	0.11	0.003	1.92E+06	1.77	1.66E+06	0.95	0.89	0.021	0.30	0.42	0.54	1.29
1.75E+06	478.88	7.91	0.11	0.11	0.007	1.92E+06	1.53	1.71E+06	0.98	0.37	0.050	0.37	0.21	0.25	1.22
1.76E+06	479.12	7.95	0.11	0.11	0.007	1.92E+06	1.52	1.65E+06	0.94	1.12	0.051	0.37	0.35	0.42	1.22
1.74E+06	478.59	7.87	0.11	0.11	0.007	1.92E+06	1.52	1.67E+06	0.96	0.70	0.051	0.37	0.28	0.34	1.22
1.75E+06	478.98	7.93	0.11	0.11	0.007	1.92E+06	1.52	1.58E+06	0.90	1.77	0.052	0.38	0.42	0.50	1.21
1.74E+06	478.72	7.89	0.11	0.11	0.011	1.92E+06	1.40	1.45E+06	0.83	2.98	0.085	0.43	0.41	0.49	1.17
1.76E+06	479.07	7.94	0.11	0.11	0.012	1.92E+06	1.37	1.69E+06	0.96	0.66	0.099	0.45	0.21	0.25	1.19
1.75E+06	478.96	7.93	0.11	0.11	0.012	1.92E+06	1.37	1.69E+06	0.96	0.66	0.099	0.46	0.21	0.25	1.19
1.75E+06	478.82	7.90	0.11	0.11	0.012	1.92E+06	1.37	1.62E+06	0.93	1.28	0.099	0.45	0.28	0.33	1.20
1.75E+06	478.95	7.92	0.11	0.11	0.012	1.92E+06	1.37	1.72E+06	0.98	0.28	0.100	0.46	0.14	0.17	1.18
1.75E+06	478.94	7.92	0.11	0.11	0.012	1.92E+06	1.37	1.53E+06	0.87	2.19	0.101	0.46	0.35	0.41	1.19

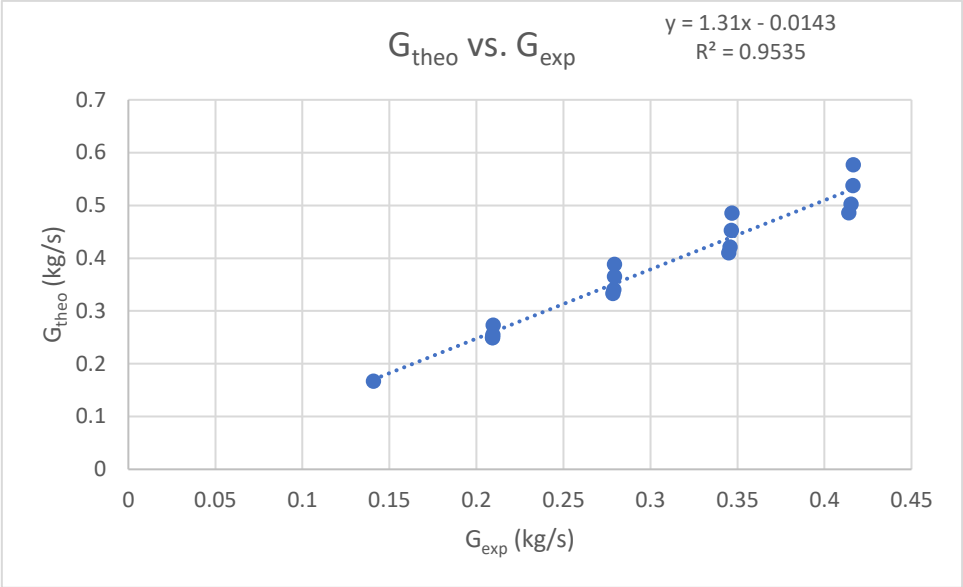

Graph 23. G_{theo} versus G_{exp} for Rank 4

It can be seen from the graphs how the theoretical and experimental fluxes do not completely coincide, which gives an idea that a discharge coefficient is needed to solve the small differences that may exist between these data. It can also be seen that for the higher and lower pressure ranks (rank 1 and 4) the predictions of the theoretical mass flow are more similar to the experimental ones provided, which gives an idea that the data, as seen in the previous model, depends on several parameters such as the initial pressure and the quality of the inlet vapour of the mixture.

To facilitate the understanding of the results, and as has been done previously in the literature, it has been decided to adopt the mass flux ratio, R, to analyse the results (the closer this parameter is to the unit value, the better the model's prediction will be).

In this case, different representations of this value have been made based on several parameters, such as inlet vapour quality, inlet pressure or pressure ratio, using the initial pressure P_{in} in the ranks described above as the input parameter. It has also been decided to use this data and these graphs to make a better comparison with the previous model.

The following graphs show the relationship between R and vapour quality at the inlet for all pressures and different ranks. In these graphs we will be able to see between which values the R-parameter moves, to see how the inlet quality affects the mass flux calculations, the closer to the unit, as mentioned above, the better the model will be able to predict.

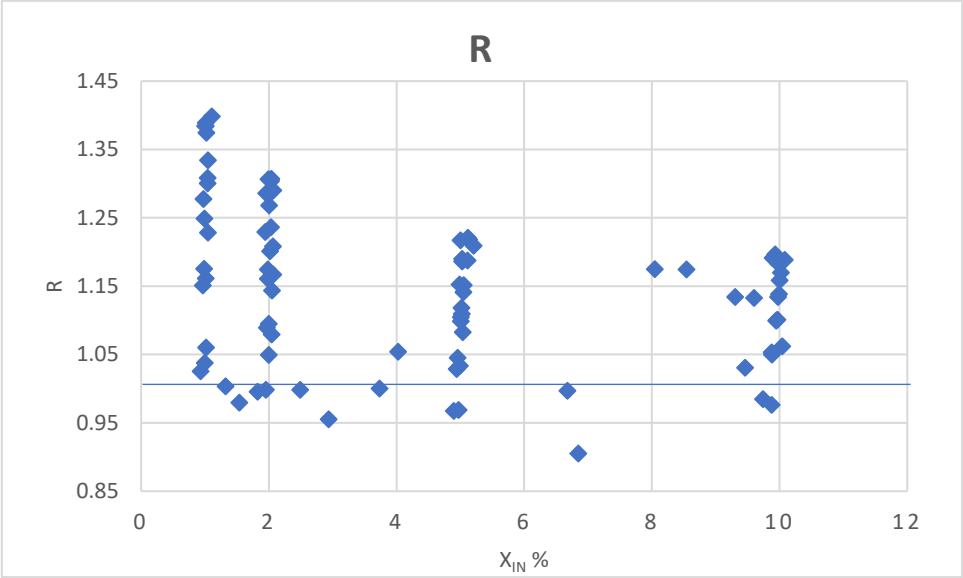

Graph 24. R versus inlet quality for all the experimental data

This graphic (Graph 24) shows the mass flux ratio in function of the inlet quality of the vapour. It can be observed that there is some diffusion in the data, the points are far apart. According to this graph, it seems that for lower pressures the diffusion of the data is greater since the R-value found between values more distant from each other.

In order to observe this better, Graph 25, Graph 26, Graph 27 and Graph 28 have been made, which compare the R-value against the inlet vapour quality according to the different pressure ranks described above.

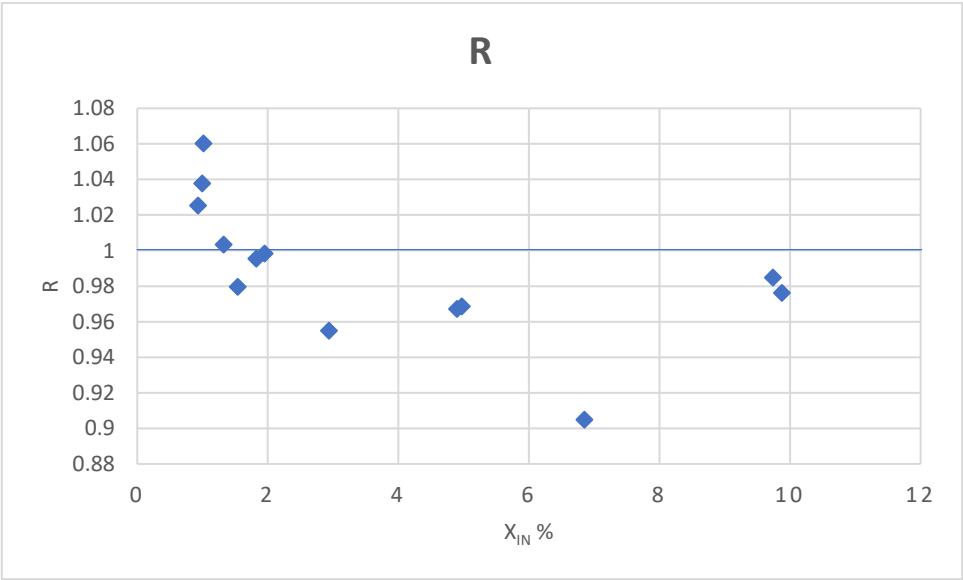

Graph 25. R versus x_{in} in Rank 1

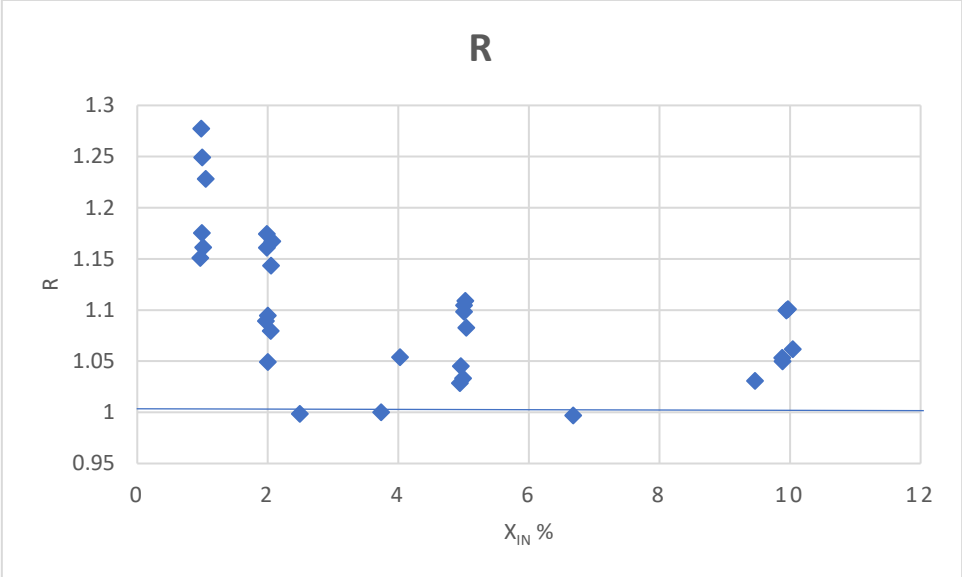

Graph 26. R versus x_{in} in Rank 2

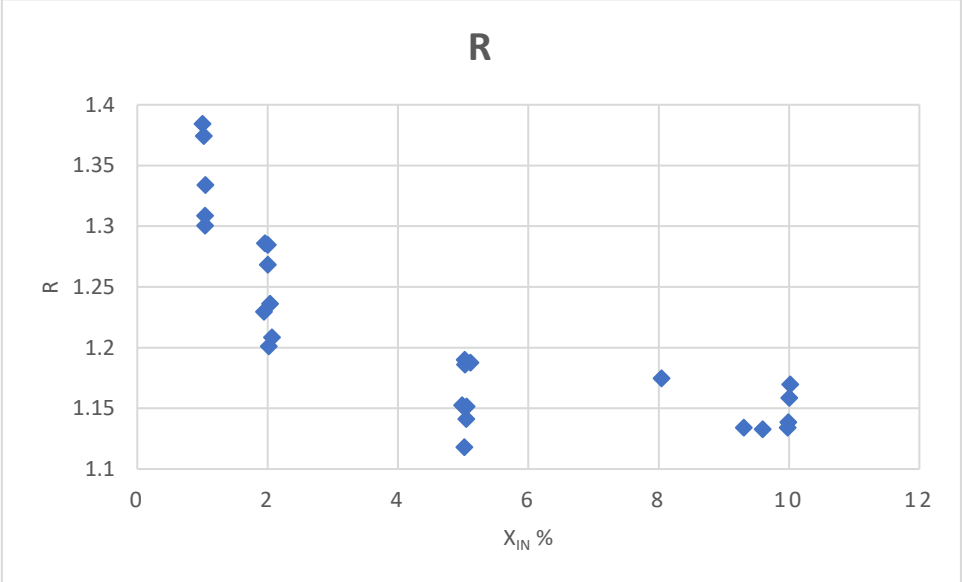

Graph 27. R versus x_{in} in Rank 3

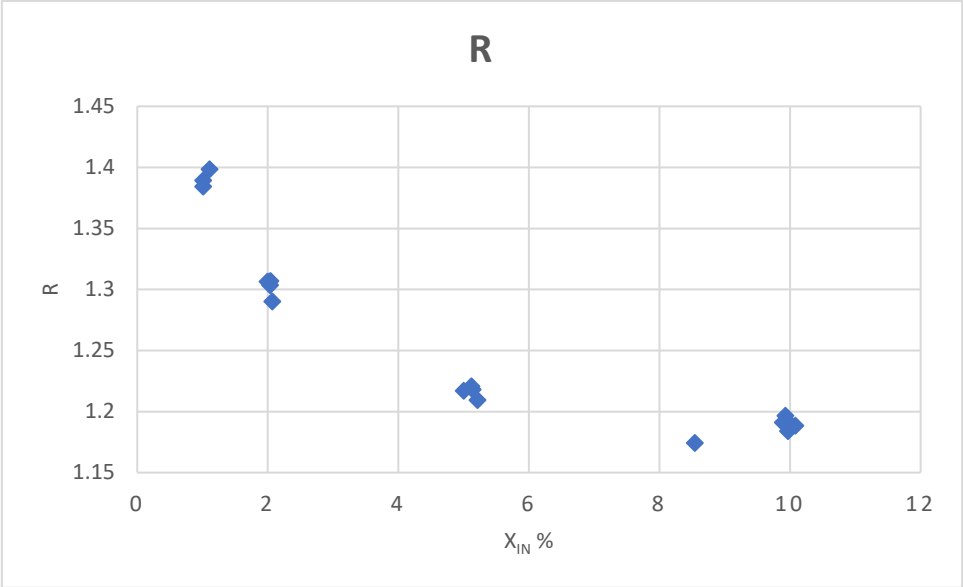

Graph 28. R versus x_{in} in Rank 4

When the R-value is below the unity value it means that the model is underestimating the theoretical mass flux rate compared to the experimental, and if it is above the unit value it is overestimating it. In this model, it is observed that for the rank 1 of pressures there are some values, not all, in which the model is underestimating the theoretical flux versus the experimental one, as well as in the rank 2 of pressures that there are two values of R that also underestimate it.

For all other cases, R-values above unity are observed, which means that the model is overestimating the value of the theoretical mass flux, which is usually the typical case in these situations since this is what usually happens in reality, since in the theoretical circle, neither instrumental nor human errors that may occur in the system are being taken into account. This overestimation of the flow rate can have detrimental consequences on the protection of the equipment if it reaches very high values.

Since most of the data are higher than 1 and very close to it, this model gives us a better prediction than the HEM model, although it does not accurately predict the system's behaviour.

Likewise, a greater dispersion of data is observed in the smaller values of the inlet vapour quality, which tends to decrease as this parameter increases, although the mass flux ratio tends to a constant's values.

It can be seen that the R values are between 0.9 and 1.4, which is a smaller range of variability than that obtained with the HEM model (0.68 and 1.32, the greater range of dispersion of the data), although this difference is still greater with lower qualities where these higher and lower R-values are found, so it gives an idea

that the parameters depend more on the pressure than on the initial quality of the vapour.

Table 16. R-values in different ranks of inlet pressures

[P]	R_{max}	R_{min}	ΔR
Rank 1	1.06	0.91	0.15
Rank 2	1.28	0.99	0.29
Rank 3	1.38	1.12	0.26
Rank 4	1.39	1.17	0.22

Table 16 shows the maximum and minimum values for each given pressure rank. These data give an idea that the values of the calculated theoretical mass flux depend not only on the quality of the inlet but also on the pressures measured.

The last column of Table 16 shows the difference between the maximum and minimum R-values in which it can be observed that for lower and higher pressures this dispersion is lower than for intermediate pressures, although the rank is very similar in all of them, in which it has been concluded that for the ranks of pressures 1 and 4 are for which better linear adjustment had the data, reason why it is in which but similar the values of the flows have been obtained, for that reason also the value of the R is nearer to 1 and has less dispersion between the qualities.

It can also be seen in both, the graphs and the tables, that this dispersion of data is reduced as the inlet vapour quality increases but that it follows the same tendency or behaviour for all pressure ranks, the lower the quality the more dispersion and the higher the less, and as this behaviour is common to all ranks it gives an idea that the data does not depend so much on the quality as on the initial pressure at which the fluids are being introduced.

Graph 29 shows a comparison for the two ranks of pressures of the extremes. It is observed that to smaller inlet qualities the difference between the mass fluxes is greater and decreases as the quality increases. There is also a major difference with the pressures so we will also analyse their effect on the system.

In this graph, it can be seen how for smaller inlet pressures the model seems to obtain a better prediction of the mass flux ratio since the values are closer to unity than for higher inlet pressures, which is already an improvement compared to the homogeneous model studied in the previous section.

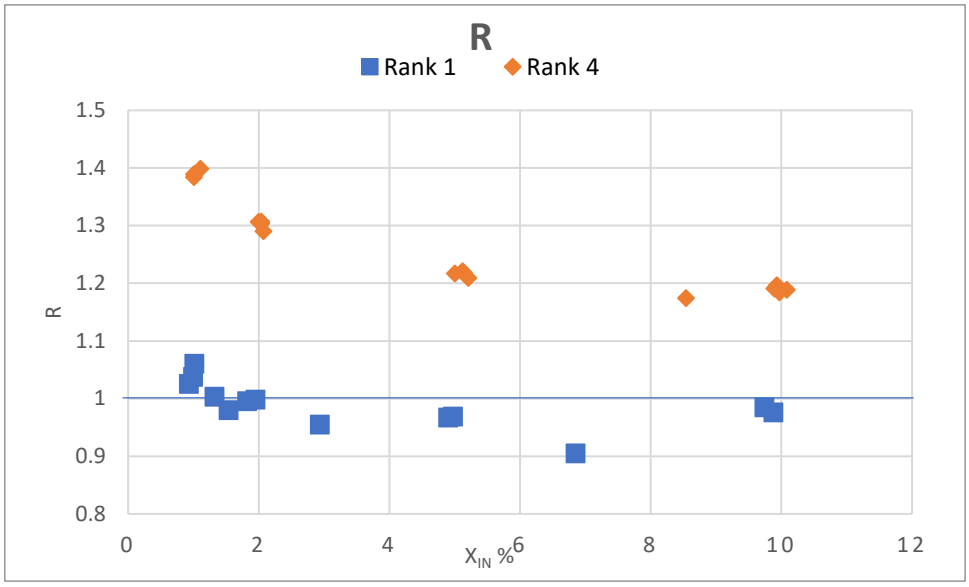

Graph 29. R versus x_{in} at two different ranks of inlet pressure

To analyse the effect of pressure, it has been decided to use the R-parameter and the pressure ranks mentioned above. Pressure is an additional variable that intervenes in the process, being important both, at the inlet and the outlet or backpressure, as we have seen in the homogeneous model and in the graphs and tables of this model (HNE-DS) the pressure is a quite important variable on which the data depend and therefore an analysis is going to be made according to it.

Taking as a reference one of the pressure ranks, for example, the same rank used in the HEM analysis, rank 3, a graph of the relationship of mass fluxes, R, as function of Dp (Pin-Pout) have been made, which refers to the pressure drop as the difference between the pressures measured at the inlet and the outlet.

When comparing the two graphs (Graph 30), it can be seen that depending on the quality of the vapour at the inlet, the R-values are closer to each other as the quality increases, but in lower qualities, this difference does not become very significant, so we find some R-values that could be considered relatively constant, but when evaluating these values as a function of the pressure drop, the graph shows something different. The R-values are higher at lower pressures and lower at higher pressures, thus seeing a tendency to decrease the R-value as the initial pressure increases. It also shows how the difference in the data of the R-values is greater at lower Dp values than when the Dp becomes higher.

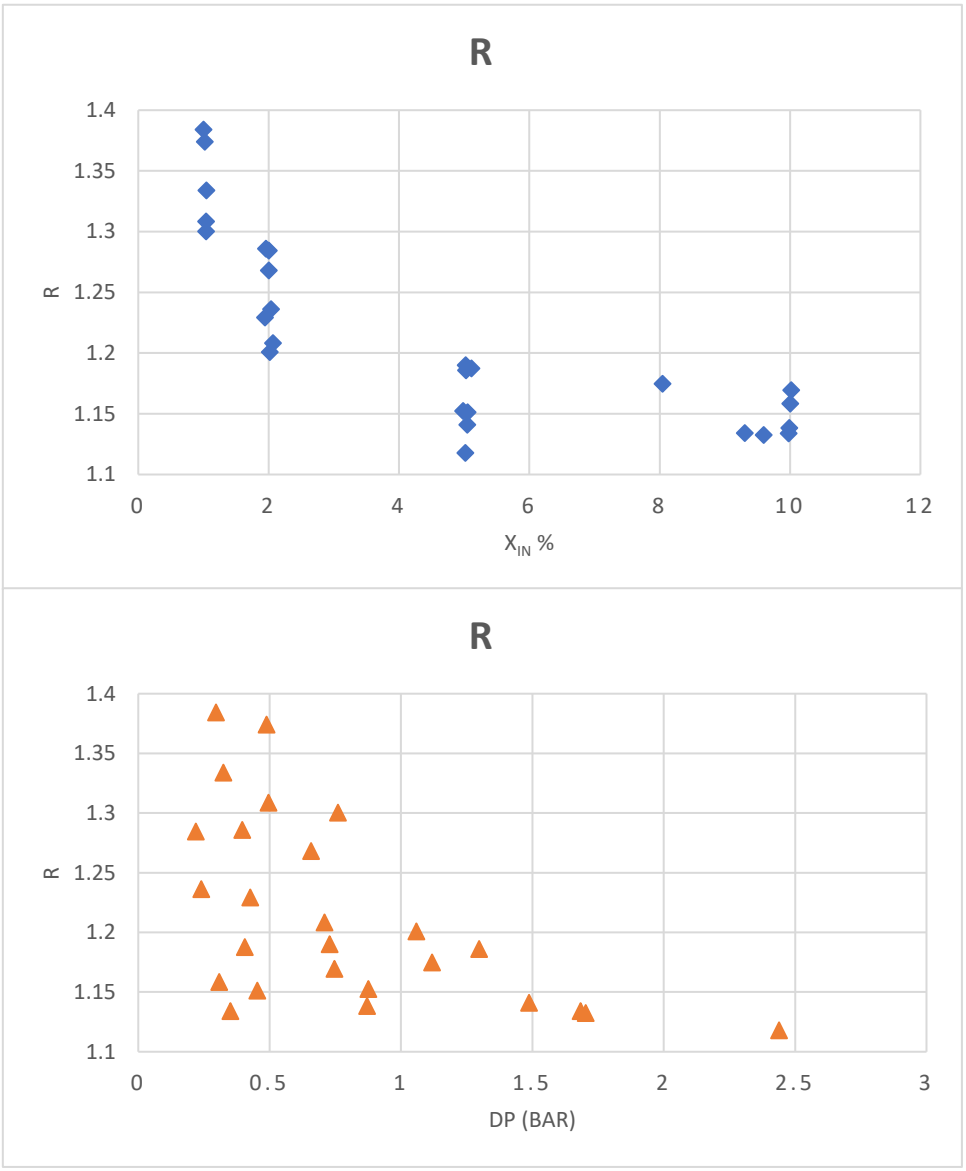

Graph 30. Comparison of the influence of the pressure difference and the vapour quality for Rank 3

Graph 30 shows how there is a tendency to decrease the R-value as the Dp increases seeing that a slight change in pressures causes greater changes in the theoretical mass flux than the changes that may occur due to the different qualities of vapour at the inlet. This influence of more marked Dp that we find can be one of the causes of the little dispersion of data that we have seen in the previous graphs and gives an idea that the model depends more on the operating conditions than on the quality of the vapour of the mixture that flows, as it has been explained before.

The comparison has also been made for the other pressure ranks, see the next graphs (Graph 31, Graph 32, Graph 33). The same tendency studied for rank 3 as for the others can be observed in the comparison of the data.

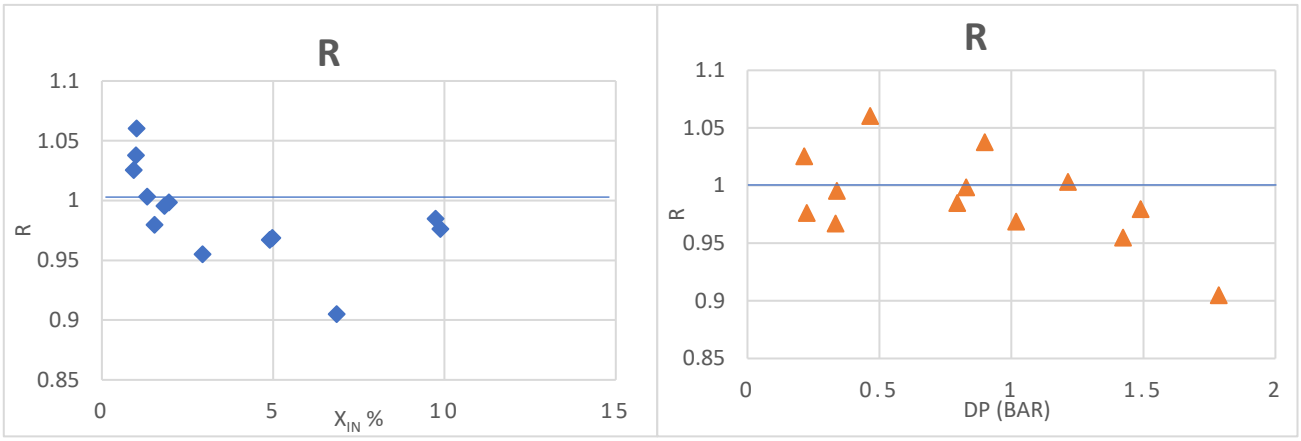

Graph 31. Comparison of the influence of the pressure difference and the vapour quality for Rank 1

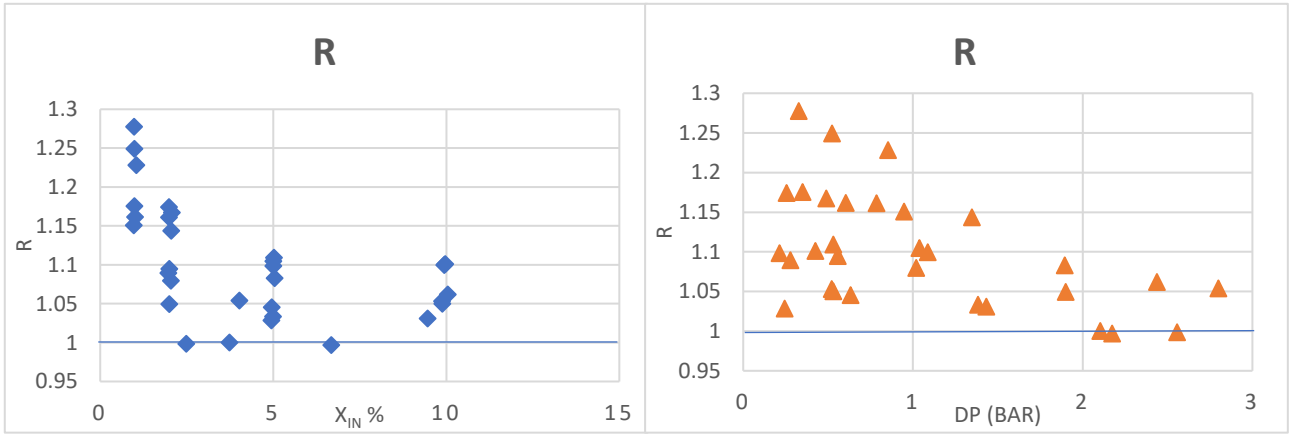

Graph 32. Comparison of the influence of the pressure difference and the vapour quality for Rank 2

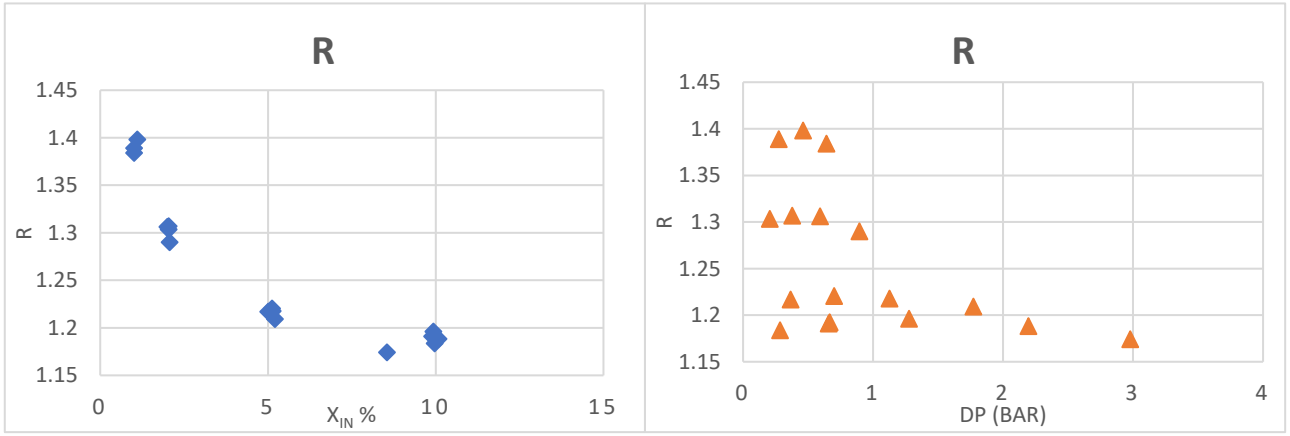

Graph 33. Comparison of the influence of the pressure difference and the vapour quality for Rank 4

As can be seen, the comparison shows that for all pressure ranks in which thesis is being done, the value of the ratio R decreases more sharply with increasing pressure drop Dp. Seeing as it has been described above, the greater influence of the upstream and downstream pressures of the system than the inlet vapour quality.

It can be seen that for the different ranks of initial pressures the dispersion and behaviour of the R-values are different, the decrease in the R-value becomes more noticeable for higher values of initial pressure, compared to the lower pressures in which it seems that the R-value follows a somewhat different tendency and not such a marked decrease; although in all cases it can be seen that the R-value decreases as the pressure difference increases

Once it has been observed that the influence of pressures is important, the different graphs comparing the R-parameter according to the pressure ratio, η, will be made. What can be observed initially in the data and the graphs are that the R-value decreases considerably as the pressure ratio η also does.

For a better understanding of the results, Graph 34 shows the R-value as function of the pressure ratio and Graph 35 shows the same data but differentiating by colours.

The R-values for the different ranks of pressures, where it is observed that the lower ratios of pressures correspond to lower values also of mass flux ratio and that as this ratio of pressures increases also the mass flux ratio does, seeing a tendency towards more constant values.

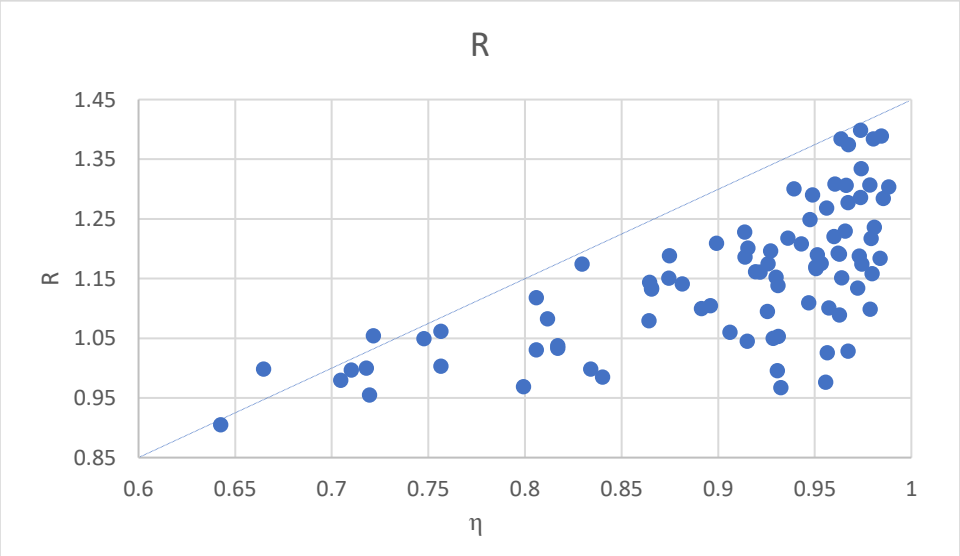

Graph 34. Mass flux ratio versus pressure ratio for all the experimental data

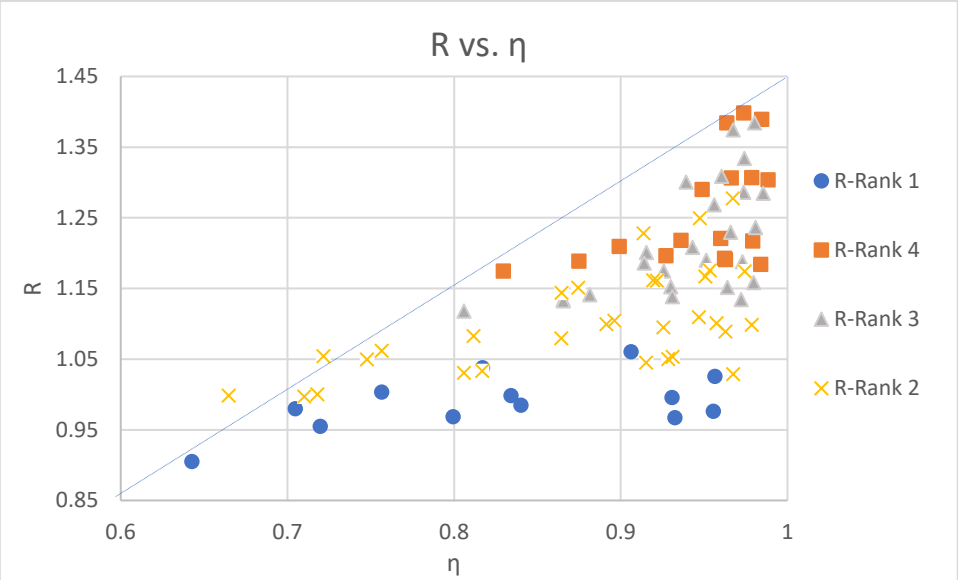

Graph 35. Mass flux ratio versus pressure ratio for the different ranks of pressure

Comparing the data for the different pressure ranks, it can be seen that they all follow an exponentially growing or increasing tendency that is not very marked, rather than linear, with the values of η which gives an idea of the growth of the R-value as the η increases, i.e., as the inlet and outlet pressures are similar (values close to the unit) it means that less pressure drop is had in the system and more constant R-values are observed so the system behaves in a more stable way when we have less pressure drop and also it is observed that for the given pressure ranks the tendency is to go towards values of R around 1.2 and 1.4 (similar to those obtained with the HEM method).

Since they are in these points in which it is observed that the data are closer to their limits and they are closer to each other for values of the pressure ratio close to the unit (which would correspond to an ideal system in which the experimental mass flux would be equal to the measured one and the HEM model studied in the previous section would perfectly predict the system if the system was in this situation, which is not the case).

In order to be able to see more clearly these results, which are affected by the pressures, it has been decided to study the value of the R as a function of η for different ranks of inlet vapour qualities in the mixture for all the pressure ranks.

So, within these experiments, the data have been divided again into other different ranks, but in this case as a function of the inlet quality of the vapour.

7.1.1.- Analysis for Rank 1

The values of the new ranks are:

- Rank 1-x1 → between 0.9-1.0 %
- Rank 1-x2 → between 1.3-3.0 %
- Rank 1-x3 → between 4.9-7.0%
- Rank 1-x4 → between 9-10%

The following table shows the results of these inlet vapour qualities ranks that have been used for the analysis.

Table 17. Data for the rank 1 of different ranks of inlet quality

	x_{in}	η	R
	%	–	-
RANK X1	0.93	0.96	1.03
	1.01	0.91	1.06
	0.99	0.82	1.04
RANK X2	1.32	0.76	1.00
	1.54	0.70	0.98
	1.95	0.83	1.00
	1.82	0.93	1.00
	2.93	0.72	0.95
RANK X3	4.90	0.93	0.97
	4.97	0.80	0.97
	6.85	0.64	0.90
RANK X4	9.74	0.84	0.98
	9.88	0.96	0.98

The following graph shows the evolution of R as function of the pressure ratio for the quality ranks explained. For these very low pressures, no very marked exponential tendency is really observed, although an increase in R-values is observed as the pressure ratio increases.

In this case it is also observed that for the inlet quality ranks, the evolution of the R-value does not change very drastically, although somewhat different values are observed since, as has been said, no tendency is seen in them; therefore, it can be said that these data do not depend on the inlet vapour quality of the mixture.

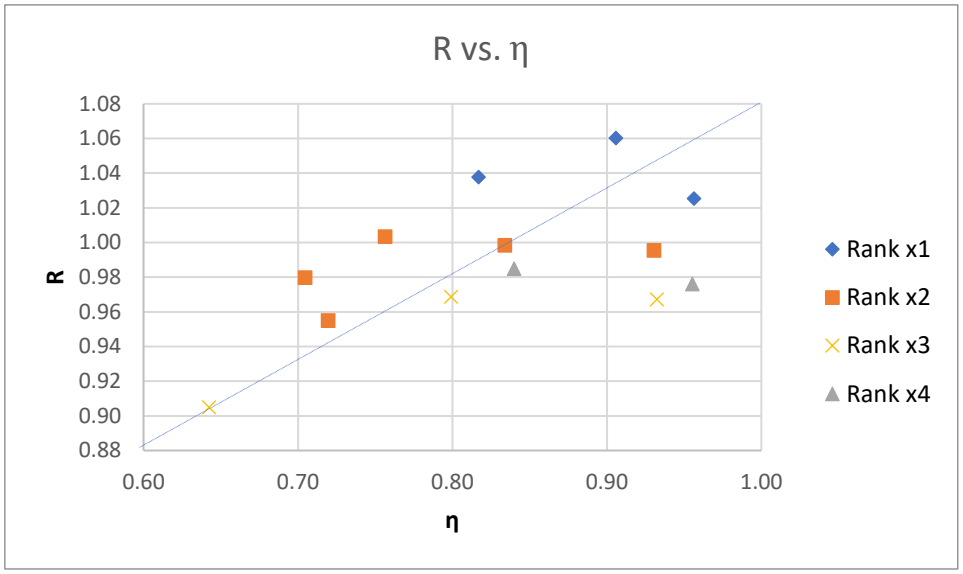

Graph 36. R versus η for the different ranks of inlet quality for Rank 1 of pressures

7.1.2.- Analysis for Rank 2

The values of the new ranks are:

- Rank 1-x1 → between 0.9-2.0 %
- Rank 1-x2 → between 2.01-4.02 %
- Rank 1-x3 → between 4.9-7.0%
- Rank 1-x4 → between 9.0-10.1%

The following table shows the results of these inlet vapour qualities ranks that have been used for the analysis.

Table 18. Data for the rank 2 of different ranks of inlet quality

	x_{in}	η	R
	%	–	-
RANK X1	0.97	0.87	1.15
	0.99	0.95	1.25
	0.98	0.97	1.28
	0.99	0.95	1.18
	1.01	0.92	1.16
	1.04	0.91	1.23
	1.97	0.96	1.09
	1.98	0.97	1.17
	2.00	0.93	1.09
	2.00	0.75	1.05
RANK X2	2.05	0.86	1.14
	2.04	0.86	1.08
	1.98	0.92	1.16
	2.07	0.95	1.17
	2.49	0.66	1.00
	3.73	0.72	1.00
	4.02	0.72	1.05
RANK X3	4.94	0.97	1.03
	4.95	0.92	1.05
	5.00	0.98	1.10
	4.99	0.82	1.03
	5.02	0.95	1.11
	5.00	0.90	1.10
	5.04	0.81	1.08
	6.67	0.71	1.00
RANK X4	9.46	0.81	1.03
	9.88	0.93	1.05
	9.88	0.93	1.05
	9.94	0.89	1.10
	9.96	0.96	1.10
	10.04	0.76	1.06

The following graph shows the evolution of R as function of the pressure ratio η for the quality ranks explained.

In this case, the exponential tendency of the data can be clearly seen, as has been deduced above, that all the data follow the same exponential tendency as the pressure ratio increases, thus corroborating what has been explained in the previous paragraphs. What is also deduced from this graph is that for all quality

ranks the evolution is the same, as seen in the previous graph for pressure rank 1, which gives the idea that the data do not depend on the inlet vapour quality since they all converge towards the same values (1.2-1.3) regardless of the quality measured in the experiments.

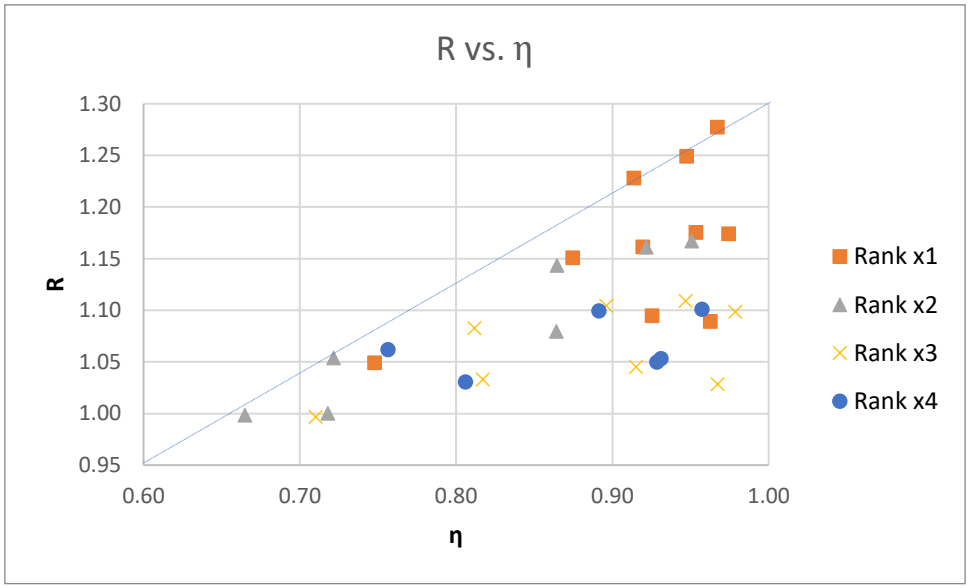

Graph 37.R versus η for the different ranks of inlet quality for Rank 2 of pressures

7.1.3.- Analysis for Rank 3

The values of the new ranks are:

- Rank 1-x1 → between 1.0-1.9 %
- Rank 1-x2 → between 2-5 %
- Rank 1-x3 → between 5.02-8.04%
- Rank 1-x4 → between 9.0-10.1%

The following table shows the results of these inlet vapour qualities ranks that have been used for the analysis.

Table 19. Data for the rank 3 of different ranks of inlet quality

	x_{in}	η	R
	%	–	-
RANK X1	1.00	0.98	1.38
	1.02	0.97	1.37
	1.04	0.94	1.30
	1.04	0.96	1.31
	1.04	0.97	1.33
	1.94	0.97	1.23
	1.96	0.97	1.29
	2.00	0.99	1.28
RANK X2	2.00	0.96	1.27
	2.02	0.92	1.20
	2.03	0.98	1.24
	2.06	0.94	1.21
	4.98	0.93	1.15
RANK X3	5.02	0.91	1.19
	5.02	0.81	1.12
	5.02	0.95	1.19
	5.05	0.88	1.14
	5.05	0.96	1.15
	5.11	0.97	1.19
	8.04	0.93	1.17
RANK X4	9.30	0.87	1.13
	9.60	0.87	1.13
	9.98	0.97	1.13
	10.00	0.98	1.16
	9.99	0.93	1.14
	10.02	0.95	1.17

The following graph (Graph 38) shows the evolution of R as function of the pressure ratio η for the quality ranks explained.

In this case, the exponential tendency of the data can be clearly seen, as has been deduced above, that all the data follow the same exponential tendency as the pressure ratio increases, thus corroborating what has been explained in the previous paragraphs. It can also be seen that, as in the case of the rank 2 data, the values do not depend on the initial quality of the vapour. It is also observed that the R data tend towards constant values between 1.2 - 1.4 and that these are more grouped together than for the previous ranks.

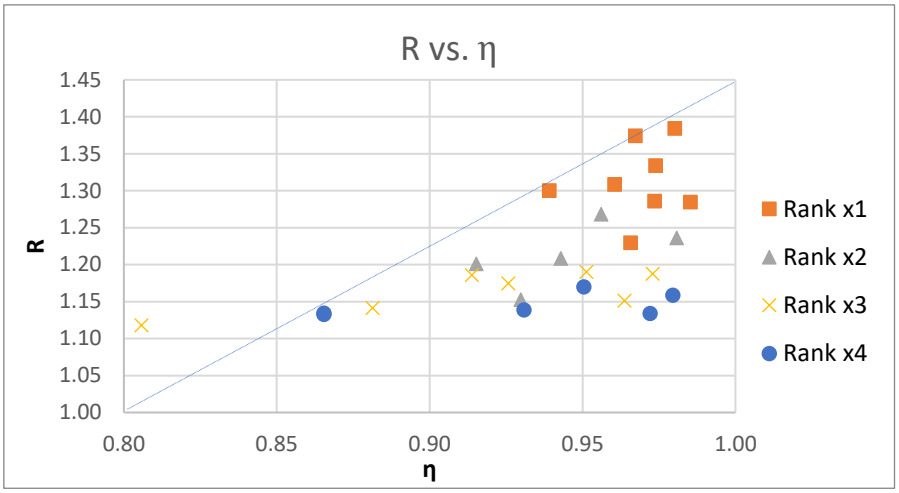

Graph 38. R versus η for the different ranks of inlet quality for Rank 3 of pressures

7.1.4.- Analysis for Rank 4

The values of the new ranks are:

- Rank 1-x1 → between 1.01-1.99 %
- Rank 1-x2 → between 2-5 %
- Rank 1-x3 → between 5.1-9.0%
- Rank 1-x4 → between 9.8-10.1%

The following table shows the results of these inlet vapour qualities ranks that have been used for the analysis

Table 20. Data for the rank 4 of different ranks of inlet quality

	x_{in}	h	R
	%	-	-
RANK X1	1.01	0.98	1.39
	1.01	0.96	1.38
	1.10	0.97	1.40
	1.99	0.97	1.31
RANK X2	2.03	0.99	1.30
	2.04	0.98	1.31
	2.07	0.95	1.29
	5.00	0.98	1.22
RANK X3	5.14	0.94	1.22
	5.12	0.96	1.22
	5.21	0.90	1.21
	8.54	0.83	1.17
RANK X4	9.89	0.96	1.19
	9.95	0.96	1.19
	9.93	0.93	1.20
	9.97	0.98	1.18
	10.08	0.87	1.19

The following graph (Graph 39) shows the evolution of R as function of the pressure ratio η for the quality ranks explained.

The same results and exponential tendency are observed as for the previous case (rank 3), which further corroborates the hypothesis of the exponential tendency of the R-values as a function of the pressure ratio, as well as the tendency to go towards constant values around 1.2 and 1.4, and the little dependence that this R-parameter has on the inlet vapour quality of the mixture.

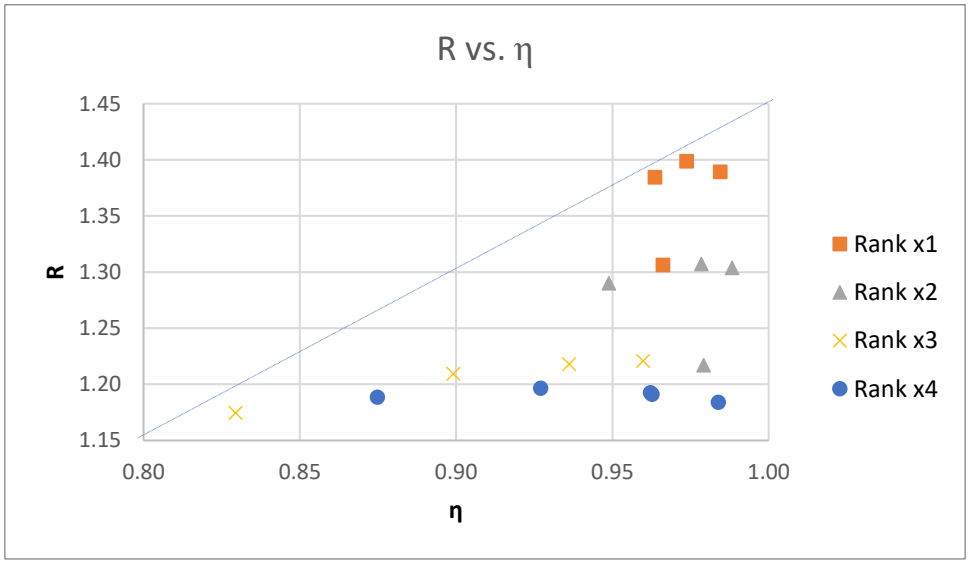

Graph 39. R versus η for the different ranks of inlet quality for Rank 4 of pressures

8.- Comparison of the models

To evaluate the accuracy of the predictions of the two methods analysed, a comparison with the R-parameter (mass flux ratio) will be made, since this is the parameter that has been decided to be used throughout the analysis to predict the results. In this section, we will compare the most important results as well as the major differences found between the two methods.

8.1.- Mass Flow Rate Comparison

To begin this section, we are going to compare the different values of R-parameter that have been obtained for all the experimental data in the two used models to see if their values are close to each other or not. In the Graph 40, the R-value obtained by the HNE-DS model is represented against the R-value obtained by the HEM model for all the experimental data as function of the inlet pressure.

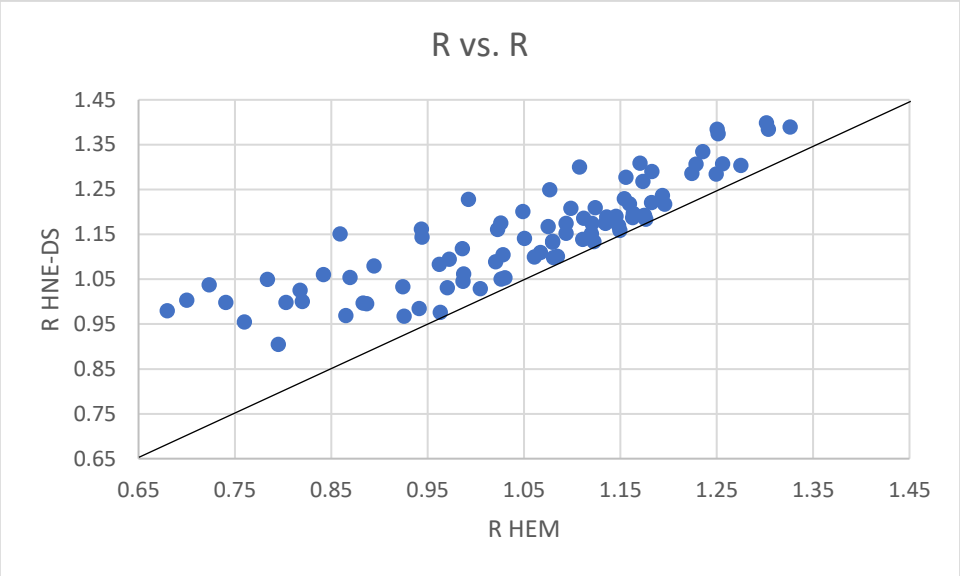

Graph 40. HNE-DS R as function of HEM R

It can be seen that the values of the R-parameter are not exact for both methods. It can be seen that the predictions for the HEM model are somewhat lower in general than for the HNE-DS model, although these differences seem to be decreasing as the graph shows a tendency in which the values are approaching to each other, although a clear general overestimation of the R-parameter can be observed for both methods.

Since this graph does not show a clear difference between the models, other comparisons will be made depending on the inlet quality of the vapour and the initial pressure at which the fluids are introduced into the system.

8.2.- Comparison of the R parameter in terms of the inlet quality of the mixture.

To make this comparison it has been decided to use the two pressure ranks (described in the analysis of the HEM model) furthest from each other (rank 1 and rank 4) since it is in these that the greatest differences have been found in the analyses of the two models separately.

The following graphs show the values of the R-parameter as a function of the inlet quality for the inlet pressure ranks, 1 and 4.

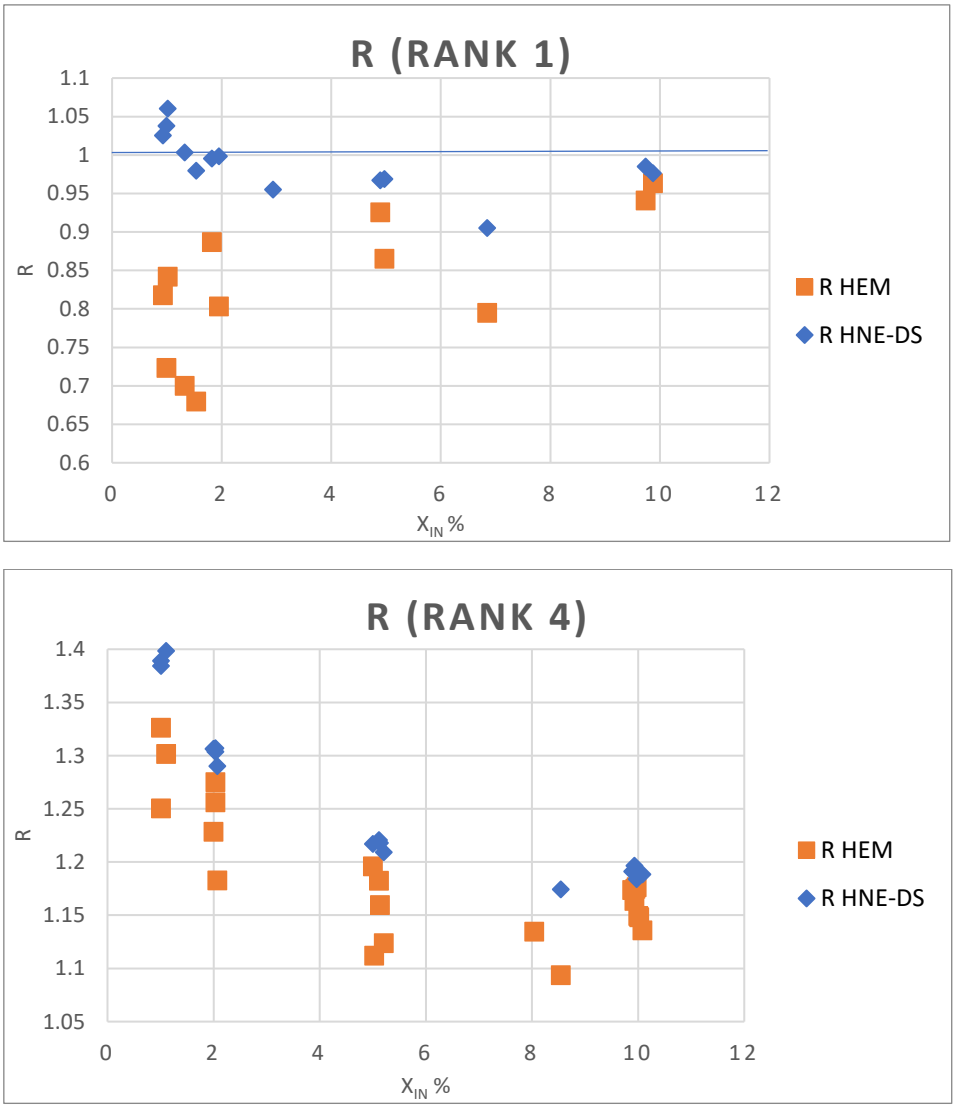

Graph 41. R HEM and R HNE-DS versus x_{in} for Rank 1 and Rank 4

In

Graph 41 it is shown that for lower inlet pressures there is an underestimation of the theoretical flux rate for the HEM model, which does not happen for higher pressures, and on the other hand for the HNE-DS model, this theoretical flux rate calculated is always somewhat overestimated since its R-parameter values are always above the unit value.

As can also be seen, the HNE-DS model seems to make a better prediction of the flux rate compared to the experimental because for the two pressure ranks being analysed, these R-values are closer to each other for this model, which means that the flux ratio values are more similar to each other.

On the other hand, in the values for the HEM model, there is a greater dispersion of data, so from these graphs we can conclude that the HEM model predicts the

behaviour of the system worse than the HNE-DS model (although in both cases a discharge coefficient would be missing to solve these small differences between the experimental and the theoretical).

It is also observed that the HNE-DS and the HEM models predicts the system behaviour better at low inlet pressures than at high inlet pressures since in the first case the R values are closer to the unit.

On the other hand, for the HEM it is observed that there is the same dispersion of data for high and low inlet pressures, so it is not a good model, which had been deduced previously since to carry out this model ideal conditions are assumed under which never work in the industry because they are very difficult to achieve and maintain.

8.3.- Comparison of the R parameter in terms of the pressure ratio

To show the last results we wanted to make a graph comparing the R-parameter as function of the pressure ratio for the two models and all the experimental data (see Graph 42)

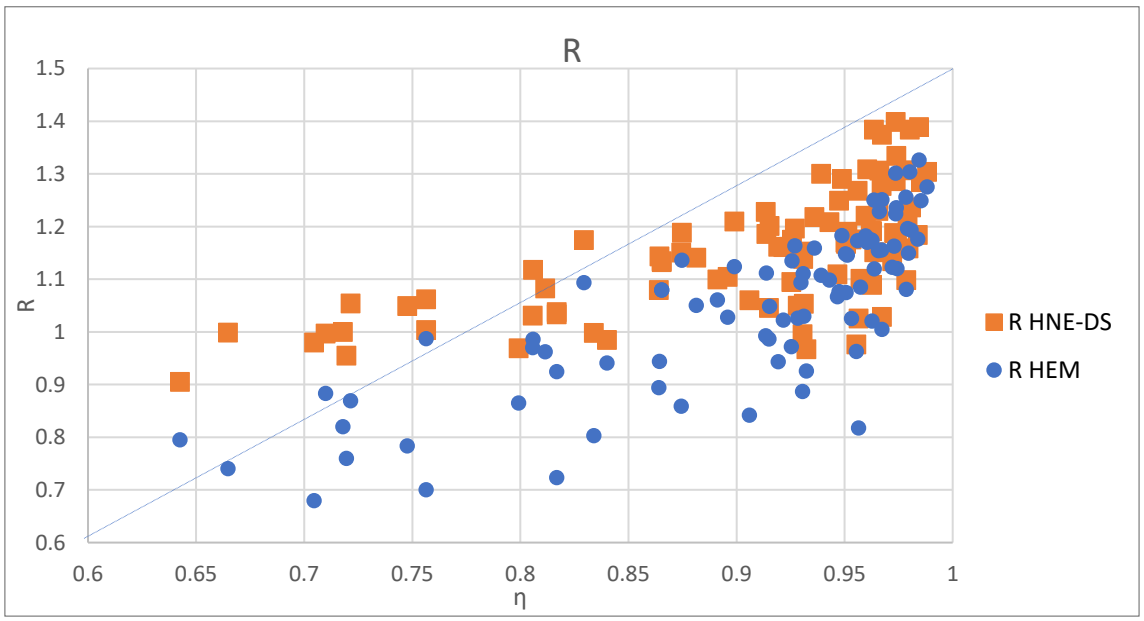

Graph 42. R HEM and R HNE-DS versus η

As can be seen, for both models, the data follow an exponential tendency, with a similar data dispersion. What we continue to observe is that the R-values continue to be higher for the HNE-DS model at any given pressure ratio, that is,

we continue to observe that the R-values are higher and closer together for both the different inlet qualities and the pressure ratios.

As the two models behave similarly, exponentially tendency to constant R-values around 1.2-1.4, it can be deduced that the influence of pressure is similar for both and does not seem to depend on the method of resolution adopted.

8.4.- Final conclusions of the comparison of the HEM and HNE-DS models

One of the main differences between the two models by definition refers to the fact that HEM model considers an ideal system in homogeneous equilibrium and on the other hand the HNE-DS takes into account the possibility of non-equilibrium thanks to the introduction of the N-parameter in which, as has been verified, this system is under conditions between equilibrium and non-equilibrium. When considering this, it influences in that with the model HNE-DS a better prediction of the behaviour of the system is obtained and it is simpler to adjust the data to this one.

Therefore, the HEM model depends a lot on the hypothesis of equilibrium and homogeneity to give accurate results, and although it is one of the most used models, more parameters are needed to characterize the system, although it is a useful model to make a first approximation of the possible behaviour of the system and thus see more or less between what ranks of flows could be found when performing new experiments. It has also been observed that the higher the input pressure in this model, the better prediction of the mass flux.

On the other hand, the HNE-DS model predicts better the behaviour of the system thanks to the introduction of the N parameter, and it is possible to observe how the data adjust better to this model since the mass flux ratio is closer to the unit value, although in this case it has been observed that this prediction is better for values or lower pressures, instead they are for the extreme values of pressures (rank 1 and rank 4) where a similar behaviour of the system is observed in which R-values follow the same tendencies.

Therefore, for this particular system and under these conditions, the HNE-DS model seems to fit better to the experimental data and should be considered when performing some model or function, either calculation or statistical, to predict the behaviour of a similar system without having to perform the experiments.

The next table shows a comparison between the experimental mass flux and the theoretical mass flux for rank 1 and rank 4 of initial pressure to clarify these results explained above.

Table 21. Comparison of theoretical and experimental mass flux for Rank 1 and Rank 4

RANK 1		
G_{theo} HEM	G_{exp}	G_{theo} HNE-DS
kg/s	**kg/s**	kg/s
0.171	**0.209**	0.214
0.235	**0.280**	0.297
0.251	**0.347**	0.360
0.242	**0.346**	0.347
0.235	**0.345**	0.338
0.225	**0.280**	0.279
0.185	**0.209**	0.208
0.212	**0.279**	0.267
0.129	**0.139**	0.134
0.180	**0.208**	0.202
0.165	**0.207**	0.188
0.131	**0.139**	0.137
0.081	**0.084**	0.082

RANK 4		
G_{theo} HEM	G_{exp}	G_{theo} HNE-DS
kg/s	**kg/s**	kg/s
0.370	**0.279**	0.388
0.521	**0.417**	0.577
0.451	**0.347**	0.485
0.426	**0.346**	0.453
0.267	**0.209**	0.273
0.351	**0.279**	0.365
0.492	**0.416**	0.537
0.250	**0.209**	0.255
0.401	**0.346**	0.421
0.330	**0.279**	0.340
0.467	**0.415**	0.502
0.453	**0.414**	0.486
0.245	**0.209**	0.249
0.246	**0.209**	0.249
0.324	**0.278**	0.333
0.166	**0.141**	0.167
0.392	**0.345**	0.410

As can be seen in the table, for lower pressures, rank 1, the mass flux ratio calculated from the HNE-DS model are better adjusted to those obtained experimentally than with the HEM model, whereas for higher pressures, rank 4, better results are obtained for the HEM model although, as can be seen in the table, the theoretical mass flow rate values between the two models do not differ so much from each other either, although they do differ more from the value obtained experimentally; therefore, it can be said that the HNE-DS model fits the data of this system better than the HEM, corroborating furthermore that the initial pressure is a factor on which the data depend because it is independent of the model to be used since the data behave in the same way for both cases.

It would also be interesting to be able to elaborate a statistical analysis on the results to see if the experiments carried out in the laboratory have repeatability or reproducibility to also check if the HNE-DS model would fit the following experiments to be carried out.

9.- Discharge coefficient

Although as has been seen before, these models do not fit well to the experimental data measured so it is necessary to use a discharge coefficient K_d to correct this error between the experimental mass flux, that is the real one that passes through the valve, and the theoretical mass flux, that is calculated by HEM and HNE-DS models.

Table 22 shows the values of the discharge coefficient K_d calculated for the experiments according to the following equation for HEM and HNE-DS models.

$$Eq\ 61 \qquad K_d = \frac{G_{exp}}{G_{theo}}$$

It also shows the calculated K_d as a function of the given discharge values, K_{dv} and K_{dl}, in the experiments. Lenzing *[29]* proposes to calculate K_d as a function of the void fraction in inlet conditions, knowing K_{dl} and K_{dv} as:

$$Eq\ 62 \qquad K'_d = K_{dv}\alpha + K_{dl}(1-\alpha)$$

In the case of the discharge coefficient calculated according to Lenzing, the same numerical value will be obtained for both models since it is a function of the K_{dl} and K_{dv} coefficients, which are the same for all the experimental data and depend on the alpha parameter, α, which in turn is a function of the quality and densities of the mixture, so, these values depend entirely on the properties of the fluid and their respective discharge coefficients for liquid and vapour and do not depend on the model being used.

However, when the coefficient is calculated according to Eq 61, different values will be obtained for each model. In Table 22 it can be seen that for lower pressures it is the HEM model that best fits the data as K_d is closer to the unit value, but in general terms and for the whole data set, it is the HNE-DS model which best fits them (as it has been explained previously).

You can also see how there is a difference when calculating K_d according to Eq 61 and according to Eq 62, which is a theoretical model. Although this thesis we will not focus on this parameter or its method of obtaining it, a more exhaustive analysis of it could be carried out to come to a linear regression of the data with K_d as a function of the pressure ratio, since it has been seen that this is one of the factors that most influences the data; in addition, carrying out a greater number of experiments as it is known from literature (explained earlier in this thesis) that the discharge coefficient can also be calculated by trial and error.

What has been able to verify with this brief analysis is that, as explained above, for low pressures the HEM model is the one that best predicts the data and for the rest the HNE-DS model is the one that best adjusts them.

Table 22. Discharge coefficient calculated by two different ways

P_{in}	K_d- HEM	K_d - HNE-DS	K_d'	P_{in}	K_d- HEM	K_d- HNE-DS	K_d'
bar	-	-	-	bar	-	-	-
4.93	1.22	0.98	0.81	**4.93**	1.08	1.03	0.84
7.56	1.16	0.87	0.80	**7.49**	1.00	0.97	0.84
9.98	0.93	0.80	0.80	**7.47**	1.01	0.96	0.84
4.94	1.19	0.94	0.82	**5.07**	1.16	1.03	0.84
17.53	0.75	0.72	0.78	**10.03**	0.93	0.91	0.84
10.00	0.87	0.78	0.79	**12.48**	0.91	0.87	0.83
7.51	0.97	0.85	0.80	**7.56**	1.08	0.97	0.84
4.91	1.38	0.96	0.82	**15.06**	0.0	0.84	0.83
17.55	0.80	0.72	0.78	**9.97**	0.94	0.90	0.84
14.92	0.77	0.72	0.78	**17.50**	0.84	0.82	0.83
7.51	1.06	0.86	0.80	**12.56**	1.01	0.89	0.83
14.93	0.80	0.73	0.78	**14.93**	0.87	0.84	0.83
12.48	0.90	0.77	0.79	**9.99**	0.97	0.91	0.84
12.53	0.85	0.76	0.79	**10.06**	1.04	0.92	0.84
12.44	0.81	0.75	0.79	**12.53**	0.95	0.88	0.83
9.89	1.01	0.81	0.80	**12.51**	0.89	0.87	0.83
17.54	0.77	0.72	0.78	**14.99**	0.86	0.84	0.83
4.99	1.43	1.00	0.82	**17.60**	0.86	0.82	0.83
5.04	1.47	1.02	0.83	**17.41**	0.85	0.82	0.83
12.43	0.87	0.81	0.81	**17.54**	0.89	0.83	0.83
7.46	0.98	0.92	0.82	**7.50**	1.13	1.00	0.84
14.99	0.82	0.78	0.81	**4.99**	1.26	1.11	0.84
4.99	1.25	1.00	0.83	**15.06**	0.88	0.85	0.84
9.97	0.89	0.85	0.82	**17.45**	0.91	0.85	0.84
7.47	1.03	0.91	0.82	**7.38**	1.03	0.97	0.84
4.87	1.13	1.00	0.83	**12.51**	0.93	0.88	0.84
7.54	1.28	0.95	0.82	**4.97**	1.06	1.02	0.85
14.94	0.80	0.78	0.81	**5.04**	1.04	1.02	0.85
14.98	0.85	0.79	0.81	**7.58**	0.97	0.95	0.84
17.46	0.81	0.77	0.80	**7.42**	0.97	0.95	0.84
12.48	0.95	0.83	0.81	**17.58**	0.85	0.84	0.84
17.47	0.78	0.77	0.80	**17.53**	0.85	0.84	0.84
17.46	0.80	0.77	0.80	**12.65**	0.93	0.88	0.84
12.48	0.84	0.81	0.81	**17.48**	0.86	0.84	0.84
9.94	1.06	0.87	0.82	**10.00**	0.94	0.91	0.84
7.51	1.12	0.93	0.82	**17.53**	0.85	0.84	0.84
10.03	0.98	0.86	0.82	**10.00**	0.92	0.91	0.84
12.42	0.91	0.83	0.81	**12.55**	0.89	0.88	0.84
17.46	0.85	0.78	0.80	**15.03**	0.87	0.86	0.84
9.96	0.93	0.86	0.82	**12.60**	0.90	0.88	0.84
7.62	1.35	1.00	0.83	**15.07**	0.87	0.86	0.84
5.07	1.32	1.05	0.84	**10.01**	1.01	0.94	0.84
7.46	1.22	1.00	0.84	**17.53**	0.88	0.84	0.84
10.06	1.15	0.95	0.83				

10.- Conclusions and future work

In this section, are going to be summarized the main results of the analysis of the two-phase flow (steam/water) from which it has been achieved thanks to the experimental data obtained by the University of La Sapienza, such as the behaviour, state of the flow and the model that best adjusts and precise these data. It will be also described a small section in which some works will be named that can be done in the future to extend this area of study.

10.1.- Conclusions

This work was begun because of the problems that the two-phase flows presented when it came to modelling them accurately as they are commonly used in the industry and there are few documents in the bibliography in which these issues have been addressed. Therefore, it was decided to try to fit some experimental data to some of the existing models to describe the behaviour of these flows. The results of the previous experiments carried out at the University of La Sapienza, Rome, were used as a starting point, in which the different outlet mass flux of a two-phase steam/water mixture were measured on a pressure relief safety valve with a diameter of 0.01 meters under different initial pressures and different initial qualities of the vapour in the mixture.

These experiments concluded in different measured data of the outlet pressure and results on the mass flux through the valve, measured in kg/s. These experimental results have been compared with the predictions of two of the most commonly used calculation methods for pressure relief valves, the homogeneous equilibrium model (HEM) and the homogeneous non-equilibrium model (derived by Diener and Schmidt, HNE-DS).

After having made the previous analyses and deductions on what state the mixture was in, it was initially found that it was in a saturation state and after the relevant calculations it was deduced that it was not in any critical situation so the calculations of the two models were quite simplified.

The two models predicted, except for some values at low pressures in the HEM model, tend to overestimate the theoretical mass flux calculated against the measured experimental ones, which corresponds to what is known from literature and at industry, which is the most common since all models have to overestimate the mass flux as they cannot take into account all aspects, both internal and external, of the system being studied.

After the analysis of the two models, some differences between them were detected. To begin with, the system is in a state between equilibrium and non-equilibrium, as demonstrated by the N-parameter in the HNE-DS model. This implied recalculating the ω-parameter that had been deduced in the HEM model since it did not take this phenomenon into account. What was found was that the

ω-parameter decreased its value in the HNE-DS model compared to the HEM model and that modifies the calculated theoretical mass flux (it should be noted that these two models follow the line of the so-called ω-methods). Therefore, as the mass flux depends on this parameter, different results are obtained depending on the model being used.

Once these specifications have been made, the theoretical mass flux rate has been calculated as function of the two models. As shown in the conclusions section of the comparison of the two models, HEM model adjusts the data better only for lower inlet pressures, for all the rest of the data, the HNE-DS model fits the data better; as well as for high pressures is different because neither models adjusts the data exactly, although they are not very far from the experimental results with which it works. Therefore, as a conclusion, it has been deduced that the HNE-DS model is the more representative of the two for this data set.

This has also been corroborated thanks to the representations made of the values of the mass flux ratio, parameter R, against different properties of the mixture such as the initial quality of the vapour, x_{in}, the pressure ratio, η, or the pressure drop in the system, Dp. In these cases, it has been possible to observe how when comparing the evolution of R, it has shown greater changes and dispersion in its data when analysed in function of Dp and without drastic changes when analysed in function of x_{in}, for the whole ran of initial pressures studied. Therefore, it has been deduced from these analyses that the data set depends more on the initial pressure and pressure drop than on the quality of the vapour.

Independently of this, the effect of this initial pressure has also been analysed for both models using x_{in} ranks instead of pressure ranks as in the previous analyses. With this analysis, it has been possible to observe that for both models the R-values follow an exponential increasing tendency, with a tendency to go towards constant values, between 1.2 and 1.4, in which the majority of the results seem to be congregated. Furthermore, it has been found that the experimental data depend on the initial pressure, as explained, but this is not a function of the model being used since for both cases studied the data follow the same tendency.

For this reason, it is believed that the data on mass flux values do depend on their properties, with greater dependence on P_{in} than on the x_{in} in this case, but that this dependence is not implicit in the model being used. Therefore, using either of the two models will lead to the same conclusion regarding system behaviour, but in this case, according to the analyses carried out, the HNE-DS model will be the most accurate and adjusted to the experimental data used. So, as a conclusion, it can be said that the best model is the HNE-DS due to its great similarity with the theorical mass flow calculates.

10.2.- Future work

As a complement to this thesis, it would be important to carry out the experiments again under the same conditions and to repeat the analysis with the two models that have been used, to check the reproducibility or repeatability of the system. And so, for future experiments, with two-phase steam/water systems, to be able to have a statistical analysis of data from which one can initially deduce the different parameters that can be obtained, and thus know the confidence of the same and even include the number of experiments that should be carried out if one wants to make a more extensive study.

It would also be desirable to vary the inlet conditions (through simulation would be a good alternative) like flows in a different state to the one that has been had in this thesis, e.g. by changing the inlets conditions of subcooled or critical, to see if the chosen models would also be able to adjust the data in the same way or substantial changes could be appreciated.

To continue with the research in which this master's thesis is framed, it could be interesting to carry out the same analysis with other calculation methods and computer simulations to see how the data behave and to be able to have a wider analysis of the two-phase flows. And as the last proposal, the same study could be done with different fluids, not only steam/water, to have a wider spectrum of study and thus be able to check the validity of the models under other conditions.

Bibliography

[1] Hewitt, G. F. (2011, February 11). *Thermopedia.* Retrieved septiembre 29, 2019, from http://www.thermopedia.com/content/3/

[2] Roul, Manmatha. (2012, January 12). Numerical investigation of single-phase and two-phase flow through thin orifices in horizontal pipes. Indian Journal of Science and Technology. Vol. 5.

[3] Hewitt, G. F. (2011, February 11). *Thermopedia*. Retrieved septiembre 29, 2019, from http://www.thermopedia.com/content/4/

[4] Hewitt, G. F. (2011, February 11). *Thermopedia*. Retrieved septiembre 29, 2019, from http://www.thermopedia.com/content/2/

[5] Hewitt, G. (1992). *Handbook of Multiphase Systems* 1982 (2nd ed., p. Chapter 2). New York: (Ed. G. Hetsroni), Hemisphere Publishing Corporation.

[6] Nedderman R. (1988). *Boiling, Condensation Gas-Liquid Flows*. By P. B. Whallwy. Oxford Science Publication, 1987. 291. Journal of Fluid Mechanics, 191, 598-599.

[7] Taitel, Y., Barnea, D. and Dukler, A. E. (1980) *Modelling flow pattern transitions for steady upward gas-liquid flow in vertical tubes*, *AIChE J*, 26, 345-354.

[8] Dukler, A. E. and Taitel, W. (1986) *Flow Pattern Transitions in Gas-Liquid Systems: Measurement and Modelling*, Chapter 1 of *Multiphase Science and Technology*, Vol. 2 (Ed. G. F. Hewitt, J. M. Delhaye and N. Zuber), Hemisphere Publishing Corporation.

[9] Cengel Y., & Boles, M. (2015). *Thermodynamics* (7th ed., p. Apendix D, Apendix C, Physiscal properties data bank). New York: McGraw-Hill Education

[10] Stefański, Sebastian & Kalawa, Wojciech & Mirek, Kaja & Stępień, Maciej. (2017). *Visualization and research of gas-liquid two phase flow structures in cylindrical channe*l. E3S Web of Conferences. Retrieved octobre 2, 2019 from https://www.researchgate.net/publication/315174654_Visualization_and_research_of_gas-liquid_two_phase_flow_structures_in_cylindrical_channel

[11] Found, N. (2019). *What is Two-phase Fluid Flow - Definition*. Retrieved 11 October 2019, from https://www.thermal-engineering.org/what-is-two-phase-fluid-flow-definition/

[12] Pálsson, H. (n.d.). *University of Iceland.* Retrieved from https://notendur.hi.is/~halldorp/UNU/twophase_concepts.pdf

[13] Pálsson, H. (n.d.). *University of Iceland.* Retrieved from https://notendur.hi.is/~halldorp/UNU/twophase_regimes.pdf

[14] Beychok, M. R. (2005 4th Edition). *Fundamentals of stack gas dispersion* (4th ed.). Irvine, California.

[15] Roberto Ibarra, J. N. (2019, August 10). Two-phase gas-liquid flow in concentric and fully eccentric annuli. Part I: Flow patterns, holdup, slip ratio and pressure gradient.

[16] (2016). *Inglenookeng*. Retrieved from http://www.inglenookeng.com/_blog/fireside_chats/post/two-phase-flow-sizing-methodologies/

[17] Paul Robert Meiller, (2000, April). *Safety relief valve sizing: Comparision of two-phase Flow models to empirical data*. A Senior Honors Thesis Submitted to the Office of Honors Programs & Academic Scholarships Texas A&M University In partial fulfillment of the requirement.

[18] Benbella, S. (2009, May 21). Mixture loss coefficient of safety valves used in nuclear plants. *Nuclear Engineering and Design*, Pages 1779-1788.

[19] American Society of Mechanical Engineers, ASME *Boiler and Pressure Vessel Code* (1986).

[20] API 520 (2000, January). *Sizing, Selection, and Installation of Pressure-Relieving Devices in Refineries.* Part I sizing and selection, 7th Edition. American Petroleum Institute.

[21] ISO/DIS-4126-10 (2006) *Safety devices for protection against excessive pressure – sizing of safety valves and connected inlet and outlet lines for gas/liquid two-phase flow*. DIN Deutsches Institute fur Normung e.V., Beuth Verlag GmbH, ¨ Berlin.

[22] Egan, J. S. (2005, November). Case Studies of Sizing Pressure Relief Valvesfor Two-Phase Flow. *Chemical Engineering & Technology*(2), Pages 263.272.

[23] William Dempstera, W. E. (2013, October). Two phase discharge flow prediction in safety valves. *International Journal of Pressure Vessels and Piping, Volume 110*, pges 61-65.

[24] N.L. Scuroa, E. A. (2018, March). A CFD analysis of the flow dynamics of a directly-operated safety relief valve. *Nuclear Engineering and Design, Volume 328*, Pages 321-332.

[25] Darby, R. (2004, July). On two-phase frozen and flashing flows in safety relief values: Recommended calculation method and the proper use of the discharge coefficient. *Journal of Loss Prevention in the Process Industries, Volume 17*(Issue 4), Pages 255-259.

[26] Gino Boccardi, Roberto Bubbico, Gian Piero Celata, Barbara Mazzarotta. (2008, January). Geometry influence on safety valves sizing in two-phase flow. *Journal of Loss Prevention in the Process Industries, Volume 21*(Issue 1), Pages 66-73.

[27] V. Dossena, F. M. (April de 2013). Numerical and experimental investigation on the performance of safety valves operating with different gases. *International Journal of Pressure Vessels and Piping, Volume 104*, Pages 21-29.

[28] lC. Bazsó, C. H. (2013, October). An experimental study on the stability of a direct spring loaded poppet relief valve. *Journal of Fluids and Structures, Volume 42*, Pages 456-465.

[29] Lenzing, T., Friedel, L., Cremers, J., & Alhusein, M. (1998). Prediction of the maximum full lift safety valve two-phase flow capacity. Journal of Loss Prevention in the Process Industries, 11, 307–321.

[30] Leung, J. C., (2004). A theory on the discharge coefficient for safety relief valve, Journal Loss Prevention Process Industrial, vol 17, (2004) pp. 301-313.

[31] CCPS of AIChE (1998) Guidlines for pressure relief and effluent handling systems. AIChE, New York.

[32] N, I. T. (25 de March de 2003). *Sizing of safety valves and connected inlet and outlet lines for gas/liquid.*

[33] A. Bernard-Champmartin, O. P. (March de 2014). Modelling of an Homogeneous Equilibrium MixtureModel (HEM). *JOUR*.

[34] Diener R, Kiesbauer J, Schmidt J (2005) Improved valve sizing for multiphase flow – HNE-DS method based on an expansion factor similar to gaseous media to account for changes in mixture density. Hydrocarb Process 84(3):59-64.

[35] Fischer HG, Forrest JS, Grossel SS, Huff JE, Muller AR, Noronha JA, Shaw DA, Tilley BJ (1992) Emergency Relief System Design Using DIERS Technology, DIERS Project Manual

[36] Leung JC (1986) A generalized correlation for one-component homogeneous equilibrium flashing choked flow. AIChE J 32(10): 1743-1746.

[37] Leung JC (1994) Flashing flow discharge of initially sub-cooled liquid in pipes. J Fluid Eng 116: 643-645.

[38] M. Epstein, R. E. Henry, W. Midvidy, R. Pauls, Thermal-Hydraulics of Nuclear Reactors II, 2nd International Topical Meeting Nuclear Reactor Thermal-Hydraulics, Santa Barbara, CA 1983.

[39] Henry, R. E., & Fauske, H. K. (1971). The two-phase critical flow of one-component mixtures in nozzles, orifices, and short tubes. Transactions of the ASME Journal of Heat Transfer, 93, 179–187.

[40] J.Schmidt, [. (2007, January 12). Sizing of nozzles, venturis, orifices, control and safety valves. *Forsch Ingenieurwes*, Pages 47-58.

[41] Diener, R., Schmidt, J., (2004) Sizing of Throttling Device for Gas/Liquid Two-Phase Flow Part 1: Safety Valves, Process Safety Progress, Vol.23, No.4, pp. 335-344.

[42] Diener, R., Schmidt, J., (2005) Sizing of Throttling Device for Gas/Liquid Two-Phase Flow Part 2: Control Valves, orifices and nozzles, Process Safety Preogress, Vol.242, No.1, pp. 29-37.

[43] Perfil V. (2014, Noviembre 14) Válvulas de presión. Retrieved November 21, 2019 from https://dewkdd.blogspot.com/2014/11/valvulas-de-presion.html

[44] Válvulas de presión. (2007). Retrieved November 21, 2019, from http://hawe.cohimar.com/valvulas_de_presion.pdf